What controls fire size in the South American Gran Chaco? Exploring atmospheric, and landscape, and anthropogenic drivers through Remote Sensing.

Rodrigo San Martín[1], Catherine Ottlé[1], Anna Sorenssön[2,3,4], Pradeebane Vaittinada Ayar[1], Florent Mouillot[5], Marielle Malfante[6]

[1]Laboratoire des Sciences du Climat et de l'Environnement, LSCE/IPSL, CEA-CNRS-UVSQ, Université Paris-Saclay, Gif-sur-Yvette, France;
[2]Centro de Investigaciones del Mar y la Atmósfera (CIMA), CONICET – Universidad de Buenos Aires, Buenos Aires, Argentina;
[3]CNRS, CNRS – IRD – CONICET – UBA, Instituto Franco-Argentino para el Estudio del Clima y sus Impactos (IRL 3351 IFAECI), Argentina;
[4]Facultad de Ciencias Exactas y Naturales, Universidad de Buenos Aires, Buenos Aires, Argentina;
[5]UMR CEFE, University of Montpellier, CNRS, EPHE, IRD, Montpellier, France;
[6]Univ. Grenoble Alpes, CEA, List, Grenoble, France;
Correspondence to: Rodrigo San Martin (rodrigo.sanmartin@lsce.ipsl.fr)

Abstract. Wildfires are key ecological agents in the Gran Chaco, one of the world's largest tropical dry forest ~~ecosystems, where fire regimes are increasingly shaped by human pressure and climate variability. However, the drivers of fire size variability remain poorly understood.~~systems. We ~~analysed over~~ analyzed more than 100,000 fire patches ~~(2001–2022) from the FRYv2.0 database to assess environmental controls on fire size and morphology~~ across the Wet, Dry~~,~~ and Very Dry Chaco~~. High-resolution fire polygon data were combined with ERA5-Land reanalysis, vegetation and topographic metrics,~~ between 2001 and 2022, to quantify environmental and anthropogenic ~~layers.~~controls on fire size. Fire sizes were ~~highly~~ strongly right-skewed: ~~>~~more than 80 % were ~~<~~smaller than 5 km², yet large ~~events (Megafires >100 km², Gigafires >1000 km²)~~ and extreme fires dominated total burned area~~ (BA). Gigafires~~. Megafires (> 100 km²) occurred in all subregions, while gigafires (> 1000 km²) were rare but ~~mostly confined to~~concentrated in the Dry Chaco~~, whereas the Wet Chaco had the highest BA, fire frequency, and Megafire count~~. Fire Weather Index ~~(FWI)~~ ~~BA~~ burned area correlations ~~reached~~exhibited strong spatial contrasts, reaching values of up to r = 0.7 in the Wet Chaco ~~but were~~and showing weaker ~~and spatially fragmented~~, more heterogeneous relationships in drier ~~subregions, where fuel continuity and ignition context played larger roles. Lag analyses showed that in drier areas, wet-season biomass buildup (4–6 months prior) increased subsequent fire activity, while in wetter areas short-term dryness (1–3 months prior) was more predictive. During fire meteorology, especially~~regions. Meteorological conditions during fires, particularly persistent strong winds, ~~better explained fire morphology than pre-fire conditions.~~were associated with larger and more elongated patches. Random Forest models ~~ranked static landscape features (elevation,~~ showed that topography and land- cover ~~evenness, slope, tree cover) highest in size prediction. Our~~composition together accounted for about 60 % of total SHAP importance, whereas demographic variables had very low SHAP contributions in the models. Human pressures shape ignition timing but showed limited direct influence on fire size once landscape structure was included in the models. These results ~~reveal region-specific fire–environment couplings, clarifying the interplay of meteorological, ecological, and anthropogenic factors, and providing actionable insights for fire risk forecasting and management~~provide a quantitative basis for improving regional fire danger assessments in the Gran Chaco.

1 INTRODUCTION

Wildfires shape global ecosystems by influencing vegetation structure, biodiversity, and landscape composition (Bowman et al., 2009; Archibald et al., 2013; Chuvieco et al., 2020). The Gran Chaco, spanning parts of Argentina, Bolivia, Paraguay, and Brazil, is one of the largest remaining dry forest ecosystems, with marked variation in precipitation, vegetation, and human land use (Morello & Adámoli, 1968; Olson et al., 2001; Ginzburg et al., 2005; Torrella & Adámoli, 2005). Fire has long modulated its forest structure and driven transitions between forests, shrublands, and grasslands (Bucher, 1982; Kunst et al., 2003; Vidal Riveros et al., 2023).

In recent decades, Gran Chaco fire regimes have shifted under land use intensification and climate variability (Gasparri et al., 2008; De Marzo et al., 2021; Baumann et al., 2022; Marengo et al., 2022; Vidal Riveros et al., 2023; San Martín et al., 2023; San Martín, 2024). These changes often produce larger, more intense fires, especially in areas with non native grasses or monocultures (D'Antonio & Vitousek, 1992; Bravo et al., 2014; Vidal Riveros et al., 2023). Natural fire breaks (e.g., water bodies) and traditional management can limit spread (Kunst et al., 2003; Bowman et al., 2011; Archibald et al., 2013; Bravo et al., 2014; Andela et al., 2017, 2019), while landscape heterogeneity further constrains propagation (Bowring et al., 2024), challenging assumptions of uniform anthropogenic effects (Bistinas et al., 2014; Archibald et al., 2018; Kelley et al., 2019). At broader scales, climatic variability — especially rainfall patterns and drought — can outweigh land use in shaping fire size and frequency (Krawchuk et al., 2009; Jolly et al., 2015; Jones et al., 2022).

The complexity of fire size drivers in the Gran Chaco is increasingly recognized, yet key mechanisms remain poorly understood (Kelley et al., 2019; Jones et al., 2022; Vidal Riveros et al., 2023, 2024). Prolonged droughts reduce fuel moisture, increasing flammability and enabling extreme events (Alencar et al., 2015; Naumann et al., 2023). Several major droughts coincided with strong negative El Niño Southern Oscillation (ENSO) phases, including the record breaking 2020–2023 La Niña (Doblas Reyes et al., 2021; De Marzo et al., 2023; Meteorological Organization et al., 2023; Arias et al., 2024).

Although recent studies have advanced understanding of Gran Chaco fire regimes, key links between patterns and meteorological or anthropogenic drivers remain unclear. Land cover and socio environmental factors play a major role: Baumann et al. (2022) found that deforestation pathways vary by actor and context, influencing fire landscape interactions; San Martín et al. (2023) showed that precipitation burned area (BA) relationships differ by land cover; and Levers et al. (2024) projected that agribusiness expansion could intensify fire impacts in ecologically and socially sensitive areas.

Fire classification efforts also overlook important drivers. Vidal Riveros et al. (2024) grouped Paraguayan Chaco fire regimes by severity, frequency, and extent, while Naval Fernández et al. (2025) applied multivariate clustering of landscape attributes to delineate pyroregions in the Argentinian Chaco.

~~Both captured spatial variability in fire activity, but neither incorporated meteorological conditions, limiting insights into atmospheric controls on fire behavior and size.~~

~~Research has further addressed post-fire vegetation recovery and cultural dimensions of fire. Saucedo and Kurtz (2025) reported rapid regrowth after the 2022 megafires, followed by climate-constrained stabilization. Sugiyama et al. (2025) highlighted Indigenous fire narratives as valuable sources of local knowledge on ignition, spread, and ecosystem recovery.~~

~~However, no study has yet combined high-resolution meteorological data, fire morphology, and landscape context to assess how fire size responds to both short-term anomalies and long-term environmental patterns in the Gran Chaco.~~

~~Advances in satellite Earth observation now make this integration possible. Global BA products such as FireCCI51 provide consistent daily burned surface estimates at moderate spatial resolutions (Chuvieco et al., 2020). Event-based datasets like FRY (Laurent et al., 2018; Chen, 2025) and the Global Fire Atlas (Andela et al., 2019) reconstruct individual fires from these burned pixels, enabling analysis of attributes such as ignition date, duration, size, and morphology (Moreno et al., 2021; García et al., 2022a; Takacs et al., 2021). In this study, we used FRYv2.0, which integrates the FRYv1.0 pixel aggregation method with FireCCI51 BA mapping (Lizundia-Loiola et al., 2020), and combined it with environmental and climate products to address gaps in understanding BA dynamics and fire size variability in the Gran Chaco.~~

Wildfires shape global ecosystems by influencing vegetation structure, biodiversity, and landscape composition (Bowman et al., 2009; Archibald et al., 2013; Chuvieco et al., 2020). The Gran Chaco, spanning around 1.1 million km^2 across Argentina, Bolivia, Paraguay, and Brazil, is one of the largest remaining dry forest ecosystems, with marked variation in precipitation, vegetation, and human land use (Morello and Adámoli, 1968; Olson et al., 2001; Ginzburg et al., 2005; Torrella and Adámoli, 2005). Fire has long modulated its vegetation structure and driven transitions between forests, shrublands, and grasslands (Bucher, 1982; Kunst et al., 2003; Vidal-Riveros et al., 2023).

In recent decades, fire regimes in the Gran Chaco have shifted under the combined influence of land-use intensification, changes in fire use and suppression practices, and increasing climatic variability (Gasparri et al., 2008; De Marzo et al., 2021; Baumann et al., 2022; Marengo et al., 2022; Vidal-Riveros et al., 2023; San Martín et al., 2023; San Martín, 2024).

Fuel characteristics and availability play a central role (Bravo et al., 2014; Argañaraz et al., 2016, 2018; Vidal-Riveros et al., 2023). In native grasslands and savannas of the Gran Chaco, fine fuels typically reach 4,000 to 5,000 kg of dry biomass per hectare per year, supporting medium to high intensity surface fires (Bravo et al., 2025). In productive systems such as silvopastoral areas or improved pastures, implanted tropical forage grasses can increase fine-fuel loads substantially (up to double the biomass), locally enhancing fire intensity (Kunst et al., 2016).

Landscape heterogeneity further controls fire propagation, as the juxtaposition of rivers, wetlands, shrublands, forests and grasslands in the Gran Chaco, together with traditional firebreak construction

and other local management practices, often restricts fire spread and creates natural or managed barriers to fire (Kunst et al., 2003; San Martín et al., 2023; Vidal-Riveros et al., 2023; Bravo et al., 2025). These interacting landscape controls challenge the idea of uniform and spatially consistent anthropogenic effects on fire regimes across global dry ecosystems (Bistinas et al., 2014; Andela et al., 2017; Archibald et al., 2018; Kelley et al., 2019; Jones et al., 2022).

Human activity is also a central component of fire regimes in the Gran Chaco. Across the region, most ignitions originate from rural land management practices, including pasture renewal burns, garbage burning, intentional clearing for agriculture or real-estate conversion, and opportunistic burning associated with hunting (Naval Fernández et al., 2023; Vidal-Riveros et al., 2023; San Martín et al., 2023; San Martín, 2024; Bravo et al., 2025). In the wetlands and floodplain grasslands of the Wet Chaco, intentional burning for pasture renovation or vegetation clearing typically occurs towards the end of winter and beginning of spring (end of the cold dry season) and, to a lesser extent, in late summer (towards the end of the wet season) (San Martín et al., 2023). Winter burns are usually controlled and produce small, patchy scars, whereas late-summer fires are more prone to escape and become larger, particularly in anomalous dry years (Saucedo and Kurtz, 2025). Despite these differences in fire behavior, vegetation often shows rapid post-fire recovery in the Wet Chaco (Bravo et al., 2025; Saucedo and Kurtz, 2025). In contrast, the central and western Dry Chaco show a higher prevalence of land-management fires linked to deforestation, rangeland conversion, and dry-season vegetation clearing (Baumann et al., 2022; Gasparri et al., 2008; Naval Fernández et al., 2023; San Martín et al., 2023). Between 2001 and 2019, nearly 40% of the 51.000 km^2 of deforested area in the Argentine Dry Chaco was associated with burned surfaces (San Martín et al., 2023).

Cultural dimensions further shape ignition patterns: indigenous and rural communities in the Dry Chaco use fire for subsistence activities and landscape maintenance, balancing risks and ecological benefits (Sugiyama et al., 2025).

In this context, the 2020 fire season illustrated how socio-environmental factors interact under exceptional circumstances. The COVID-19 pandemic altered mobility, enforcement capacity and on-the-ground fire management across many regions worldwide. As discussed by Naval Fernández et al. (2023), in several fire-prone landscapes, such as the Brazilian Pantanal and other tropical savannas, the reduction or suspension of field surveillance and firefighting activities during lockdowns led to increased fire activity (Garcia et al., 2021; Kumar et al., 2022; Eklund et al., 2022). In contrast, in other regions, strict mobility restrictions reduced human-caused ignitions, highlighting the strong coupling between human presence and fire occurrence, as reported for regions in Asia and North America (Paudel, 2021; Poulter et al., 2021). In the Gran Chaco and adjacent drylands of central Argentina, mobility also declined sharply during the peak fire months, yet suppression capacity remained relatively stable due to the continued availability of volunteer brigades (Naval Fernández et al., 2023). Recent socio-anthropological work further shows that the lockdown period through 2020 overlapped with ongoing agrarian expansion and land-clearing dynamics, with deforestation, burning and road-

infrastructure projects proceeding despite mobility restrictions, reinforcing long-standing territorial inequalities and weak institutional fire governance (Castilla, 2021; Schmidt and Castilla, 2023). This combination indicates that many ignitions were not accidental or urban in origin, but instead linked to rural land-clearing practices, pasture renewal and other management activities, underscoring the central role of human agency even under atypical social conditions (Naval Fernández et al., 2023; San Martín, 2024).

At broader temporal and spatial scales, climatic variability, especially the occurrence of prolonged droughts related to the intensification of episodes of multi-year strong El Niño–Southern Oscillation (ENSO) negative phases (La Niña), has been associated with large fire seasons in the Chaco and neighboring biomes (Alencar et al., 2015; Naumann et al., 2023). These climate anomalies reduce fuel moisture and extend the window for fire spread (Doblas-Reyes et al., 2021; De Marzo et al., 2023; Arias et al., 2024). In particular, several recent extreme fire seasons coincided with the 2020–2023 La Niña, which strongly affected moisture availability and fire activity throughout the Gran Chaco and its surroundings (Kumar et al., 2022; Naval Fernández et al., 2023; San Martín, 2024).

Although individual drivers of fire occurrence are increasingly well understood, the way these factors interact to determine the final size of fires in the Gran Chaco remains poorly quantified. Existing studies highlight the importance of drought, fuel moisture deficits and human land use in shaping ignition patterns and BA totals, yet the mechanisms that control how far fires spread under contrasting environmental and land-use contexts remain unresolved (San Martín et al., 2023; Vidal-Riveros et al., 2023, 2024; Bravo et al., 2025). Baumann et al. (2022) showed that deforestation pathways vary by actor and context, altering fuel configurations and fire–landscape interactions, San Martín et al. (2023) demonstrated that precipitation–BA relationships differ markedly across land-cover types, and Levers et al. (2024) projected that continuing agribusiness expansion could intensify fire impacts on ecologically and socially sensitive areas. Together, these studies reveal substantial spatial heterogeneity in fire dynamics, but none explicitly evaluate how meteorological variability interacts with landscape structure and human pressures to shape final fire size.

Some classification efforts have begun to map regional fire diversity but still overlook key atmospheric determinants. Vidal-Riveros et al. (2024) grouped Paraguayan Chaco fire regimes by severity, frequency and extent, while Naval-Fernández et al. (2025) used multivariate clustering of landscape attributes to delineate pyroregions in the Argentine Chaco. These approaches captured meaningful spatial patterns, yet they did not incorporate high-resolution meteorological conditions, limiting their ability to identify the atmospheric processes that influence fire expansion.

In summary, no study has yet combined meteorological anomalies, fire morphology metrics, and landscape context to assess how short-term weather and long-term environmental gradients determine fire size in the Gran Chaco. This gap is critical given the biome's diverse ignition sources, propagation through heterogeneous fuels, and sharp transitions in hydrology, vegetation structure, and land-use intensity.

Advances in satellite Earth Observation now allow for such integration. Global burned area (BA) products such as FireCCI51 offer consistent daily burned surface estimates at moderate spatial resolution (Chuvieco et al., 2020). Event-based datasets including FRY (Laurent et al., 2018; Mouillot et al., 2023) and the Global Fire Atlas (Andela et al., 2019) reconstruct individual fires and enable the analysis of attributes such as ignition date, duration, size and morphology (Moreno et al., 2021; Takacs et al., 2021; García et al., 2022). In this study, we use FRYv2.0, which integrates the FRYv1.0 pixel aggregation method with the latest version of FireCCI51 BA mapping (Lizundia-Loiola et al., 2020), and we combine it with environmental and meteorological datasets to quantify how different drivers influence fire size across the Gran Chaco.

Specifically, we aim to answer the following scientific questions:

(1) What are the primary fire--size characteristics and their frequency ~~in~~across the Gran Chaco between 2001 and 2022? (2) To what extent do meteorological conditions influence the size and expansion of ~~these~~individual fires? (3) Beyond weather, what roles do vegetation type, topography~~,~~ and human activity play in shaping fire size and fire occurrence across the region? (4) Which of these drivers best ~~explains~~explain the spatial and temporal variability ~~in~~of fire size ~~across~~among the different subregions of the Gran Chaco ~~subregions~~?

~~This study adds value by providing a spatially explicit, multiscale analysis of BA and individual fire events, clarifying fire size dynamics across landscapes from wet to arid ecosystems. By quantifying the relative contributions of climate, landscape, and human factors, it advances understanding of fire regimes in one of the world's most dynamic yet understudied deforestation and fire frontiers (Kuemmerle et al., 2017; Baumann et al., 2022; Vidal-Riveros et al., 2023; Levers et al., 2024; San Martín, 2024).~~

2 METHODS

2.1. Study area

The Gran Chaco is an extensive tropical and subtropical region of South America, covering approximately 1,100,000 km² (**Fig. 1**).

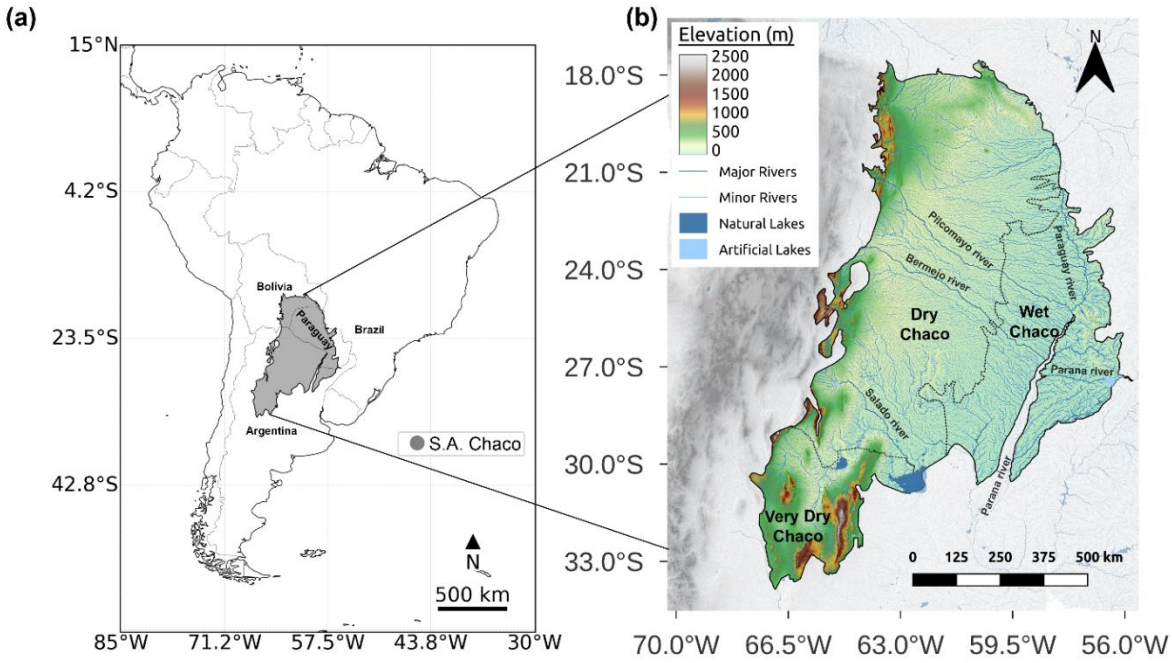

It contains the world's largest continuous dry tropical forest and extensive wetland systems (Bucher, 1982; Olson et al., 2001). In the literature, terminology varies with references to the South American Chaco, the Gran Chaco, or just Chaco. To avoid confusion, we only use Gran Chaco in this work.

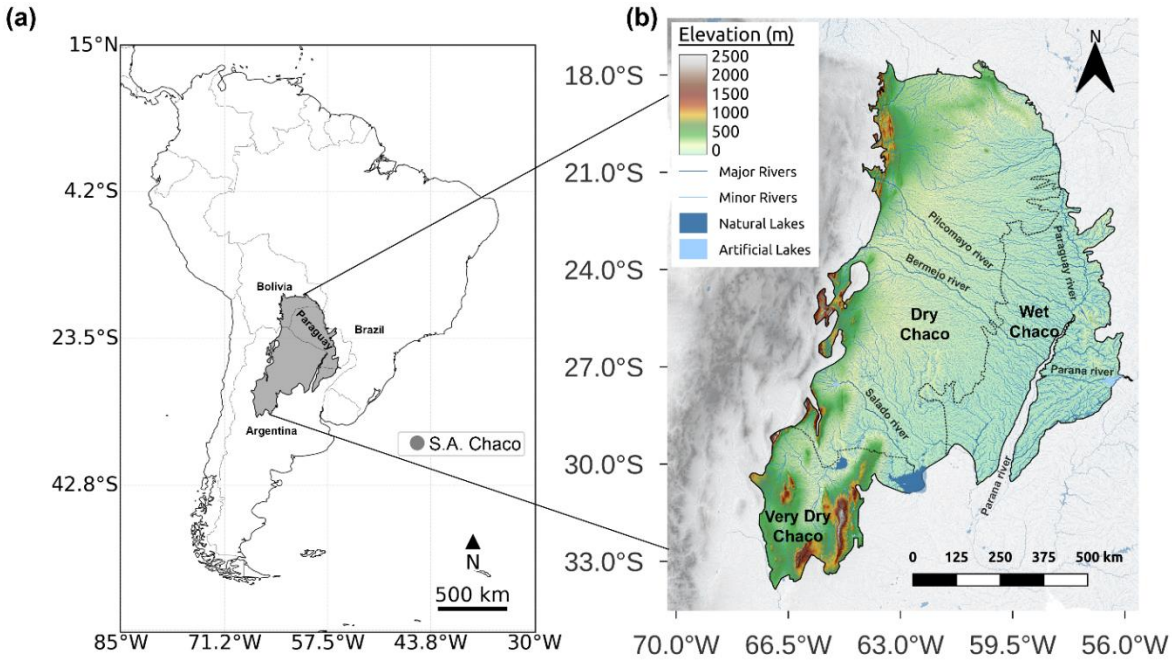

Fig. 1. The Gran Chaco location in South America (a) and its topography (b) with its different subregions, main rivers, and lakes. Based on Shuttle Radar Topography Mission (SRTM) at 90m (SRTM | NASA Earthdata, 2024) and HydroSHEDS (Lehner et al., 2008).

The region is mostly flat and low (<200 m.), with higher and undulating terrain towards the northeast limit (~500 m), the western Andean foothills (~2,000 m), and the southwestern Sierras de Córdoba (~2,900 m). Following Olson et al. (2001), we distinguish a humid eastern Wet Chaco from a drier western Dry Chaco, shaped by west–east gradients in precipitation, vegetation, and hydrology (Morello and Adámoli, 1968; Bucher, 1982; Ginzburg et al., 2005; Torrella and Adámoli, 2005). The Wet Chaco receives up to 1,800 mm/year and supports wetlands and palm savannas, while the Dry Chaco gets 300–800 mm/year and is dominated by drought-adapted forests and shrublands. Following Baumann et al. (2018), we identify a drier subregion in the southwest called the Very Dry Chaco, characterized by lower biomass, greater aridity, higher elevations, and distinct fire regimes. Its area is delimited using the borders of the Argentine provinces of Mendoza, San Luis, Córdoba, San Juan, and La Rioja.

The Gran Chaco forms part of the La Plata basin (Musser, 2024). Rivers such as the Pilcomayo, Bermejo, and Salado originate in the Andes, cross the Dry Chaco, and disperse into alluvial megafans, streams, and wetlands in the eastern Wet Chaco. This west–east hydrological gradient drives seasonal contrasts: in dry months, the Dry Chaco faces water scarcity, whereas the Wet Chaco retains permanent wetlands that sustain ecological processes and fauna (Naumann et al., 2023).

The region harbors exceptional biodiversity, with over 3,400 plant species and hundreds of vertebrates, many endemic (Redford et al., 1990; Bucher and Huszar, 1999; Nori et al., 2016).

Fire activity shows pronounced subregional contrasts across the Gran Chaco. The Wet Chaco presents a bimodal fire season, with peaks at the end of the warm wet season (late summer–autumn) and again at the end of the cold dry season (late winter–spring), while the Dry Chaco exhibits a unimodal pattern

restricted to the end of the cold dry season, towards late winter–spring (San Martín et al., 2023). Mean annual BA is about 15,000 km²/yr in the Wet Chaco and roughly 8,500 km²/yr in the Dry and Very Dry Chaco together, based on annual BA totals for 2001–2019. Despite its higher annual BA, the Wet Chaco burns repeatedly on much of the same land; about 57% of its burned surface experienced at least two fire events between 2001 and 2019, indicating high recurrence rather than continuous spatial expansion. In contrast, about 66% of the burned surface in the Dry Chaco represents one-time fires, with burns advancing over previously unburned forests. In this western subregion, fires typically follow deforestation rather than acting as the primary clearing mechanism (San Martín et al., 2023). These contrasts reflect the greater continuity of fine fuels and higher fire recurrence in the eastern Wet Chaco, compared with the more intermittent and fuel limited conditions characterizing the Dry and Very Dry Chaco.

~~The Gran Chaco is an extensive tropical and subtropical region of South America, covering approximately 1,100,000 km² (**Fig. 1**). It contains the world's largest continuous dry tropical forest and extensive wetland systems (Bucher, 1982; Olson et al., 2001). Terminology varies in the literature (South American Chaco, Gran Chaco, Chaco); here we use Gran Chaco for clarity.~~

~~The region is mostly flat (<200 m a.s.l.), with higher terrain in the northeast (to 500 m), Sierras de Córdoba (to 2,900 m), and Andean foothills (~2,000 m). Following Olson et al. (2001), we distinguish a humid eastern Wet Chaco from a drier western Dry Chaco, shaped by west–east gradients in precipitation, vegetation, and hydrology (Bucher, 1982; Ginzburg et al., 2005; Morello and Adámoli, 1968; Torrella and Adámoli, 2005). The Wet Chaco receives up to 1,800 mm/year and supports wetlands and palm savannas, while the Dry Chaco gets 300–800 mm/year and is dominated by drought-adapted forests. To refine this scheme, we follow Baumann et al. (2018) and designate a Very Dry Chaco in the southwest (Mendoza, San Luis, Córdoba, San Juan, La Rioja), characterized by lower biomass, greater aridity, higher elevations, and distinct fire regimes.~~

~~The Gran Chaco forms part of the La Plata basin (Musser, 2024). Rivers such as the Pilcomayo, Bermejo, and Salado originate in the Andes, cross the Dry Chaco, and disperse into megafans, streams, and wetlands in the eastern Wet Chaco. This west–east hydrological gradient drives seasonal contrasts: in dry months, the Dry Chaco faces water scarcity, whereas the Wet Chaco retains permanent wetlands that sustain ecological processes and fauna (Naumann et al., 2023).~~

~~The region harbors exceptional biodiversity, with over 3,400 plant species and hundreds of vertebrates, many endemic (Redford et al., 1990; Bucher and Huszar, 1999; Nori et al., 2016).~~

2.2 Datasets

2.2.1 Fire patches

~~In this study, we used FRYv2.0, a comprehensive global database dedicated to the functional traits (morphology, fire spread, and timing) of fire patches (FPs), to investigate fire dynamics and their~~

~~underlying drivers in the Gran Chaco. FRYv2.0 incorporates burned area (BA) data from the FireCCI51 dataset as well as from MODIS MCD64A1 in two different versions, with different temporal cut-offs of 6, 12, or 24 days, as described in Laurent et al. (2018). It offers medium resolution FPs covering the period from 2001 to 2022, including metrics for FPs, such as morphological traits (e.g., area, shape index), temporal traits (e.g., burn dates, duration), dynamic traits (e.g., rate of spread, fire radiative power, and burn severity), and land cover.~~

~~For this work, we selected the FRYv2.0 dataset based on FireCCI51 over the MODIS MCD64A1 version, due to the higher spatial resolution of the FireCCI51 input data (250 m compared to 500 m), its suitability for the heterogeneous Chaco landscapes, and its consistency with our previous FireCCI51-based analysis (San Martín et al., 2023), avoiding uncertainties from mixing datasets. The dataset is available at https://osf.io/rjvz5/files/osfstorage (last accessed on 10 June 2025).~~

In this study, we used FRYv2.0, a recent global database of fire patch (FP) functional traits (morphology, fire spread, and timing) to investigate fire dynamics and their underlying drivers in the Gran Chaco (Laurent et al., 2018; Mouillot et al., 2023). FRYv2.0 is an updated, second-generation version of the original FRY database that aggregates burned area (BA) pixels from the latest FireCCI51 dataset and from the MODIS MCD64A1 product into individual FPs using fixed temporal cut-offs of 6, 12, or 24 days to delimit the extent of a fire event or the onset of a new one. Compared with the original release, it provides extended patch-level information, including morphology (for example area, perimeter, shape index, core area), temporal traits such as burn dates and duration, dynamic traits such as rate of spread, fire radiative power (FRP) and severity indicators, and associated land cover. The FRYv2.0 morphological metrics describe the geometry and structure of each FP: *n_cell* quantifies the number of burned pixels from the input BA product that form the fire patch; area represents the total burned surface; the *shape index* captures deviations from a compact circular shape; the *core-area index* indicates the proportion of interior, non-edge area; *eccentricity* measures patch elongation; and the *perimeter-to-area ratio* characterizes boundary complexity and compactness.

Patch-level functional traits are computed only for patches composed of at least five burned pixels, to avoid geometric and orientational instability in very small patches. FRP-based diagnostics, including ignition timing derived from active-fire detections, are assigned only to patches larger than 100 ha (approximately sixteen FireCCI51 pixels). This ignition dating offers a more accurate estimate of fire onset than the default burn-date information in FireCCI51 or MODIS MCD64A1, which relies on the day of first BA detection.

For this work, we selected the FRYv2.0 version based on FireCCI51 rather than the version based on the MODIS MCD64A1 BA product, because the FireCCI51 input has higher spatial resolution (250 m compared to 500 m), provides better spatial detail for the heterogeneous landscapes of the Gran Chaco, and ensures consistency with our previous FireCCI51 based analysis (San Martín et al., 2023), thus

avoiding additional uncertainty from mixing BA products. The FRYv2.0 FireCCI51-based dataset used here is publicly available at https://osf.io/rjvz5/files/osfstorage (last accessed on 10 June 2025).

2.2.2 Meteorological Data

To study meteorological and climate time series in the region, we used the ERA5-Land global reanalysis dataset focused on land surface variables, developed by the European Centre for Medium-Range Weather Forecasts (ECMWF) ~~(Muñoz Sabater et al., 2021).~~(Muñoz-Sabater et al., 2021). It provides high-resolution data for land–atmosphere interactions, designed to improve the ERA5 dataset by offering finer detail (0.1° instead of 0.25° spatial resolution) for variables affecting the land surface. The product is available in the Copernicus Data Store (CDS) in NetCDF at https://cds.climate.copernicus.eu/cdsapp#!/dataset/reanalysis-era5-land (last accessed on 30 May 2024). We downloaded hourly data arrays covering January 2001 through January 2023.

2.2.3 Environmental and Anthropogenic Data

We compiled ~~multiple~~several spatial datasets ~~to~~that represent ~~landscape~~biophysical conditions and human-related drivers ~~of~~relevant to fire activity~~.~~ in the Gran Chaco.

Topography was ~~derived~~obtained from the ~~Shuttle Radar Topography Mission (~~NASA SRTM v3 product (https://srtm.csi.cgiar.org, accessed 26 May 2025). This product provides a 3 arc-second (approximately 90 m) digital elevation model ~~at 30 m resolution (https://srtm.csi.cgiar.org, accessed 26 May 2025) and resampled to 0.01° (~1 km).~~(DEM) in WGS84 geographic coordinates. Slope ~~was~~ and aspect were calculated from ~~the elevation surface~~this DEM using ~~standard GIS tools.~~the Horn algorithm as implemented in the *richdem TerrainAttribute* function, which estimates local gradients over 3 by 3 cells (Horn, 1981).

~~Land cover (LC) was obtained from the ESA Climate Change Initiative Moderate Resolution Land Cover (ESA CCI MRLC) product (https://cds.climate.copernicus.eu/datasets/satellite-land-cover, accessed 26 May 2025), reclassified into groups relevant to the Gran Chaco (e.g., forests, shrublands, grasslands, seasonally flooded herbaceous vegetation) for 2001–2022.~~

~~Human pressure variables included population density from the Gridded Population of the World v4 (CIESIN, 2017; https://www.earthdata.nasa.gov/data/projects/gpw, accessed 26 May 2025) and road density from OpenStreetMap networks (https://www.openstreetmap.org, accessed 26 May 2025) calculated via kernel density estimation.~~

~~Livestock density came from the Gridded Livestock of the World v4 (https://dataverse.harvard.edu/dataverse/glw_4, accessed 26 May 2025), resampled to match the analytical resolution.~~

~~Soil properties (bulk density, sand content, and organic carbon at 0–5 cm depth) were obtained from SoilGrids250m (Hengl et al., 2017; https://soilgrids.org, accessed 26 May 2026).~~

Land cover (LC) was obtained from the ESA Climate Change Initiative Moderate Resolution Land Cover product (CCI MRLC; https://cds.climate.copernicus.eu/datasets/satellite-land-cover, accessed 26 May 2025). This product provides annual maps at 300 m spatial resolution for the period 1992 to 2022. We selected CCI MRLC because its resolution is appropriate for the regional extent of this study, which covers more than 1,100,000 km^2. The product has undergone extensive validation, is widely used in regional land surface studies, and ensures consistency with our previous analyses in the Gran Chaco (Defourny et al., 2023; Harper et al., 2023; San Martín et al., 2023). Using MapBiomas Chaco would have required a dedicated comparison and validation exercise that was beyond the scope of this fire size study.

Fuel accumulation before each fire was characterized using MODIS LAI at 500 m resolution and 8-day intervals. We used MOD15A2H (Terra) for 2001 to 2002 and MCD15A2H (Terra and Aqua combined) for 2002 to 2023. Only observations with quality level 0 were retained. For each fire, we extracted all LAI values from MODIS pixels that overlapped the fire patch. To represent the accumulated biomass that could contribute to fire spread, we defined the pre-fire period as the interval between 1 August of the year before the fire and the ignition date. This window captures the seasonal minimum at the end of the winter dry season and the entire subsequent growing season. A 4-step rolling mean with a minimum of one valid value was applied to reduce high frequency noise. The final pre-fire LAI value for each fire patch was the mean LAI across this August to ignition interval. This variable, which we refer to as the mean LAI of the previous growing season, served as a proxy for the biomass accumulated before the fire.

Soil properties were obtained from the SoilGrids250m database. The variables used were soil organic carbon at 0 to 5 cm depth, sand fraction, and bulk density. We used the one-kilometer aggregated layers provided by *SoilGrids* and computed means for each fire patch.

Population density was taken from the Gridded Population of the World version 4 (GPWv4) (CIESIN, 2017; https://www.earthdata.nasa.gov/data/projects/gpw, accessed November 25, 2025). The native resolution of this product is approximately 30 km. Since the dataset was not modified, population values were assigned to each fire patch using nearest neighbor extraction.

Livestock density was obtained from the Gridded Livestock of the World version 4 (GLWv4; https://dataverse.harvard.edu/dataverse/glw_4, accessed November 25, 2025). This dataset is available at roughly 10 km resolution. The original values were used as provided. For each fire patch, livestock density (number of cattle / km^2) was summarized using zonal means.

Road density was derived from two global road network datasets to account for uncertainties in road mapping, particularly the incomplete representation of informal, unpaved or irregular roads in some regions of the Gran Chaco. We used two independent sources: OpenStreetMap (OSM; https://www.openstreetmap.org, accessed November 25, 2025), which is community-curated and

generally more complete in populated areas, and the Microsoft Bing AI Global Roads dataset (MS; https://github.com/microsoft/RoadDetections, accessed November 25, 2025), which is algorithmically extracted from high-resolution satellite imagery and tends to provide broader coverage in rural and sparsely populated landscapes. For all main analyses, road density was computed from the OSM dataset, while the MS product was used only in a sensitivity experiment to evaluate the robustness of road-related effects (see *Section 2.3.9*).

Roads were maintained in vector format and intersected with a regular 0.03° grid (~3 km), projected onto an equal-area coordinate system for accurate calculations of road length and cell area. Road density (km km^{-2}) was computed for each grid cell, and fire patches were assigned an area-weighted mean value based on all overlapping cells. The 0.03° resolution was selected after testing coarser and finer grids, providing the best trade-off between capturing road density within each patch and preserving the surrounding spatial context while maintaining consistency across both road datasets. Using both products in this way ensured that the inferred influence of human accessibility on fire behavior was not dependent on a single mapping dataset, while keeping OSM as the reference road layer for the core RF configurations.

2.2.3 Climate Oscillations

To account for the influence of large-scale climate variability, we included the Multivariate El Niño–Southern Oscillation (ENSO) Index version 2 (MEI.v2), developed by NOAA's Physical Sciences Laboratory. The MEI.v2 time series was obtained from NOAA PSL at https://psl.noaa.gov/enso/mei/ (last accessed 26 May 2025).

2.3 Data processing and analysis methods

2.3.1 Fire Weather Index (FWI)

We built an ERA5-Land-based Canadian Fire Weather Index (FWI; ~~Van Wagner, 1987)~~Van Wagner, 1987) dataset for the Gran Chaco at 0.1° resolution and daily time steps. We converted hourly accumulated precipitation to hourly rainfall by differencing successive steps and ~~summed~~summing totals from 15 UTC (day D-1) to 15 UTC (day D), matching the FWI daily window and corresponding to local noon~~.~~ in most of the Gran Chaco. We applied this fixed 15 UTC cutoff to the full region to avoid inconsistencies ~~from~~caused by varying national time zones and daylight-saving changes.

We extracted daily meteorological inputs— (i.e., air temperature, relative humidity, wind speed at local noon, and 24-h precipitation—) to compute the six FWI sub-indices: Fine Fuel Moisture Code (FFMC), Duff Moisture Code (DMC), Drought Code (DC), Initial Spread Index (ISI), Build-Up Index (BUI), and FWI. We performed calculations with an adapted version of the *FireDanger* Python package

(https://github.com/steidani/FireDanger) compatible with *xarray* and ~~netCDF~~*NetCDF*, including pixel-level day length for DMC and hemisphere-specific drying factors for DC.

We initialized the system on 1 January 1981 using Copernicus ERA5–FWI moisture codes at 0.25° ~~(Vitolo et al., 2020)~~(Vitolo et al., 2020) interpolated to 0.1°. ~~For anomaly analysis, we restricted the time series to 2001–2022 to match satellite-based burned area (BA) records and calculated daily climatologies for all variables and indices using 2001–2020 as the baseline.~~

2.3.2 Land Cover processing

For this work, the original classes of CCI MRLC were grouped into eight categories relevant to the Gran Chaco fire regime. These categories included tree cover, shrublands, grasslands, seasonally flooded herbaceous vegetation, croplands, two mixed mosaics containing combinations of herbaceous and woody vegetation, and an extra class we called "Others", grouping the remaining underrepresented classes in the Gran Chaco. For each FP we extracted the fractions of LC at the year of fire ignition, and these fractions were used to calculate the following landscape heterogeneity indices:

In order to quantify the landscape heterogeneity within each FP and assess how the mix and spatial balance of LC types influence fire outcomes, we calculated the Shannon diversity index (*H*) and Pielou's evenness (*E*). They were computed as follows:

(**Eq. 1**) Shannon Diversity Index (Shannon, 1948):

$$H = -\sum_{i=1}^{m} p_i \log(p_i)$$

Where *m* is the number of land cover classes present in the fire patch, p_i is the proportion of land cover type i, and the sum includes all classes with $p_i > 0$.

(**Eq. 2**) Pielou's evenness (Pielou, 1966):

$$E = \frac{H}{\log(m)}$$

Where *H* is the Shannon Diversity Index and *m* is the number of land cover classes present in the fire patch.

2.3.3 Wind indices

Using ERA5-Land data, we calculated for each FP a metric specifically designed to capture the role of strong, persistent winds in shaping fire behavior: the Extreme Wind Directionality Index (*EW_dir_index*). This index measures both how often extreme winds occurred and how steady their direction was.

The first component, fraction of extreme-wind days (*EW_frac*), is the proportion of burning days when the daily maximum wind speed exceeded 25 km h^{-1}:

(**Eq. 3**) *Extreme Wind Fraction Index*:

$$EW\_frac = \frac{EW}{N}$$

where *EW* is the number of days with extreme winds and *N* is the total fire duration (days). High values indicate that strong winds occurred on many burning days.

The second component, wind direction steadiness (*wind_dir_R*), reflects how consistent the wind direction was across the fire's duration (N). Each day's mean wind direction (θ_i, in radians) is represented as a unit vector, summed across all days, and normalized by the fire duration:

(**Eq. 4**) *Wind Directionality Index*:

$$wind\_dir\_R = \frac{\sqrt{\left(\sum_{i=1}^{N}\cos\theta_i\right)^2+\left(\sum_{i=1}^{N}\sin\theta_i\right)^2}}{N}$$

Values near 1 mean that winds blew in a stable direction throughout the event, while values near 0 mean that wind directions shifted substantially from day to day.

The *EW_dir_index* is the product of *EW_frac* and *wind_dir_R*:

(**Eq. 5**) *Extreme Wind Directionality Index*:

$$EW\_dir\_index = EW\_frac \times wind\_dir\_R$$

It reaches high values only when strong winds occur on many burning days and blow consistently from the same direction, identifying fires likely driven by sustained, unidirectional wind conditions.

2.3.4 Burned Area vs Fire Counts

To examine the interannual relationship between fire counts and total BA, we compared annual BA and annual fire counts for each of the three Gran Chaco subregions using FRYv2.0. For every year in 2001–2022, total BA was computed as the sum of the burned surface of all fire patches within each subregion, while fire counts were obtained as the number of individual patches whose ignition date fell within that year. We then fitted simple linear regressions between annual BA and annual fire counts for each subregion to quantify how ignition frequency explains interannual variability in BA and to assess whether this relationship differs among the subregions and between the wet and dry seasons.

2.3.5 Fire size classification

To ~~better~~ characterize how fires of different magnitudes contribute to overall fire activity ~~across~~in the Gran Chaco, we classified all ~~fire polygons (~~FPs~~)~~ from FRYv2.0 into six size categories~~, ranging from very small fires (<1 km²) to gigafires (>1000 km²), following and adapting the~~. Fire events can be classified according to multiple criteria, including behavior (rate of spread, intensity), ecological impact (severity), structure (number of ignition points), or final extent. Because this study focuses specifically on the determinants of final fire size, we adopted a size-based classification system. This choice allows

us to map directly the response variable of interest and to interpret the climatic, landscape, and anthropogenic factors that control it.

To avoid ad-hoc or region-specific thresholds, we followed the standardized fire-size typology proposed by Linley et al. ~~(2022). We used this to assess both the frequency and relative contribution of different fire sizes across regions and seasons~~(2022), who conducted the first global assessment aimed at harmonizing terminology for large fires. They argue that terms such as "*megafire*" or "*large wildfire*" had been used inconsistently across disciplines and agencies, often referring to different orders of magnitude depending on national contexts or management traditions. They show that this lack of standardization complicates cross-regional comparison and the interpretation of extreme events. To resolve this, they propose clear, size-based definitions applicable worldwide: megafires as events with BA > 10,000 ha (100 km²), gigafires > 100,000 ha (1000 km²), and terafires > 1,000,000 ha (10,000 km²). Their framework is explicitly designed for satellite-derived BA products, including those used to build FRY, and provides a consistent basis for global and regional analyses.

~~2.3.3~~Using Linley's typology ensures that extreme fire classes in the Gran Chaco are comparable to global assessments and avoids relying on operational thresholds used in some countries (e.g., 40,000 ha) that lack a physical or ecological rationale. At the same time, the empirical distribution of FRYv2.0 patch sizes in the Chaco is strongly right-skewed, with most events being small and only a few exceeding the megafire threshold. For this reason, and to retain regional relevance, we adapted Linley's standardized thresholds into operational size classes suitable for the Gran Chaco, while preserving the key Linley cut-offs at 100 km² and 1000 km². FRYv2.0 imposes a practical lower limit on measurable patch size: functional traits are computed only for patches composed of at least five FireCCI51 pixels (~0.3 km²), and FRP-based diagnostics, including ignition dating, are provided only for patches larger than 100 ha (1 km²; see *Section 2.2.1*). This naturally defines the smallest reliable category in our system. The resulting scheme spans from a "very small" class (0–1 km²), which is more uncertain because FRY patches in this range often lack complete geometric or FRP-based diagnostics, through small (1–5 km²), medium (5–10 km²), and large (10–100 km²) events, up to megafires (100–1000 km²) and gigafires (>1000 km²). No fire in the Gran Chaco exceeded 10,000 km², and therefore the terafire class defined by Linley et al. is not used in this work.

2.3.6 Gridded burned area

To enable a ~~spatio-temporal~~spatiotemporal comparison between fire activity from FRYv2.0 ~~polygons~~fire patches and meteorology, we developed a pipeline to transform the FP-based data into a monthly gridded product at 0.1°, matching the ERA5-Land grid ~~-~~(**Fig. 2**).

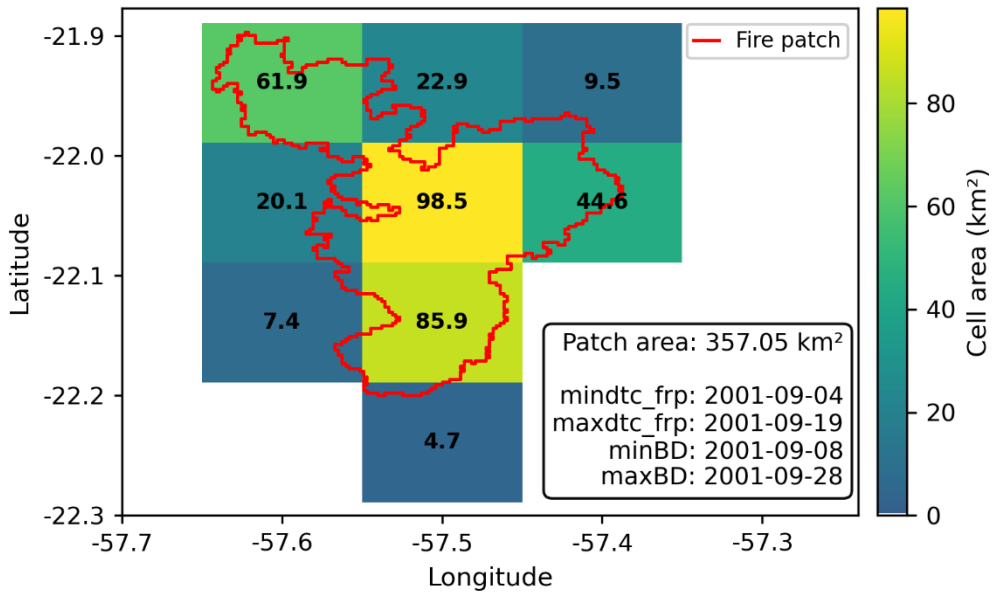

Fig. 2. Example of ~~a~~one FRY ~~polygon~~fire patch (red line) over the gridded FRY dataset. Each grid cell at 0.1º is assigned the burned area corresponding to the total fraction of the ~~polygon~~patch that overlaps it. The values printed over each grid cell correspond to these values.

The temporal assignment of fires to months followed a hybrid strategy: where MODIS-derived hotspot detection dates (*mindtc_frp* and *maxdtc_frp*) were available in a given FP (typically absent in very small FPs) they were used. Both FireCCI51- and MODIS-based versions of FRYv2.0 include these hotspot date variables when available for the FP. When hotspot dates were missing, we used the FireCCI51-derived burn dates (*minBD* and *maxBD*), which are based on surface reflectance changes and are available for all FPs. For FPs spanning multiple months, we assigned the fire to the month in which it started, unless its duration in a subsequent month exceeded that of the starting month by more than two days.

Each FP was rasterized ~~over the ERA5~~on a 0.01° grid by intersecting it with individual cells. The intersected area in square kilometers was computed using the WGS84 ellipsoid model. These contributions were aggregated per cell and per assigned month to build a three-dimensional array of monthly BA (*lat x lon x time*). A similar procedure was implemented for fire counts, using ignition (first detection) coordinates ~~when available~~and dates. Each FP's fire ignition coordinate was allocated to the closest cell in the 0.1º grid. The resulting monthly gridded dataset included two variables: BA and counts.

To compute monthly BA anomalies, we derived pixel-level monthly climatologies for the period 2001–2020 from the gridded BA dataset. Anomalies were defined as the difference between each monthly BA value and the corresponding monthly climatological mean, following the same temporal normalization applied to meteorological variables.

2.3.4~~7~~ Anomalies and climatologies

For all ERA5-Land variables, as well as the FWI index and its sub-indices, we computed pixel-level daily climatologies using the 2001–2020 mean as the baseline. Meteorological anomalies were then defined as the daily deviation from this climatology and subsequently aggregated to monthly values to match the temporal scale of the BA analysis.

To compute monthly BA anomalies, we derived pixel-level monthly climatologies for the period 2001–2020 from the gridded BA dataset. Anomalies were defined as the difference between each monthly BA value and the corresponding monthly climatological mean, following the same temporal normalization applied to meteorological variables. This anomaly-based formulation was used only for the correlation analysis with FWI anomalies and not for any other statistical or spatial analyses in the manuscript.

For the specific analysis comparing monthly BA anomalies with monthly FWI anomalies, only pixels with at least four fire-active months (BA > 0) during 2001–2022 were retained to avoid artefacts from sparsely populated or highly skewed anomaly series. Correlations were computed using both Pearson's coefficient and Spearman's rank coefficient.

We did not apply an FWI95-based threshold or similar fixed-percentile metrics, as these are less comparable across the strong climatic gradient of the Gran Chaco and may artificially amplify or dampen fire–weather relationships depending on local baseline conditions. Using pixel-level anomalies instead allows each location to be evaluated relative to its own climatology, yielding a spatially consistent and locally meaningful basis for comparison.

2.3.8 Fire-weather types

~~We classified fire patches (FPs) into three groups based on associated atmospheric conditions using the K-means clustering algorithm (MacQueen, 1967) in scikit-learn v1.3. This approach follows prior applications in fire studies (Ruffault et al., 2016, 2020; Vidal-Riveros et al., 2024) and aimed to identify distinct fire-weather types and assess their influence on fire size and shape.~~

~~We~~We classified fire patches (FPs) into three groups based on associated atmospheric conditions using the K-means clustering algorithm (MacQueen, 1967) in *Python's scikit-learn v1.3*. This approach follows prior applications in fire studies (Ruffault et al., 2016, 2020; Vidal-Riveros et al., 2024) and aimed to identify distinct fire-weather types (FWTs) and assess their influence on fire size and shape.

For this clustering analysis, we retained only ~~FPs~~fire patches between 1 and 100 km² (N = ~~76,263) to reduce biases~~ 78,052). At the lower end, this choice is consistent with the construction of the FRYv2.0 database, where the FP functional traits are computed only for patches composed of at least five burned pixels and smaller patches are filtered out because their geometry and orientation are considered unreliable (see *Section 2.2.1*). In addition, FRP based diagnostics, including ignition timing derived from ~~very small or very large~~active fire detections, are only provided for FPs larger than 1 km² (approximately 16 FireCCI51 pixels), so the smallest events~~.~~ lack both robust geometric traits and FRP timing

information. At the upper end, fires larger than 100 km² were excluded from the K-means analysis. In addition to their low frequency, these very large, long duration patches often span heterogeneous landscapes and experience several distinct weather situations over their burning period, so the associated ERA5-Land and FWI time series mix conditions from distant locations and different days. This mixing makes the patch-averaged meteorological descriptors difficult to interpret as a single coherent FWT and would likely introduce substantial biases in the clustering and in the Random Forest (RF) models used later to analyze fire size drivers (see *Section 2.3.9*).

For each FP within the 1–100 km² range, we extracted daily ERA5-Land meteorological data and ~~generated~~the computed FWI time series from 7 months before ignition to 7 months after~~. Two~~, and then built two feature sets~~ were built:~~, one ~~for~~representing pre-fire conditions and one ~~for during fire~~representing conditions~~.~~ during the fire.

~~For the *Pre-Fire* set, we used normalized anomalies of 2-m air temperature, 10-m wind speed, relative humidity (RH), drought code (DC), and duff moisture code (DMC) (Ruffault et al., 2020). Pre-fire values were calculated as the 3-day mean from ignition day (D) to D-2 to limit detection date bias (Lizundia-Loiola et al., 2020; Pettinari et al., 2021) while avoiding noise from longer lags.~~

For the *Pre-Fire* set, we used normalized anomalies of 2-m air temperature, 10-m wind speed, relative humidity (RH), drought code (DC), and duff moisture code (DMC) (Ruffault et al., 2020). Pre-fire values were calculated as the 3-day mean from ignition day (D) to D-2 to limit detection-date bias (Lizundia-Loiola et al., 2020; Pettinari et al., 2021) while avoiding noise from longer lags.

For the *During-Fire* set, we computed the same variables averaged over the fire's duration and added ~~a metric specifically designed to capture the role of strong, persistent winds in shaping fire behavior:~~ the *Extreme Wind Fraction Index* and the *Extreme Wind Directionality Index* ~~(*EW_dir_index*). This index measures both how often extreme winds occurred and how steady their direction was.~~

~~The first component, fraction of extreme wind days (*EW_frac*), is the proportion of burning days when the daily maximum wind speed exceeded 25 km h^{-1}:~~

~~**(Eq. 1)**:~~

$$\text{EW\_frac} = \frac{EW}{N}$$

~~where *EW* is the number of days with extreme winds and *N* is the total fire duration (days). High values indicate that strong winds occurred on many burning days.~~

~~The second component, wind direction steadiness (*wind_dir_R*), reflects how consistent the wind direction was across the fire's duration (N). Each day's mean wind direction (θ_i, in radians) is represented as a unit vector, summed across all days, and normalized by the fire duration:~~

~~**(Eq.**~~, described in *Section 2*~~)~~:

$$\text{wind\_dir\_R} = \frac{\sqrt{\left(\sum_{i=1}^{N}\cos\theta_i\right)^2 + \left(\sum_{i=1}^{N}\sin\theta_i\right)^2}}{N}$$

~~Values near 1 mean winds blew in a stable direction throughout the event, while values near 0 mean wind directions shifted substantially from day to day.~~

~~The *EW_dir_index* is the product of *EW_frac* and *wind_dir_R*:~~

~~(**Eq.** .3)~~:.3.

$$EW\_dir\_index = EW\_frac \times wind\_dir\_R$$

~~It reaches high values only when strong winds occur on many burning days and blow consistently from the same direction, identifying fires likely driven by sustained, unidirectional wind conditions.~~

All variables in both sets were standardized ~~(mean = 0, σ = 1)~~ before clustering~~.~~ (mean = 0, σ = 1). The resulting data matrix ~~(nnn fires × ppp variables)~~ was clustered with k = 3, squared Euclidean distance, *k-means++* initialization, 50 random restarts, and a convergence tolerance of 10^{-4}. We retained three clusters based on a prior hypothesis (wind-driven, drought-driven, and neutral), an elbow in the within-cluster sum-of-squares curve, and a peak in the silhouette coefficient at k = 3.

Cluster labels were assigned by interpreting centroid positions in principal component space and examining the temporal evolution of variables (**Fig. ~~A1~~S1**). Robustness was assessed using mean silhouette coefficients and their distribution across clusters. The first two principal components explained more than 60 % of the variance and clearly separated cluster centroids.

2.3.~~5~~9 Fire size drivers

To investigate the role of environmental and anthropogenic variables in ~~shaping~~determining fire ~~activity~~size, we extracted a diverse set of FP-level potential predictors encompassing topographic, climatic, anthropogenic, vegetation, and landscape heterogeneity dimensions. These variables, listed in **Table 1**, were used as inputs in the ~~Random Forest (~~RF~~)~~ models to assess their relative importance in explaining fire size ~~and frequency~~.

~~**Table 1.** Polygon-level predictor variables used in the Random Forest models, grouped by variable type.~~

~~**Category**~~	~~**Variables**~~
~~**Topographic**~~	~~Mean Slope (%)~~ ~~Mean Elevation (m)~~
~~**Climatic (during fire)**~~	~~Precipitation (mm)~~ ~~Maximum Wind Speed (km/h)~~ ~~Extreme Wind and Direction Index (EW_dir_index)~~ ~~Extreme Wind Days Fraction (EW_frac)~~
~~**Anthropogenic**~~	~~Cattle Density (heads/km²)~~ ~~Road Density (km/km²)~~ ~~Population Density (p/km²)~~

Vegetation productivity	LAI for previous growing season (MODIS-derived)
Land Cover Composition	Flooded Herbaceous vegetation (%) Tree Cover (%) Shrublands (%) Trees/Shrubs/Herbs Mosaics (%) Natural/Croplands Herbaceous Mosaics (%)
Landscape Heterogeneity	Land Cover Diversity (Shannon Index, H) Land Cover Evenness (Pielou Index, E)

The Shannon diversity (*H*) and Pielou's evenness (*E*) were computed as follows:

(Eq. 4) Shannon Diversity Index (Shannon, 1948):

$$H = -\sum_{i=1}^{m} p_i \log(p_i)$$

Where *m* is the number of land cover classes present in the polygon, p_i is the proportion of land cover type i, and the sum includes all classes with $p_i > 0$.

(Eq. 5) Pielou's evenness (Pielou, 1966):

$$E = \frac{H}{\log(m)}$$

Where *H* is the Shannon Diversity Index and *m* is the number of land cover classes present in the polygon.

Once all potential predictor variables were derived, we trained RF models using a set of 17 explanatory variables to analyze the drivers of fire behavior, using the variable *n_cell* from the FRY dataset as the response variable. This variable represents the number of FireCCI51 pixels within each FP and was preferred over polygonpatch-based *area* due to the latter's dependency on latitude, which introduced artificial discontinuities. In contrast, *n_cell* provided a discrete and spatially consistent proxy for BA, improving model stability and interpretability.

We implemented 12 primary RF models across five configurations: (i) a global model using all 76,263 polygons (the 78,052 fire patches used for the clustering analysis (patches with area between 1– and 100 km^2);^{2}), (ii) three subregion-specific models for the Wet, Dry, and Very Dry Chaco;, (iii) two seasonal models based on ignition season (wet vs dry);), and (iv) two sets of three cluster-based models (pre-fire and during-fire conditions) derived from the meteorologicalFWT classification (see *Section 2.3.*48).

Table 1. All models were trained using the *ranger* R package (Wright and Ziegler, 2017) with quantile regression forests (Meinshausen, 2006). We used 500 trees, a minimum node size of 5, variance-based importance, and the Poisson split rule, with 4 variables considered at each split. Feature selection

~~included correlation filtering (r > 0.8 threshold) and preliminary importance scores. Each model was trained on 75% of the data and validated on the remaining 25%. We evaluated feature contributions using SHAP (SHapley Additive exPlanations) values.~~

Target and potential predictor features extracted from each FRY fire patch within the Gran Chaco region, grouped by variable types. These features were used for the Random Forest models trained in this work.

Category	Variables
Fire Size (target feature)	Number of pixels within the fire patch (250 m pixels from FireCCI51)
Topography	Mean Slope (%) Mean Elevation (m)
Meteorology (during fire mean)	Precipitation (mm) Maximum Wind Speed (km/h) Extreme Wind and Direction Index (EW_dir_index) Extreme Wind Days Fraction (EW_frac)
Anthropogenic proxies (year of fire ignition)	Cattle Density (heads/km²) Road Density (km/km²) Population Density (p/km²)
Vegetation productivity (previous growing season)	LAI for previous growing season (MODIS-derived)
Land Cover Composition (year of fire ignition)	Flooded Herbaceous vegetation (%) Tree Cover (%) Shrublands (%) Trees/Shrubs/Herbs Mosaics (%) Natural/Croplands Herbaceous Mosaics (%)
Landscape Heterogeneity (year of fire ignition)	Land Cover Diversity (Shannon Index, H) Land Cover Evenness (Pielou Index, E)

All models were trained using the *ranger* R package (Wright and Ziegler, 2017) with quantile regression forests (Meinshausen, 2006). We used 500 trees, a minimum node size of 5, variance-based importance, and the Poisson split rule, with 4 variables considered at each split. Feature selection included correlation filtering ($r > 0.8$ threshold) and preliminary importance scores. Each model was trained on 75% of the data and validated on the remaining 25%. We evaluated feature contributions using SHAP (SHapley Additive exPlanations) values.

In addition to these primary configurations, we trained two diagnostic RF models to assess the robustness of our results. First, a "No Topography" model was built by removing elevation and slope from the predictor set while keeping all other variables and settings identical to the Full Chaco configuration. Second, an "MS Roads" model replaced the OSM-based road-density layer with the MS-based road density, again using the same sample of fire patches, hyperparameters, and training / test split as the Full Chaco RF. These sensitivity experiments were analyzed with the same SHAP-based diagnostics as the primary models and were used to evaluate whether the RF results were robust to changes in the predictor set and road-data source.

3 RESULTS

3.1 Burned area and ignitions

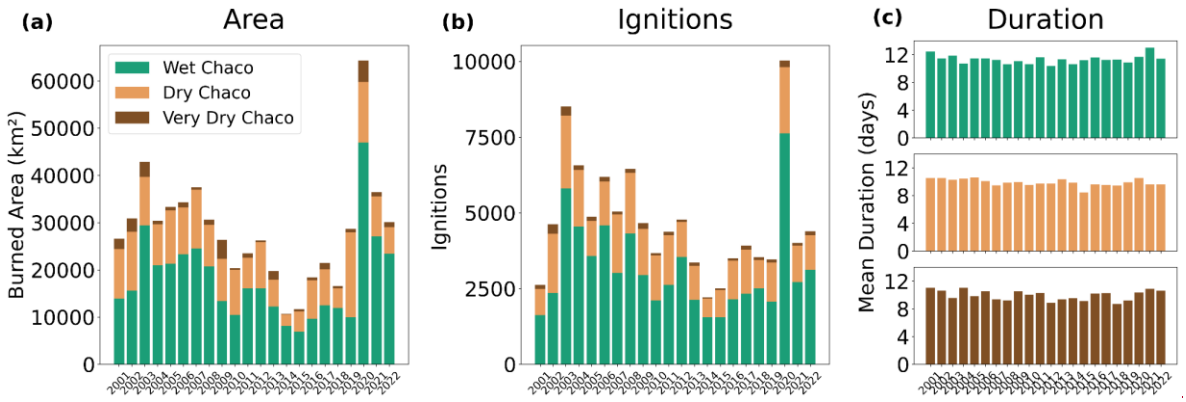

We examined the interannual variability of burned area (BA), fire counts, and mean fire duration across the Gran Chaco between 2001 and 2022 (**Fig. 3**~~,~~**; Fig. S3**). To complement these indicators, we quantified the relationship between total BA and annual fire counts for each subregion and season, using linear correlations (**Fig. S2**).

The time series reveals a sustained decrease in annual fire counts and BA from the early 2000s to the late 2010s, followed by a pronounced peak in 2020–2021. Because the observational window begins in 2001, it is difficult to determine whether the downward phase reflects a longer-term trend or a segment of decadal variability. These two peak years also show the largest BA of the record, particularly in the Wet and Dry Chaco, and stand out clearly relative to the preceding trajectory.

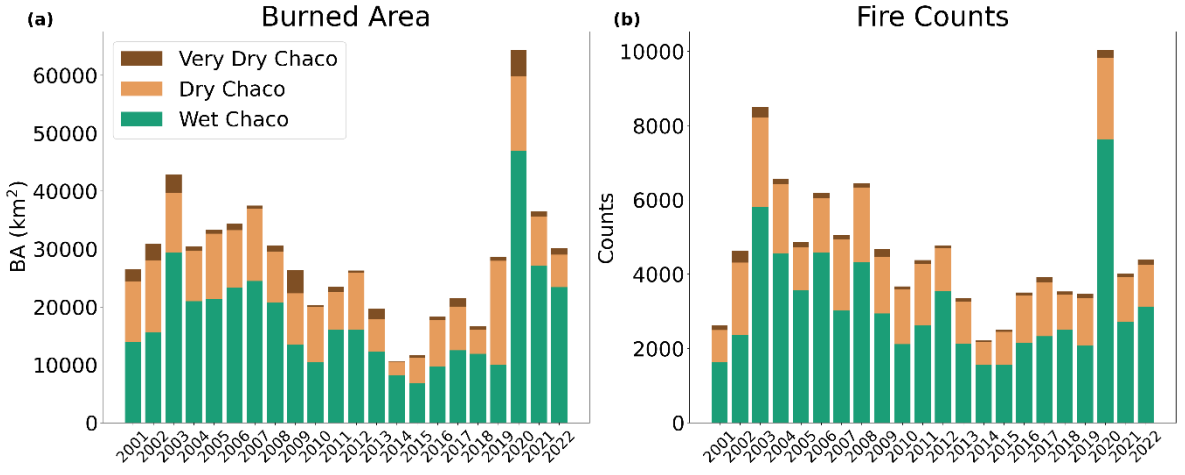

Fig. 3. Interannual evolution of fire activity in the Gran Chaco from 2001 to 2022, derived from FRYv2.0 fire patches. (a) Total annual burned ~~areas (a), ignitions~~ area and (b~~), and mean~~) total annual fire ~~durations (c), between 2001 and 2022 in~~counts, with stacked bars showing the contributions of the Wet, Dry, and Very Dry Chaco ~~regions. Extracted from FRYv2.0~~subregions.

~~We examined the interannual relationship between total burned area (BA) and the number of fire polygons (FPs) across the Chaco (**Fig. 3**). Overall, BA and ignition counts show a~~ BA and fire counts showed a broadly positive ~~association, though~~relationship, but with substantial regional and seasonal ~~variability~~differences. In the Wet Chaco, ~~strong correlations~~ BA and fire counts were ~~found~~ strongly correlated in both wet and dry seasons (R^2 = 0.96 and 0.91; **Fig. S2**), indicating ~~fire extent~~that interannual BA variability is largely ~~proportional to ignition frequency (**Fig. A2**).~~ explained by the annual number of fire patches rather than by individual fire sizes. Mean fire duration remained stable (approximately 10–12 days; **Fig. S3**).

The Dry Chaco ~~also showed~~exhibited a high wet-season correlation between BA and fire counts (R^2 = 0.87; **Fig. S2**), but a much weaker dry-season ~~one~~relationship (R^2 = 0.45~~), suggesting a greater role of other drivers in the latter.~~). This implies that, during the dry season, fluctuations in BA are not tightly linked to fire counts, consistent with a larger contribution of size extremes. Fire duration was also stable through the period (**Fig. S3**).

In the Very Dry Chaco, wet-season fires were ~~sparse and weakly correlated with BA~~ infrequent and showed almost no relationship between BA and fire counts (R^2 = 0.11~~), while a stronger correlation emerged in the dry season~~; **Fig. S2**). In contrast, dry-season BA correlated strongly with the number of fires (R^2 = 0.78). Mean fire duration ~~remained~~was relatively ~~stable over time, implying that~~ constant, with no clear interannual ~~variability in~~ trend (**Fig. S3**).

Overall, fire duration exhibited limited variation across subregions (**Fig. S3**), reinforcing that BA ~~is~~fluctuations were controlled primarily ~~linked to ignition frequency~~by changes in fire counts and the distribution of fire ~~size~~sizes, rather than by changes in the duration of individual fires.

3.2 Land Cover and Fire size distribution~~ and regional differences~~

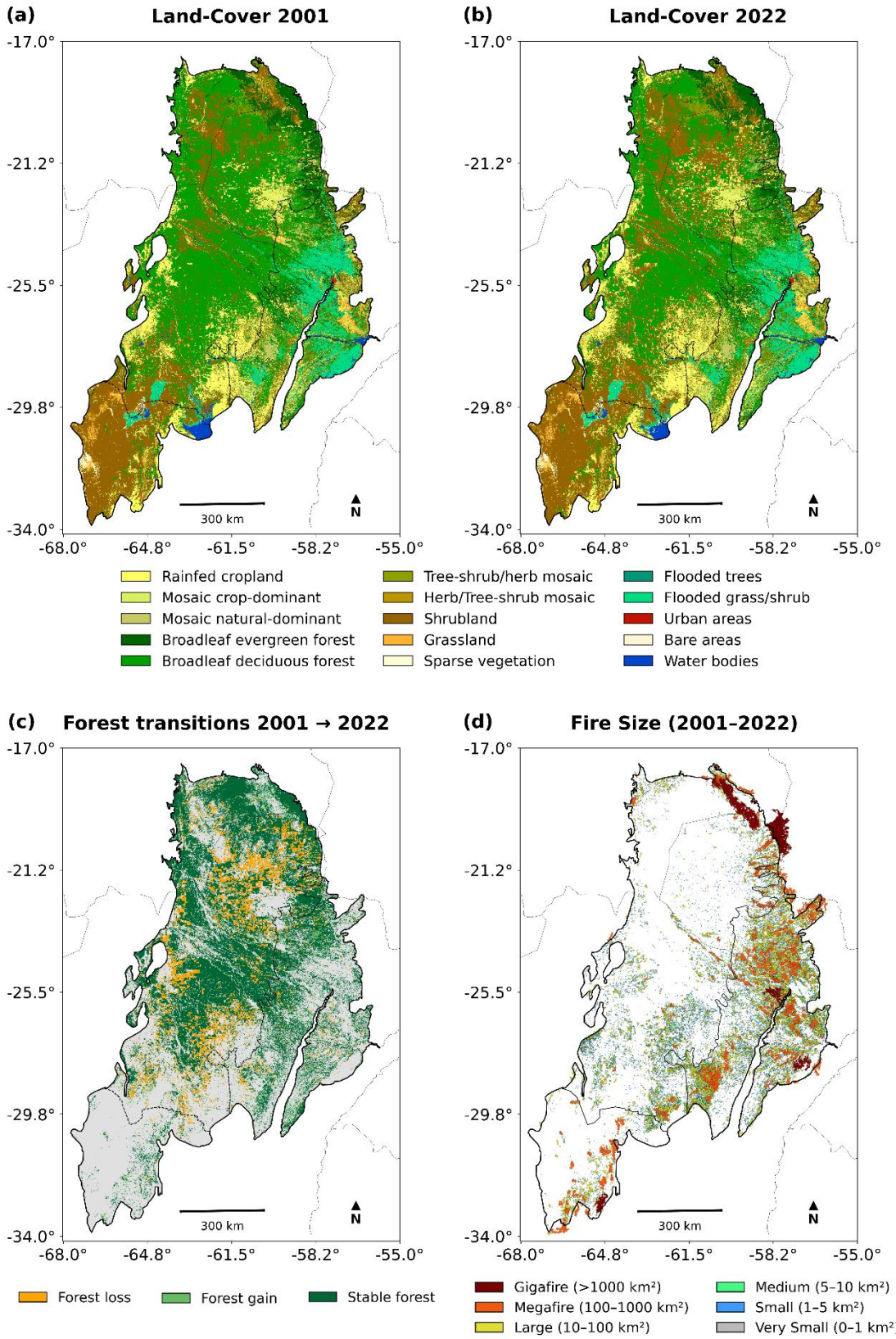

~~**Fig. 4.** (a) and (b) Land-cover distribution in the Gran Chaco based on ESA-CCI-MRLC for 2001 and 2022, respectively. (c) Forest transition classes between 2001 and 2022, showing forest loss (forest to non-forest), forest gain (non-forest to forest), and stable forest. Forests include all tree cover classes; non-forest pixels appear in grey. (d) Spatial distribution of fire events (2001–2022) categorized by fire size using FRYv2.0 data. Fire-size classes range from Very Small (< 1 km²) to Gigafires (> 1000 km²). Fires polygons overlapping the Chaco boundary are retained~~

Fig. ~~4~~ **4** shows the ~~LC~~ land-cover distribution, forest transition patterns, and spatial distribution of ~~the Gran Chaco in 2001 and 2022 (panels a and b), the spatial pattern of forest transitions~~fire events categorized by size between 2001 and 2022 ~~(panel c), and all fire events recorded during 2001–2022 categorized by fire size (panel d).~~. The Wet Chaco is dominated by seasonally flooded herbaceous vegetation, forest mosaics, productive grasslands, and croplands, and it exhibits the highest fire frequency. In contrast, the Dry and Very Dry Chaco regions show increasing proportions of shrublands, fragmented forests, and agricultural frontiers. These long-term LC shifts are summarized in **Fig. S4**, which illustrates the main transitions between 2001 and 2022 and highlights the substantial expansion of shrublands and mosaic vegetation, together with a marked reduction in tree cover.

Fire size distribution is strongly right-skewed across all subregions: over 80 % of events fall within the Very Small (< 1 km²) and Small (1–5 km²) categories (**Table** ~~A1~~**S1; Fig.** ~~A3~~**S6**). Larger fires, although less frequent, account for a disproportionate share of total ~~burned area~~BA. While Very Small to Large (10–100 km²) fires are widespread, Megafires (100–1000 km²) are most common in the Wet Chaco, likely due to continuous fuel beds in grasslands and wetlands. These large fires often occur in areas dominated by seasonally flooded herbaceous vegetation, which can generate high flammability during dry periods. Gigafires (> 1000 km²), although rare, are almost exclusively observed in the Dry ~~and Very~~ Chaco.

Forest loss is widespread across the Chaco in all three countries, with extensive deforestation frontiers in both Argentina and Paraguay. However, the association between fires and these frontiers differs regionally. In Argentina, deforestation zones often coincide with clusters of small and medium fires, whereas in Paraguay and Bolivia fire activity is less evident along recent forest loss edges. In all regions, most large fires occurred in non-forest areas. Shrublands were excluded from the forest class definition, which here only includes tree-cover categories. The Sankey diagram in **Fig. S3** also shows that much of the increase in shrublands and mixed vegetation mosaics originates from former tree-cover classes, reinforcing the link between vegetation degradation and the fuel complexes that support the largest fires.

Across the full Chaco, BA were dominated by open formations: seasonally flooded grasses and herbs account for more than 26% of the total, shrublands for 23% and mosaic vegetation for roughly 12%. Tree cover represents about 24% of all BA, indicating that fires also affect forested and semi-forested landscapes, particularly in the wetter and transitional subregions.

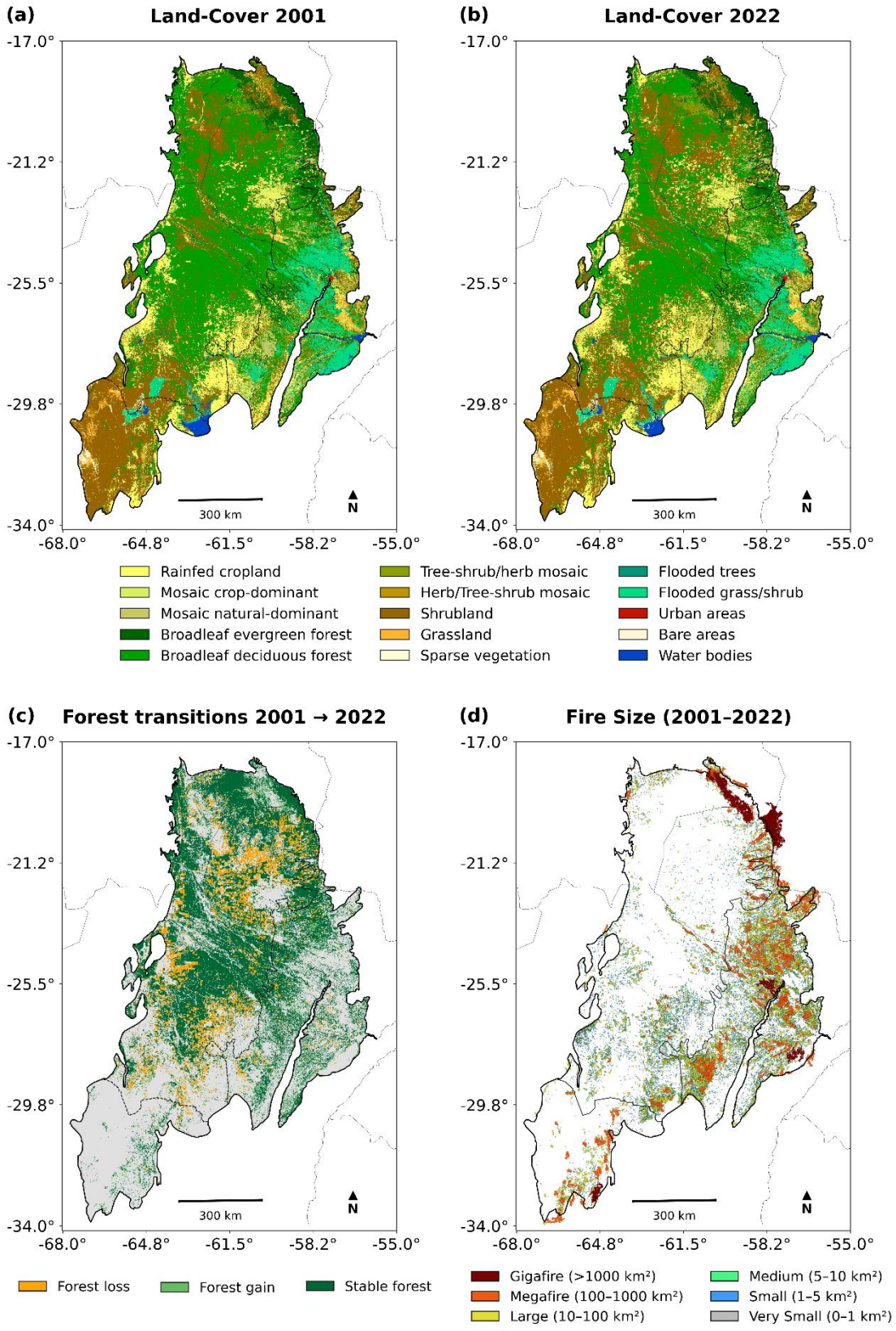

Fig. 4. (a) and (b) Land-cover distribution in the Gran Chaco based on ESA-CCI MRLC for 2001 and 2022, respectively. (c) Forest transition classes between 2001 and 2022, showing forest loss (forest to non-forest), forest gain (non-forest to forest), and stable forest. Forests include all tree cover classes (shrubs not included); non-forest pixels appear in grey. (d) Spatial distribution of fire events (2001–2022) categorized by fire size using FRYv2.0 data. Fire-size classes range from Very Small (≤ 1 km²) to Gigafires (≥ 1000 km²). Fires patches overlapping the Chaco boundary are retained.

Subregional patterns reveal strong gradients. In the Wet Chaco, flooded grasses and herbaceous vegetation together contribute more than 36% of the BA, followed by tree cover (24%), showing that fires extend beyond the floodplain system into forest–savanna transitions. In the Dry Chaco, shrublands dominate the burned LC composition (almost 39%), accompanied by substantial fractions of mosaic vegetation and tree cover, consistent with the vegetation degradation and forest-to-shrub transitions shown in **Fig. S3**. In the Very Dry Chaco, fires overwhelmingly affect shrublands, which represent more than 75% of all BA.

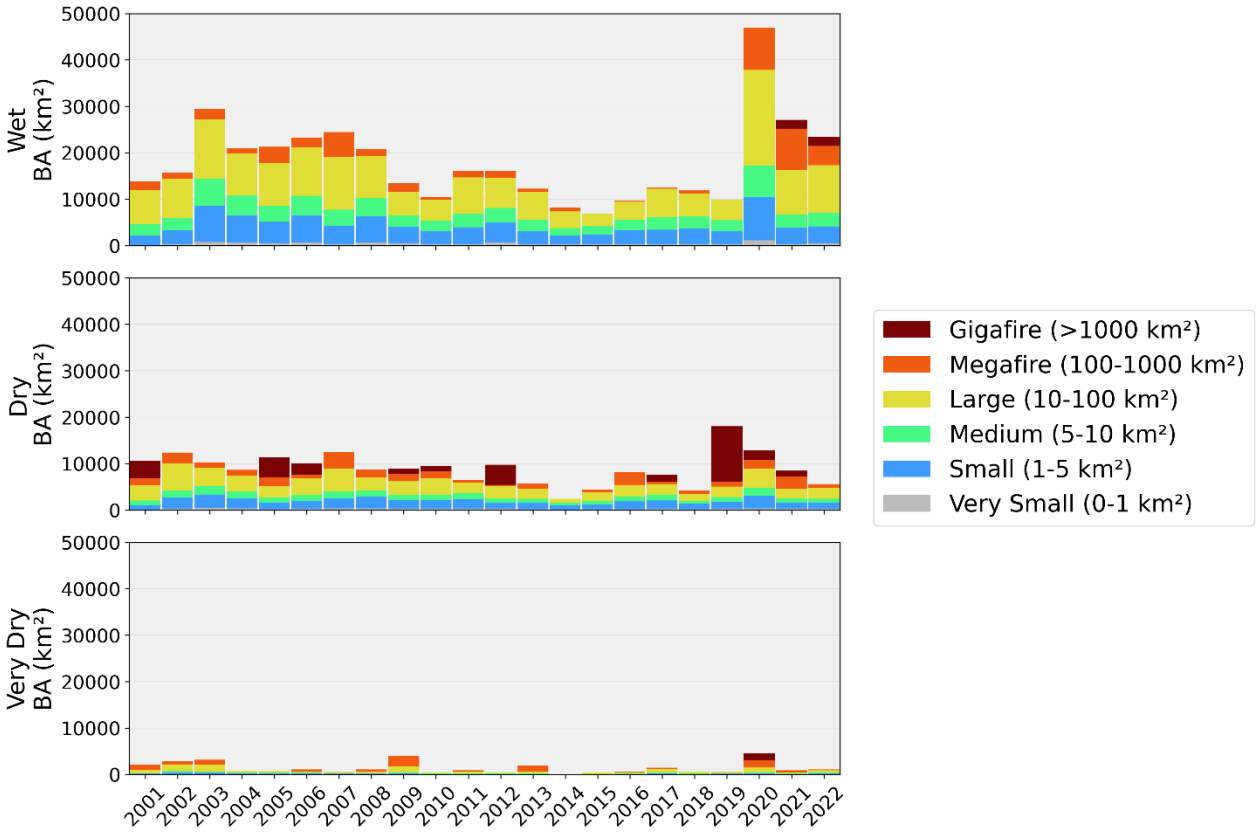

Fig. 5. Cumulative burned area (2001–2022) by fire-size class across the Wet, Dry, and Very Dry Chaco subregions.

According to **Fig. 5**, the Wet Chaco registers the highest total burned area, nearly double that of the Dry and Very Dry regions. In this subregion, ~~Large~~large fires contribute ~40% of annual BA, and ~~Small~~small fires ~20% (**Fig.** ~~A4~~ S5). Despite their modest size, small fires contribute substantially to BA in the Wet Chaco due to their high frequency between 2001 and 2022 (>36,000). Extreme years such as 2003 and 2020 were marked by widespread outbreaks.

In the Dry Chaco, fire ~~frequency~~count is lower, but large fires play a more prominent role. Large fires account for about 25% of the annual ~~burned area~~BA, and ~~Gigafires~~gigafires can dominate totals in some years. For example, in 2019, just three ~~Gigafires~~gigafires in the Dry Chaco burned approximately 10,000 km², which corresponds to the region's mean annual BA and represented more than 50% of the total for that year.

The Very Dry Chaco, while recording the lowest overall BA, exhibits abrupt interannual peaks driven by isolated ~~Megafires~~megafires and ~~Gigafires~~gigafires, pointing to a more stochastic fire regime. Between 2020 and 2022, the Wet Chaco experienced an unprecedented number of ~~Megafires~~megafires and ~~Gigafires~~gigafires, both in terms of event counts and their contribution to total BA. These patterns align with the extreme fire-~~ ~~weather anomalies described in *Section 3.3*.

3.3 Fire–weather relationship

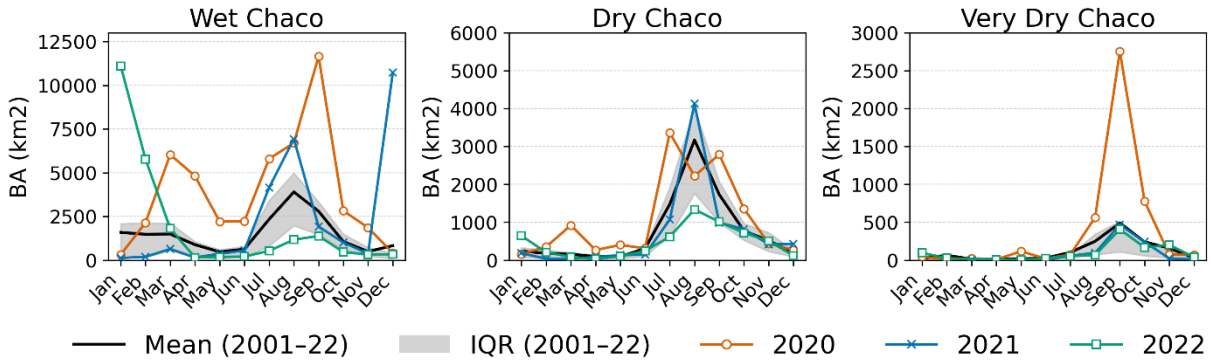

Fig. 6. Seasonality of burned area (BA, km²) in the Wet, Dry, and Very Dry Chaco. The black curve is the 2001–2022 monthly BA mean and the grey band shows the interquartile range (25–75%). Colored curves overlay monthly BA for 2020 (orange circles), 2021 (blue crosses), and 2022 (green squares), highlighting differences from the climatological envelope. Y-axis limits differ by panel.

Fig. 6 presents the monthly BA climatology (2001–2022) with 2020–2022 overlaid for the Wet, Dry, and Very Dry Chaco. In the Wet Chaco, BA in 2020 is above average for most months, with a secondary pulse in March–April (late wet season) preceding pronounced peaks in August–September (winter/dry season). In contrast, anomalies in 2021–2022 are concentrated in the summer/wet season (December–March), reaching levels similar to the typical late-winter/early-spring maximum, while post-winter months in 2022 remain mostly below average. In the Dry Chaco, 2020 stands out as extreme, particularly in July and September, whereas 2021 records an exceptional August at or above historical maxima and 2022 stays near or below the mean. In the Very Dry Chaco, positive anomalies are dominated by 2020, with a sharp ~~October~~September maximum; 2021 shows only minor increases, and 2022 remains subdued. Overall, 2020 shows widespread positive anomalies lasting several months across all subregions. In contrast, 2021 and 2022 generally feature shorter peaks, often concentrated in summer, although 2021 also records exceptional winter fires in the Dry Chaco. Activity during the canonical late-winter fire season is otherwise limited, particularly in 2022.

~~Spatial~~The spatial patterns of fire–weather coupling ~~are explored~~shown in Fig.~~ 7, which shows~~ 7 depict the per-pixel Pearson correlation between monthly Fire Weather Index (FWI) anomalies ~~and BA~~from ERA5-Land and BA anomalies derived from the gridded FRY dataset, both at 0.1° resolution, during

the wet and dry seasons. FWI anomalies exhibit an approximately normal distribution, and after filtering pixels with fewer than four fire-active months, most BA anomaly series are quasi-normal, justifying the use of Pearson correlation as described in *Section 2.3.7.* Significant positive correlations ($p < 0.05$) are concentrated in the Wet Chaco, where R coefficients reach up to 0.7 during the wet season. In contrast, the Dry and Very Dry Chaco show weaker and more spatially scattered relationships, partly due to lower fire frequency. Spearman correlations were also calculated, resulting in similar patterns with lower coefficients (maximum R of 0.52; **Fig. S7**)

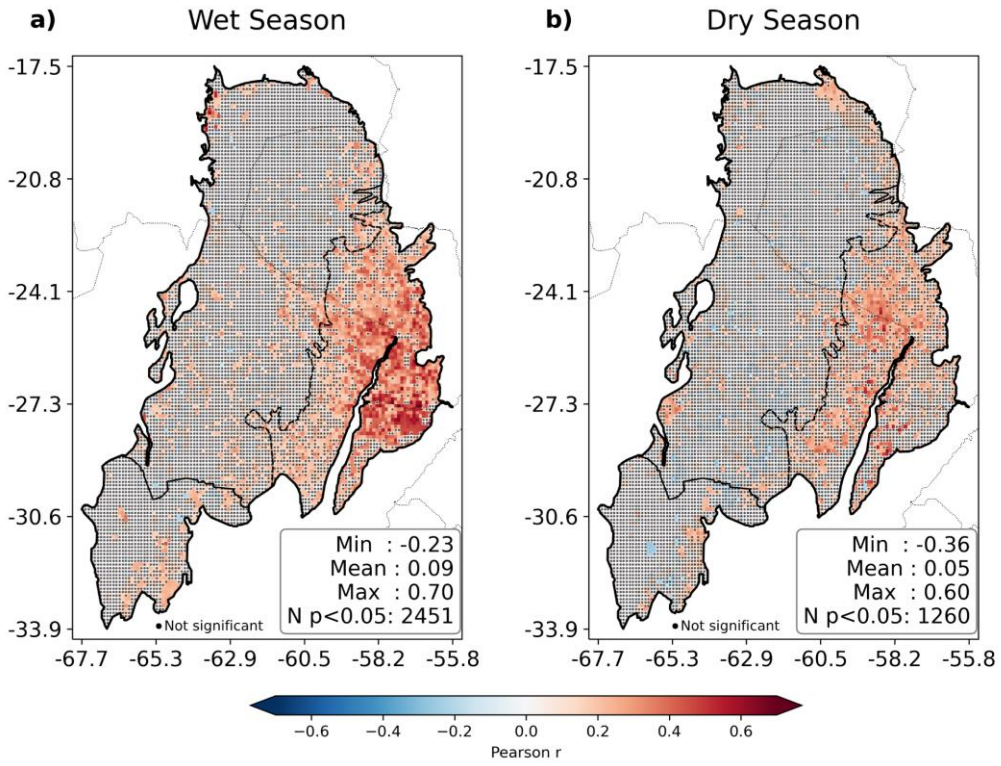

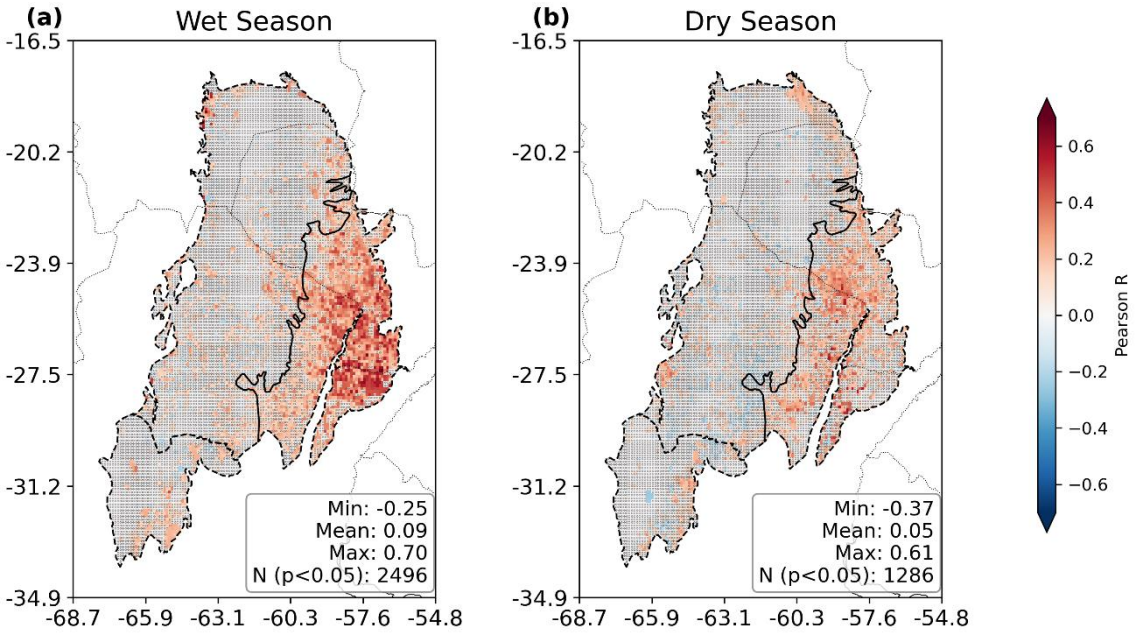

Fig. 7. Spatial distribution of pixel-wise Pearson correlation coefficients between monthly Fire Weather Index (FWI) anomalies and monthly burned area (BA) for the period 2001–2022: (a) Wet Season and (b) Dry Season. The color bar indicates the strength and direction of the correlation (from negative in blue to positive in red). Inset statistics summarize the distribution of coefficients (Min, Mean, Max). Pixels marked with small black circles represent non-significant correlations (p-value > 0.05), while unmarked pixels indicate significant correlations (p-value < 0.05). Only pixels with more than 3 time steps with burned area >0 were kept to avoid biased correlations related to very few or no fires.

To further explore the spatial sensitivity of fire activity to fire weather, **Fig. 8** compares per-pixel correlations between monthly FWI anomalies (see *Section 2.3.7*) and two metrics: fire counts ~~(ignitions)~~ and BA. Each dot represents a 0.1° grid cell, and quadrants classify response types. In the Wet Chaco, 93% of cells fall in Q1, where both metrics show positive correlations with FWI, with moderate mean values (0.17 ± 0.12 for ignitions, 0.19 ± 0.13 for BA) and strong inter-metric correlation ($r = 0.76$). The Dry and Very Dry Chaco show more heterogeneous patterns, with Q1 proportions of 59% and 61%, and weaker mean correlations (~0.04–0.06). Still, inter-metric spatial correlations remain high ($r = 0.81$ and $r = 0.72$), indicating that regions more sensitive to fire weather in terms of ignitions also tend to be more sensitive in terms of fire extent.

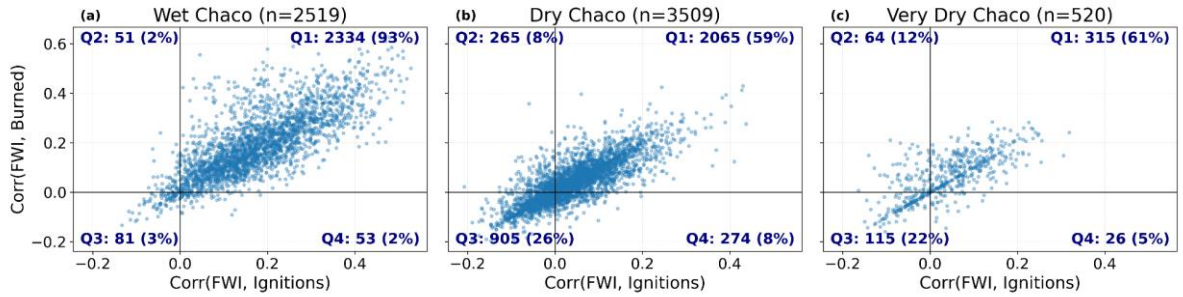

Fig. 8. Each panel shows a scatterplot of per-pixel Pearson correlation coefficients between the Fire Weather Index (FWI) and two fire activity metrics—ignition frequency (x-axis) and burned area (y-axis)—over the period 2001–2022. The panels correspond to the Wet, Dry, and Very

Dry Chaco subregions, and each dot represents a 0.1° × 0.1° grid cell. Quadrants are defined by the sign of each correlation coefficient to classify spatial patterns of fire–weather association: Q1 (top-right) includes pixels with positive correlations for both ignitions and burned area; Q3 (bottom-left) includes negative correlations for both; Q2 and Q4 represent divergent cases. For each subregion, quadrant counts, percentages, and summary statistics (mean ± standard deviation of each correlation axis and Pearson r between them) are annotated.

Finally, the temporal co-evolution of annual BA and FWI anomalies is illustrated in the appendix (**Figs.** ~~A5–A6~~ **S9–S10**). Several years, especially in the Wet Chaco, show strong spatial correspondence between extensive fire activity and positive FWI anomalies (e.g. 2012, 2020–2022). However, other years (e.g. 2003) reveal extensive BA without matching FWI extremes, underscoring that weather is not the sole driver of interannual variability.

3.4 Temporal dynamics of fire–environment interactions

To explore how conditions evolve before and after fire events, we analyzed both regional time series and lagged correlations between BA anomalies and three key drivers: FWI, rainfall, and vegetation greenness (EVI), over the period 2001–2022.

The time series analysis (**Fig.** ~~**A07**~~ **S10**) reveals a coherent pattern in all subregions. Typically, positive rainfall anomalies (which automatically decrease FWI) are followed by increased EVI, indicating vegetation growth and fuel accumulation. When this is then followed by elevated FWI values (due to negative rain and humidity anomalies, extreme heat and/or strong winds), peaks in BA are frequently observed. This pattern supports the interpretation of a fire-favoring sequence: moisture enables biomass build-up, which is later dried and made flammable under high fire-weather conditions, culminating in fire activity. This cycle is particularly evident in major fire years such as 2020 and 2022, especially in the Wet Chaco, where the alignment between environmental anomalies and BA peaks is striking. In the Dry and Very Dry Chaco, the sequence is also well defined, although slightly more variable probably due to limited fuel accumulation.

The influence of large-scale climate variability, particularly the El Niño–Southern Oscillation (ENSO), is also reflected in the fire–environment dynamics. During La Niña phases (negative ENSO), we observe reduced rainfall and elevated FWI values, often coinciding with increased BA. Conversely, El Niño episodes (positive ENSO) are associated with wetter conditions, lower fire-weather pressure, and reduced fire activity (**Fig.** ~~**A7**~~ **S10** and **Fig.** ~~**A8**~~ **S11**).

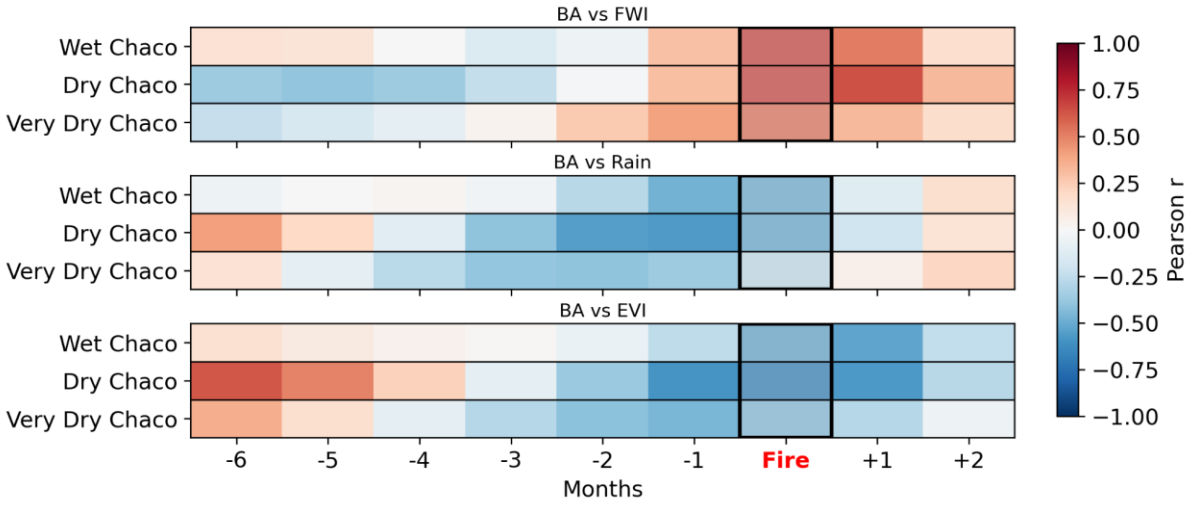

Fig. 9. Lagged correlations between monthly anomalies of FWI, rainfall, and EVI with burned area in the Chaco. Each heatmap shows the Pearson correlation coefficient between the anomaly of a given variable (FWI, rainfall, or EVI) at different time lags and the burned area anomaly, for each Chaco subregion. Negative lags indicate the variable leads burned area; positive lags indicate it follows. Correlations are computed from pixel-based, region-averaged monthly time series for 2001–2022.

Fig. 9 shows lagged Pearson correlations between monthly anomalies of BA and FWI, rainfall, and EVI for the three Chaco subregions. Positive correlations between BA and FWI at lags 0 to +1 months, indicate that peak fire activity coincides with high fire-weather conditions. Rainfall and EVI display negative correlations with BA at short negative lags (−1 to −3 months), consistent with dry, senescent vegetation promoting flammability. At longer negative lags (−5 to −6 months), especially in the Dry and Very Dry Chaco, both variables correlate positively with BA, suggesting that wetter, greener periods months earlier promote fuel build-up. In the Wet Chaco, lag correlations are weaker and less structured, likely due to consistently moist conditions that buffer fire–environment coupling.

3.5 Fire-weather types

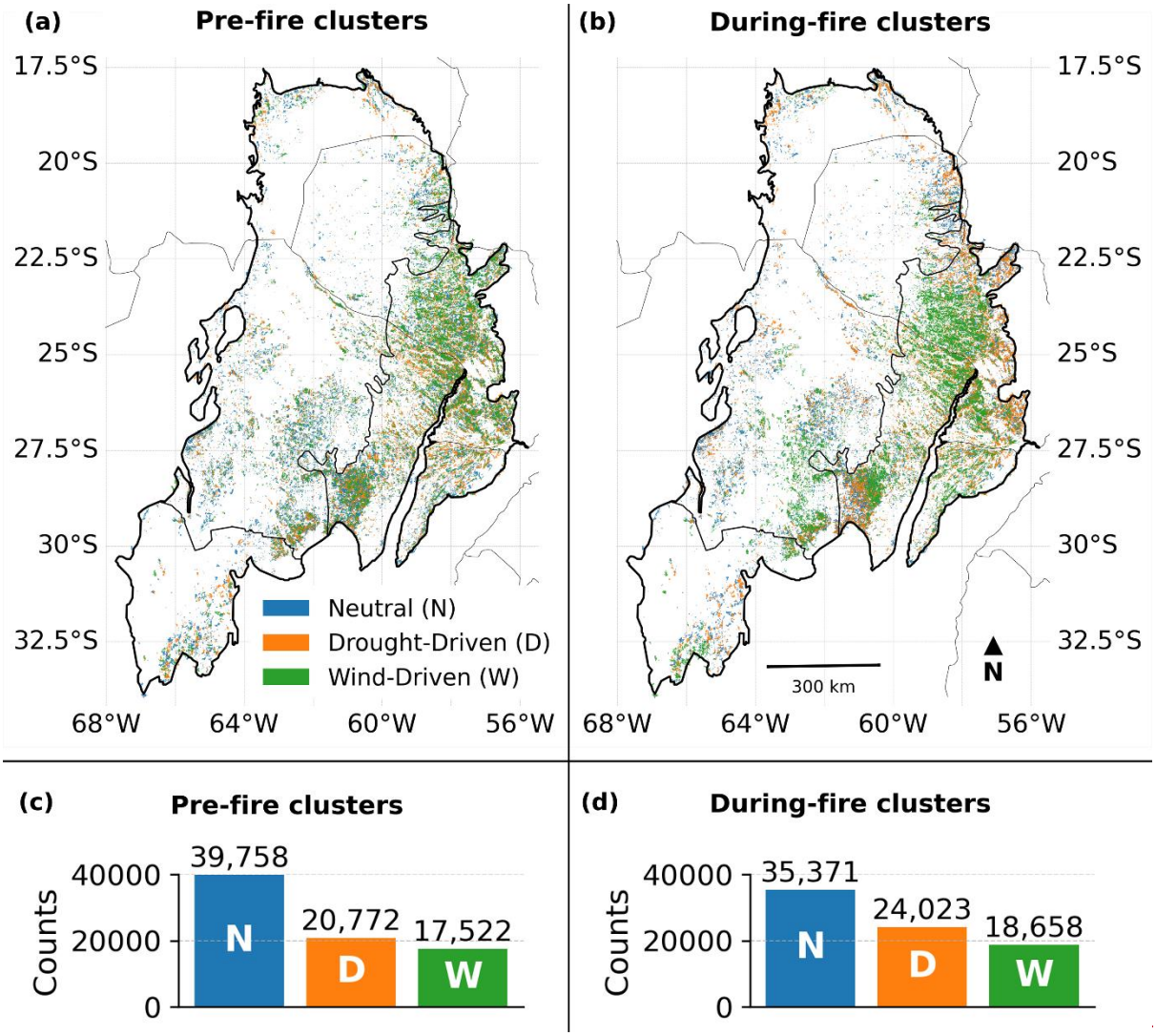

To characterize the atmospheric conditions associated with fire occurrence and fire growth, we analyzed the Fire–Weather Types (FWTs) assigned to each fire patch during the days preceding ignition (*Pre-Fire* clusters) and during the active burning period (*During-Fire* clusters). **Figure 10** presents the spatial distribution and frequency of the three FWT categories (Neutral, Drought Driven and Wind Driven) for both clustering types.

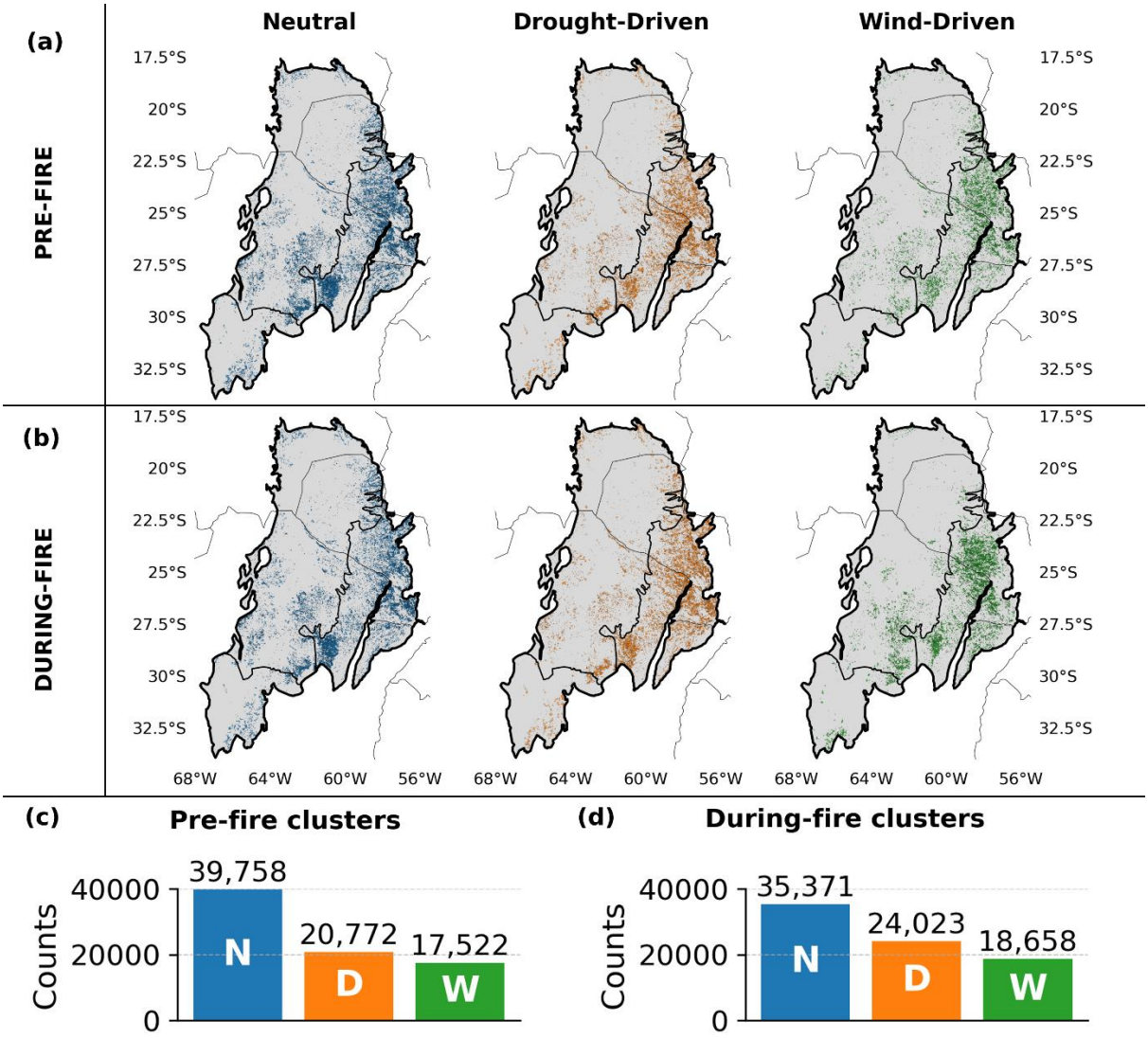

Fig. 10. Spatial distribution and frequency of pre- and during-fire meteorological clusters across the Gran Chaco (2001–2022). Panels (a) and (b) show the geographic location of fire patches classified into three Fire–Weather Types (FWTs)—Neutral (blue), Drought-Driven (orange), and Wind-Driven (green)—for the pre-fire and during-fire periods, respectively, overlaid on Chaco sub-region boundaries Some patches overlap through the years and may partially or totally cover each other. Panels (c) and (d) display the total number of patches assigned to each FWT for pre-fire and during-fire clustering methods, respectively.

~~**Fig. 10** shows the spatial distribution and frequency of three Fire–Weather Types (FWTs)—Neutral, Drought-Driven, and Wind-Driven—for the pre-fire and during-fire periods. Using k-means clustering with $k = 3$, each FP was assigned an FWT twice: first based on conditions in the 0–3 days before ignition (*Pre-Fire*) and then based on mean conditions during the active burning period (*During-Fire*).~~

Neutral FWTs dominate both ~~clusterings~~clustering groups, but their share decreases from 50.9 % to 45.3 % overall, while Drought-Driven rises from 26.6 % to 30.8 % and Wind-Driven from 22.4 % to 23.9 % (**Fig. 10c–d and Fig. ~~A9~~S12**). ~~In the Wet Chaco, Neutral drops~~This indicates that when fires are clustered according to the meteorology during the fire rather than before ignition, a larger fraction falls into drought or wind related conditions and fewer remain neutral. In the Wet Chaco, Neutral FWTs drop from 49 % to 42 % with a marked increase in Drought-Driven; in the Dry Chaco, both non-neutral types

grow moderately; in the Very Dry Chaco, Wind-Driven ~~increases~~types increase sharply (from 15 % →to 26 %), especially in the south where complex topography may strongly influence fire–atmosphere dynamics (see *Section 2.1*). These regional shifts suggest that dryness is particularly important in the Wet Chaco, while stronger winds become comparatively more relevant in the southern Very Dry Chaco.

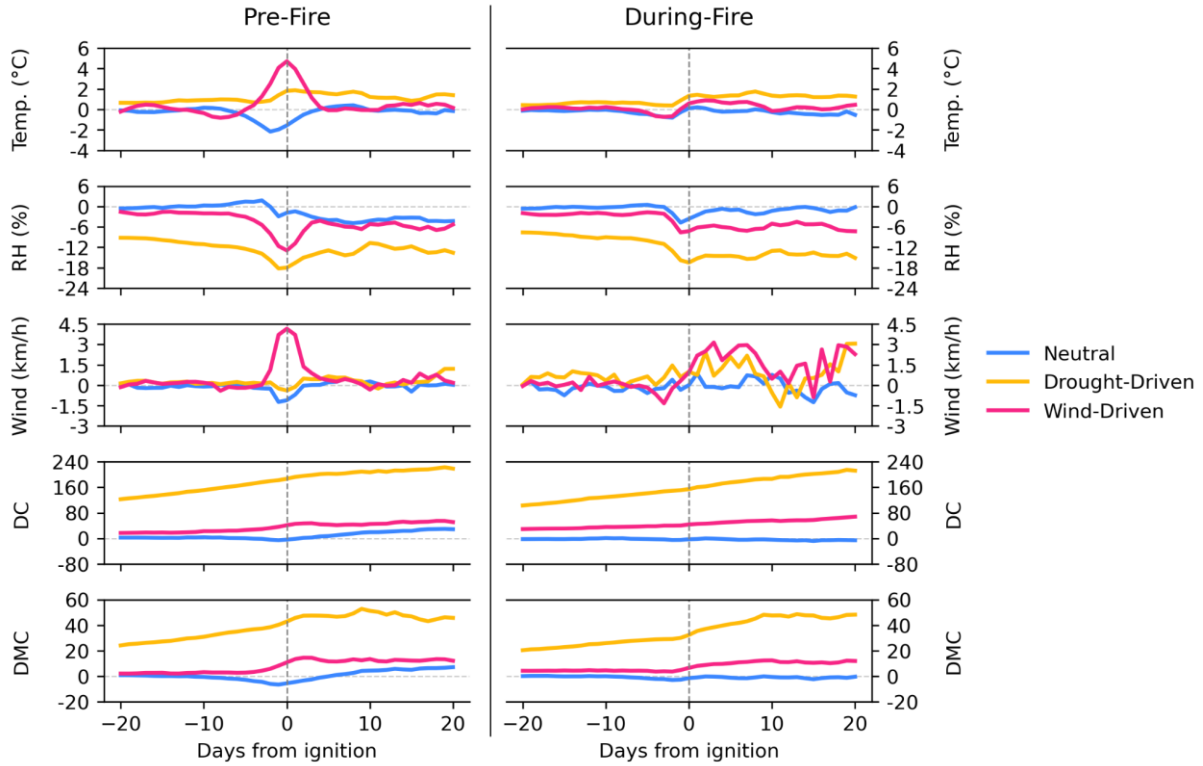

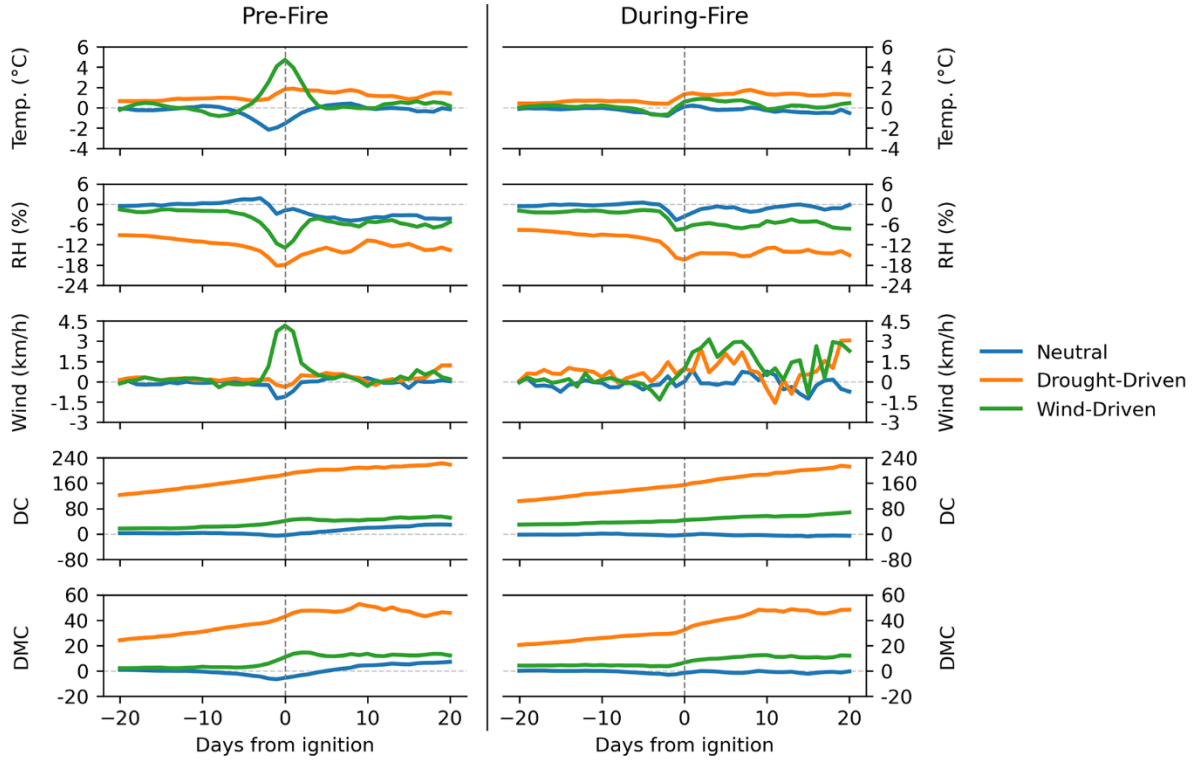

Fig. 11. Mean daily anomalies of temperature (Temp.), relative humidity (RH), 10-meter wind speed, Drought Code (DC), and Duff Moisture Code (DMC) from 20 days before to 20 days after fire ignition, averaged over fire ~~polygons~~patches assigned to the Neutral, Drought-Driven, and Wind-Driven clusters for Pre-Fire (left) and During-Fire (right) clustering approaches.

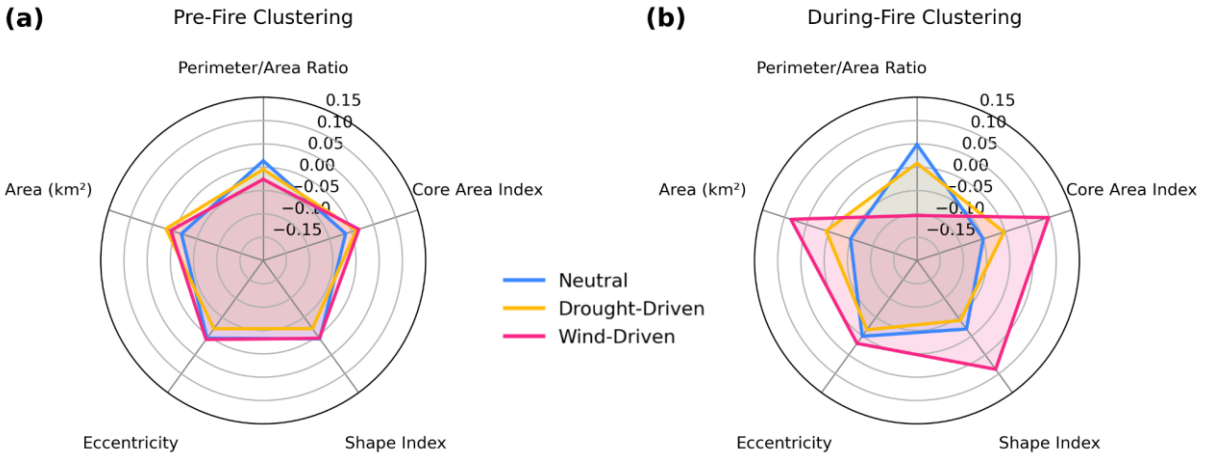

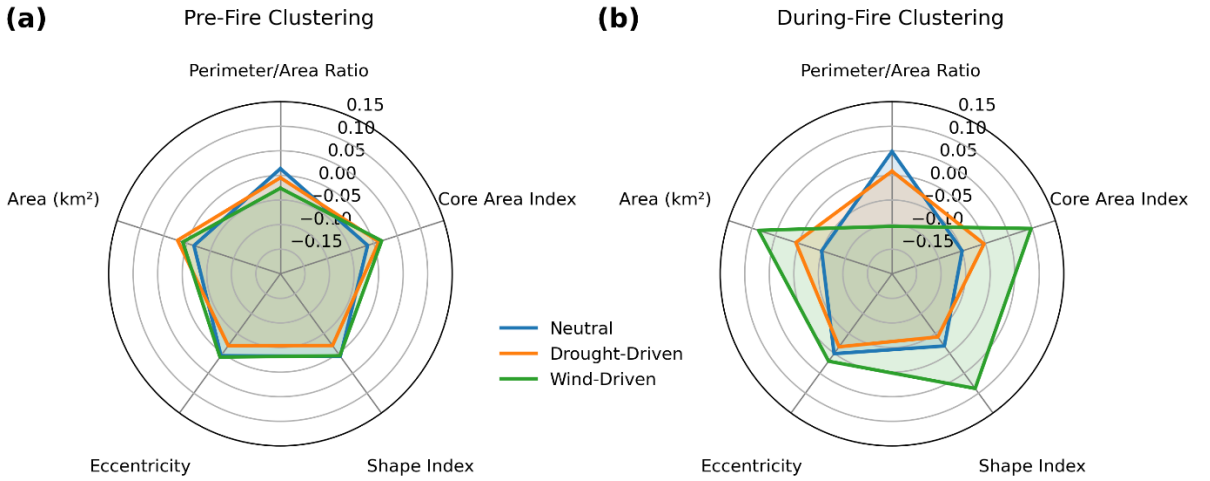

Fig. 12. Clusters mean morphology profiles for (a) Pre-Fire and (b) During-Fire ~~clusterings~~clustering. Each axis represents a ~~standardised~~standardized morphology variable (z-score), and each colored polygon shows the mean profile for one cluster. The radial extent indicates the relative value of each variable within the dataset.

Fig. 11 shows mean daily anomalies from 20 days before to 20 days after ignition for each FWT~~.~~ for both clustering types. In the *Pre-Fire* FWT, we see that the Wind-Driven fires present a sharp rise in wind speed and temperature in the days around ignition, coupled with a drop in RH, creating highly flammable conditions. Drought-Driven fires exhibit a long build-up of dryness before ignition, with persistently high DC and DMC values and low RH, indicating extended fuel curing. Neutral fires occur under conditions close to climatology, with only small fluctuations in all variables.

~~Morphology~~The time series of the *During-Fire* FWTs show that the dry conditions characteristic of the Drought-Driven cluster begin to develop before ignition and remain well differentiated during the fire, with very low RH and high DC and DMC values. Wind speed anomalies are also elevated in this cluster, although not as sharply as in the Wind-Driven cluster. This indicates that dryness and wind can co-occur in Drought-Driven fires, whereas Wind-Driven fires are characterized by a clear and sustained peak in

wind speed combined with dry conditions, but without the prolonged build-up of drought observed in the Drought-Driven cluster. The Neutral cluster remains close to climatology throughout, with only a slight decrease in RH immediately prior to ignition, suggesting a minimum dryness threshold for fire initiation across clusters.

When comparing FP morphology across clusters, *Pre-Fire* FWTs ~~is~~appear broadly similar (**Fig. 12, ~~A10–A11~~S13–S14**), with comparable FP area, shape index~~,~~ (deviation from compactness), core-area index~~,~~ (interior cohesion), eccentricity~~,~~ (elongation), and perimeter-to-area ratio~~.~~ (boundary complexity). In contrast, *During-Fire* FWTs ~~display~~show clear differences: Wind-Driven fires tend to be larger, more elongated~~,~~ (higher eccentricity), and more cohesive (higher core-area index~~,~~ and lower perimeter-to-area ratio) than Drought-Driven fires, consistent with a directional spread under strong and sustained winds.

The combination of high eccentricity and low perimeter-to-area ratio reflects elongated but relatively smooth fire perimeters produced by the rapid advancement of the fire under strong winds. In contrast, Drought-Driven fires tend to generate more irregular boundaries for a given size, consistent with a stronger dependence on the spatial distribution of cured fuels, which causes the fire to advance unevenly across fuel patches and results in more complex and less smooth perimeter shapes.

Overall, *Pre-Fire* FWTs capture the atmospheric ~~context~~conditions leading to ignition, whereas *During-Fire* FWTs better reflect the conditions that shape the eventual size and geometry of the ~~burned area. Other factors such as fuel continuity, topography, and human interventions likely modulate these outcomes~~fire. These results show that both clustering types capture different aspects of fire–weather interactions, but that the *During-Fire* FWTs provides clearer separation in terms of final fire size and morphology.

3.6 Fire size drivers

Our RF analysis identified static topographic and vegetation structure variables as the dominant predictors of final fire size in the Gran Chaco (**Fig. 13a**). *Mean elevation* showed the highest mean SHAP value (17.4%), followed by *LC evenness* (10.8%), *tree/shrub/herbs mosaics* (9.79%) and m*ean slope* (9.1%). These four variables consistently occupied the top positions across the global model and all twelve specific models (**Fig. 14**). LC fractions within the FPs, including cropland or flooded herbaceous cover, made moderate contributions, whereas meteorological and social variables such as maximum wind speed, precipitation, population density or cattle density ranked markedly lower in importance. **Fig.** ~~To identify drivers of fire size and shape beyond meteorological conditions, we trained Random Forest (RF) models using 17 landscape and environmental predictors for all FPs between 1 km² and 100 km² (**see Section 2.3.5**).~~

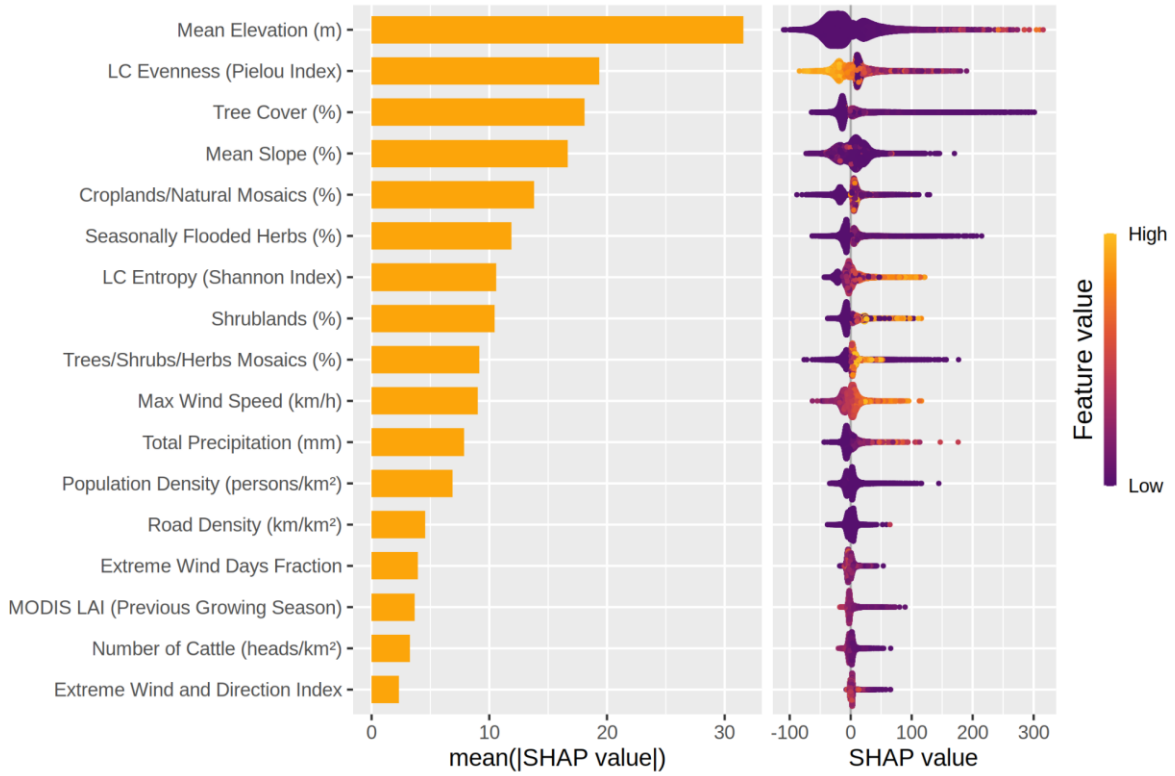

14 demonstrates that this hierarchy is almost unchanged across regional, seasonal and fire-weather subsets, underscoring that the dominance of topography and vegetation structure is not an artefact of spatial domain or sample composition.

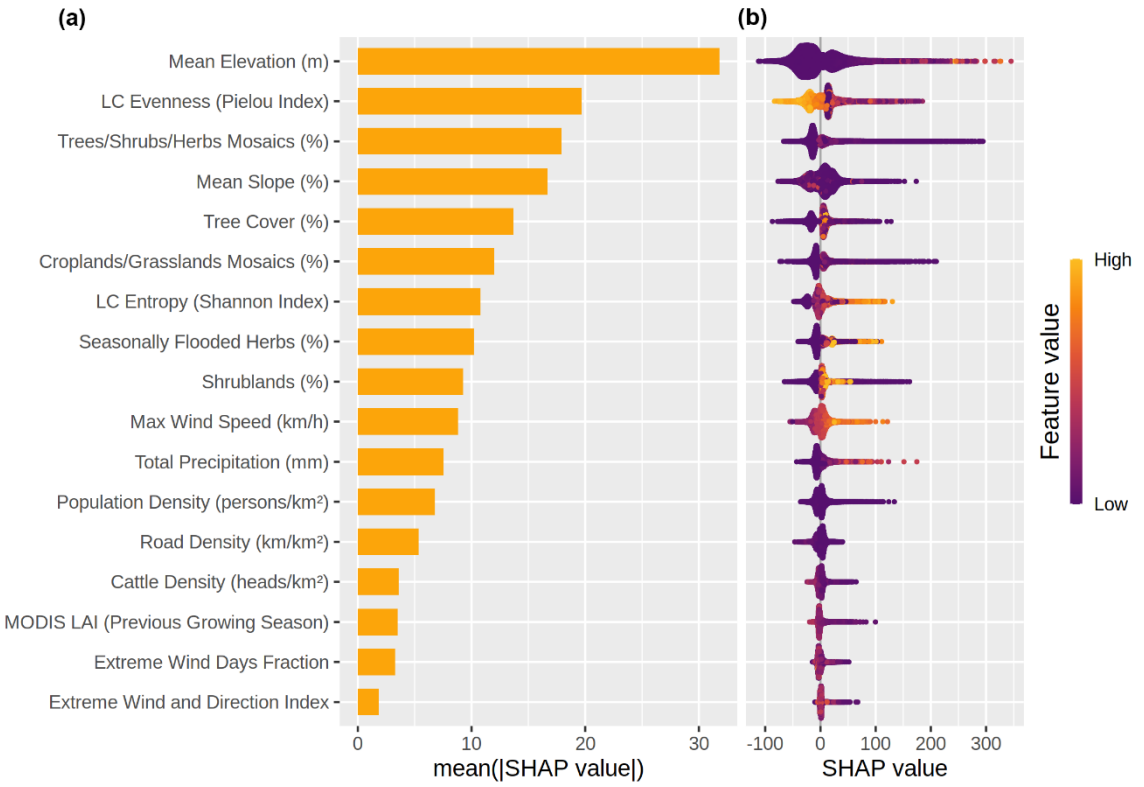

Fig. 13. ~~SHAP summary plot~~ Feature importance ranking for the Random Forest model predicting fire ~~polygon~~patch (FP) size ~~(n_cell) using all fire patches in the FRY dataset with areas between 1 km^2 and 100 km^2, with 17 explanatory features extracted for each polygon. The left panel~~across the entire Gran Chaco. (a) shows the average importance of each variable, expressed as the mean absolute SHAP value ~~for,~~ which reflects how strongly each feature~~, ranking them by overall importance. The right panel displays the distribution of~~ contributes to model predictions on average. (b) shows the SHAP values for ~~each feature~~ all individual fire patches, indicating how low (purple) or high (yellow) feature values influence the prediction toward smaller or larger fires. SHAP values are used here to quantify feature importance consistently across the dataset.

Model performance was satisfactory, with the global RF achieving a correlation of 0.74 on the test set and a test RMSE of ~110 burned pixels, compared with 0.96 and ~54 pixels on the training set (**S14).** These values indicate limited overfitting and show that the model captures a substantial fraction of the variance in fire size despite the inherent noise and strong skewness of the response variable. Because the target variable is the number of burned FRY pixels within each FP, RMSE values are interpreted directly in pixel units; with the 250 m FireCCI51 resolution, 110 pixels correspond to approximately 6.9 km², less than 7 % of the 1–100 km² size range analyzed here. Comparable performance was obtained across all ~~observations, with color indicating the feature value (purple = low, yellow = high).~~ regional, seasonal and fire-weather configurations (**Table S3**).

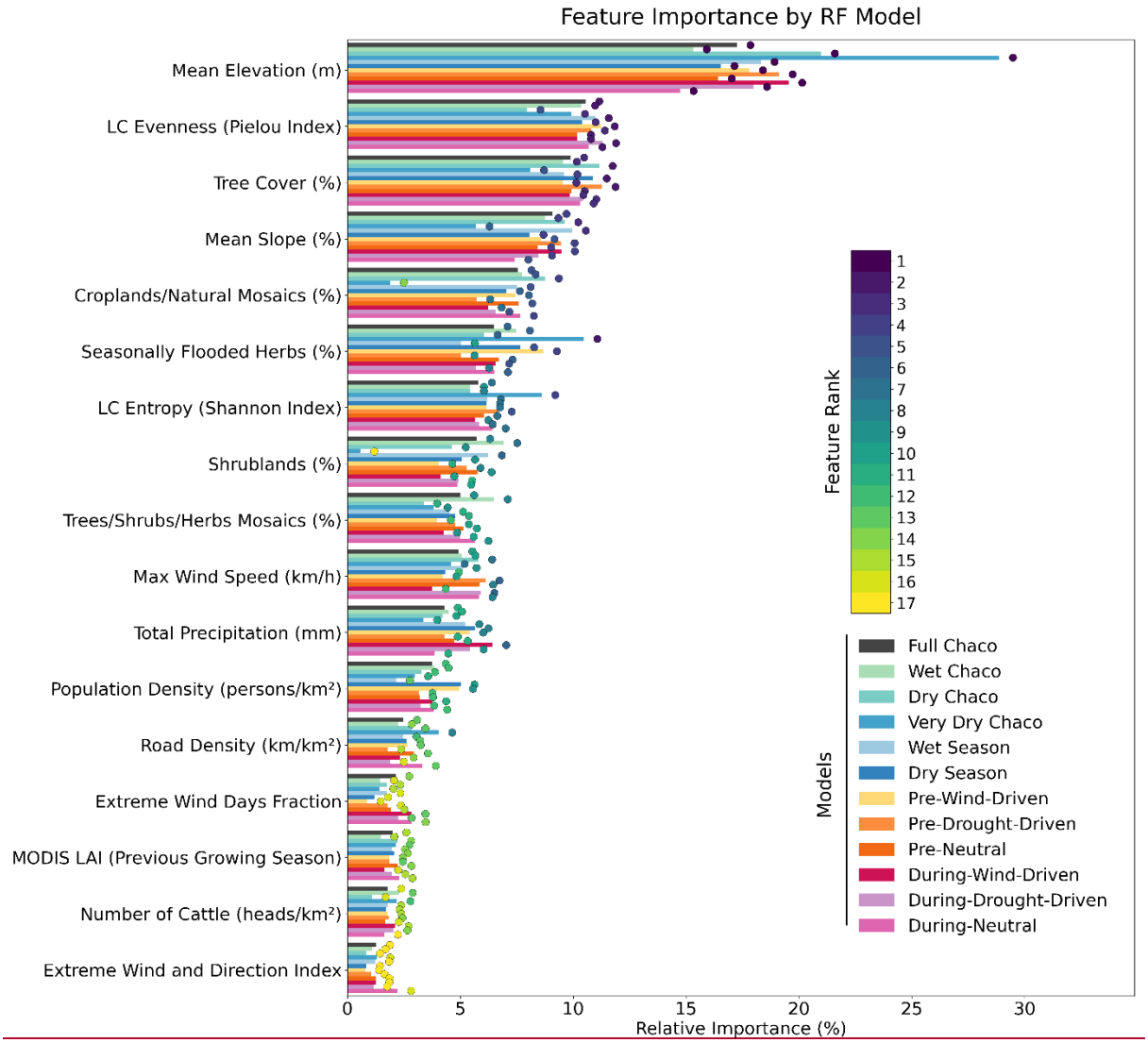
Feature Importance by RF Model
Mean Elevation (m)
LC Evenness (Pielou Index)
Tree Cover (%)
Mean Slope (%)
Croplands/Natural Mosaics (%)
Seasonally Flooded Herbs (%)
LC Entropy (Shannon Index)
Shrublands (%)
Trees/Shrubs/Herbs Mosaics (%)
Max Wind Speed (km/h)
Total Precipitation (mm)
Population Density (persons/km²)
Road Density (km/km²)
Extreme Wind Days Fraction
MODIS LAI (Previous Growing Season)
Number of Cattle (heads/km²)
Extreme Wind and Direction Index
0
5
10
15
20
25
30
Relative Importance (%)
Feature Rank
1
2
3
4
5
6
7
8
9
10
11
12
13
14
15
16
17
Models
Full Chaco
Wet Chaco
Dry Chaco
Very Dry Chaco
Wet Season
Dry Season
Pre-Wind-Driven
Pre-Drought-Driven
Pre-Neutral
During-Wind-Driven
During-Drought-Driven
During-Neutral

1031

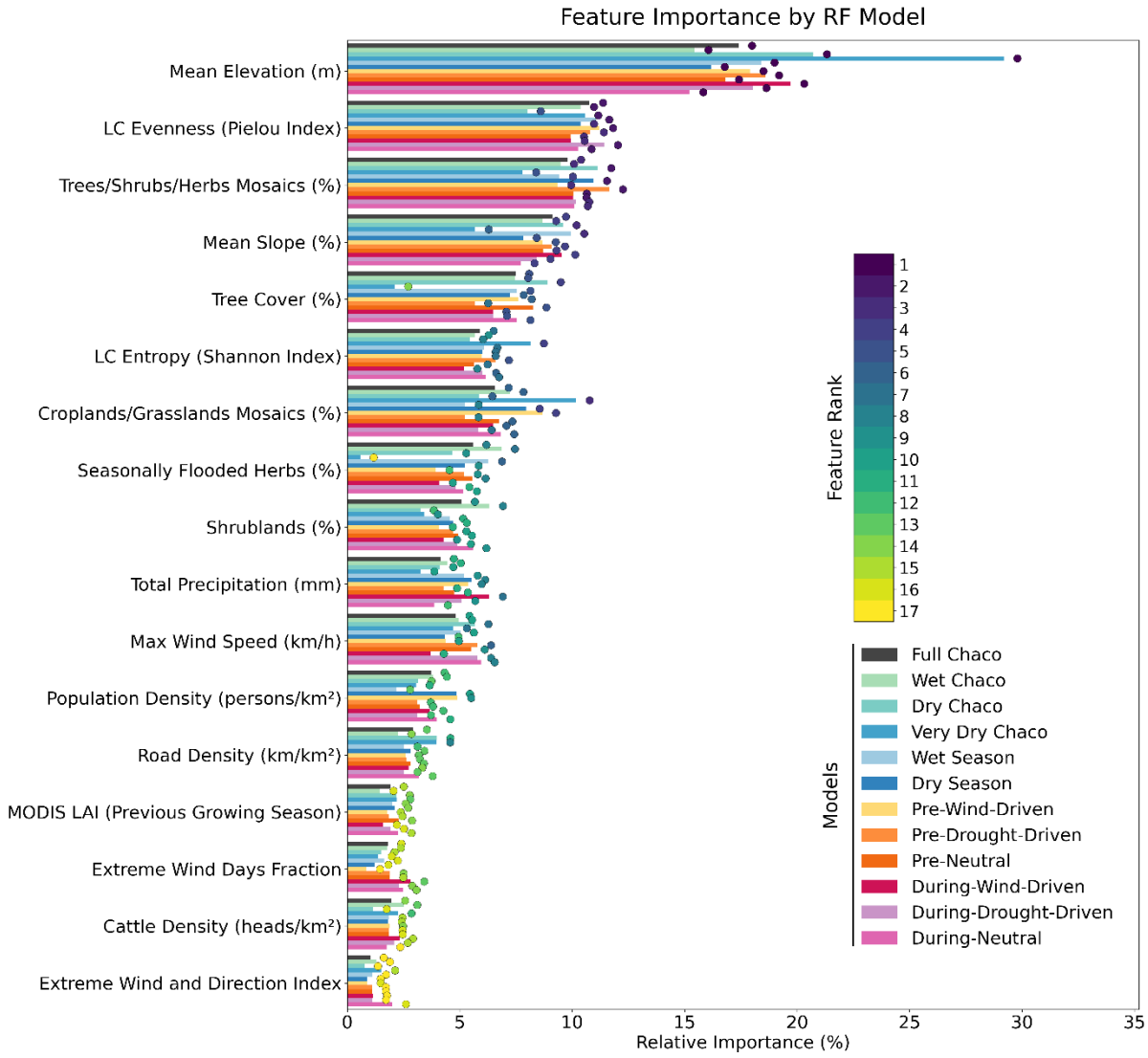

Fig. 14. SHAP feature importance ranks across all trained Random Forest models used to predict fire ~~polygon~~patch size (n_cell) based on 17 explanatory variables. Colored dots at the end of bars shows the rank of a variable's importance (1 = most important, 17 = least important) for a given model.

~~In the global RF model (**Fig. 13**), static topographic and vegetation structure variables dominated: mean elevation had the highest mean SHAP value (31.3), followed by land cover (LC) evenness (21.0), tree cover (19.3) and mean slope (15.2). These four variables consistently ranked in the top positions across all twelve cluster-specific and global models (**Fig. 14**). Land cover composition metrics such as cropland or flooded herbaceous cover showed moderate contributions, while meteorological and social variables (e.g. maximum wind speed, precipitation, population or cattle density) were surprisingly of lower importance.~~

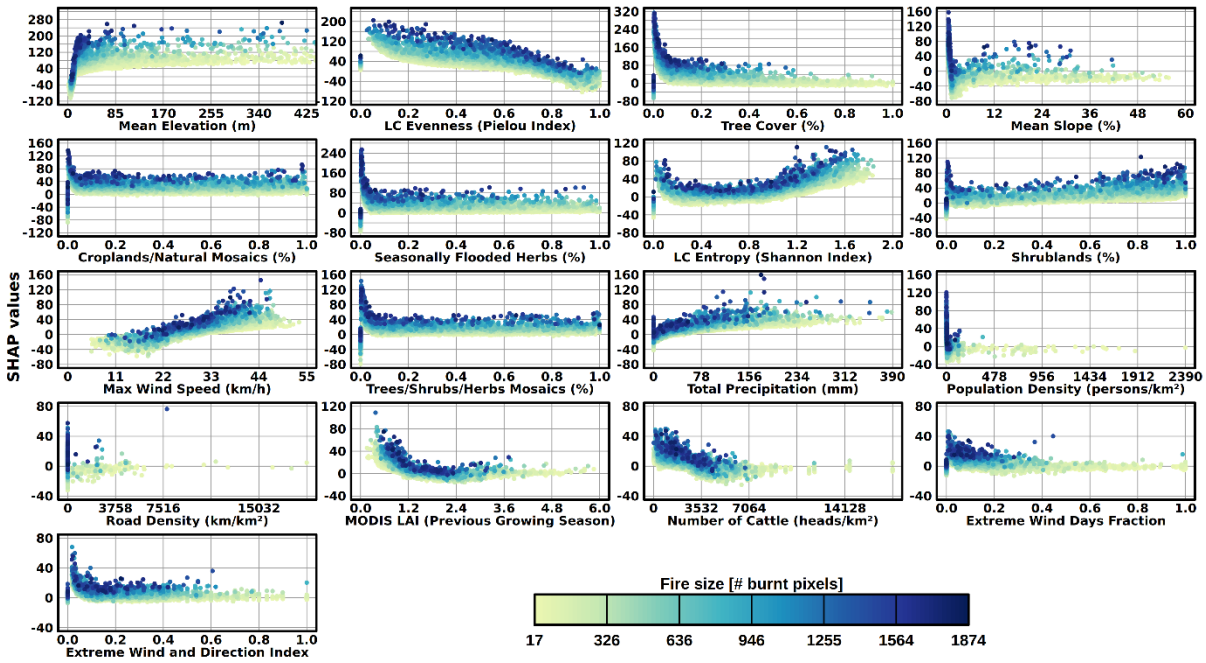

Predictor distributions were strongly skewed for many variables (e.g., LC fractions, anthropogenic densities), with high proportions of zeros and long upper tails, whereas elevation and slope varied mostly within narrow low-lying ranges with few high-elevation observations (**Table S2; Fig. S15**). These empirical distributions are critical for interpreting SHAP behavior in **Fig. 13** and **15**, as they define the domains within which the RF partitions landscape conditions.

The global SHAP distribution (**Fig. 13b**) shows that elevation exerts a consistently positive influence on predicted fire size across most of its range, with the PDP in **Fig. 15** revealing a steep rise in SHAP values between 0 and ~40–60 m, followed by a broad plateau. Large fires dominate this low to mid elevation interval, while higher elevations generally host smaller events. This pattern indicates that elevation is acting not as a physical driver but as a proxy for geomorphological and ecological gradients that determine fuel structure and continuity. In the lowlands of the Chaco, shallow depressions, seasonal marshes ("bañados"), and permanent wetlands ("esteros") develop over silty clay soils with poor infiltration and minimal slope, accumulating abundant herbaceous biomass that cures during dry periods and supports extensive fire spread (Bravo et al., 2025). Slightly elevated terraces and woody islets ("montes", "albardones") act instead as natural barriers. Because the RF does not encode these fine spatial transitions explicitly, elevation functions as an integrative descriptor of landscape contexts conducive to large fires. Regional PDPs (**Figs. S17–S19**) confirm and refine this interpretation. In the Wet Chaco, SHAP values rise sharply from 0 to ~20–40 m and stabilize above that threshold, while in the Dry Chaco the increase is concentrated in the 0–20 m band and flattens near 50–100 m, reflecting transitions from floodplain matrices to agricultural or post-deforestation mosaics. In contrast, the Very Dry Chaco exhibits a nearly linear positive gradient up to ~700 m, with large fires clearly associated with higher elevation.

Mean slope refines this topographic signal. Although its global importance is slightly lower than elevation, its SHAP dependence curve (**Fig. 15**) mirrors the elevation-driven distinction between flat floodplain fuels and more fragmented uplands. SHAP values decline sharply between 0 and ~2–3 % slopes, where the largest fires are concentrated, and then stabilize. Regional PDPs show the same structure in the Wet and Dry Chaco, with large fires almost entirely confined to slopes below ~2-3 %, whereas steeper terrain hosts only small fires. The Very Dry Chaco departs from this pattern, showing a monotonic negative gradient with a small cluster of large fires at intermediate slopes (~20–30 %), likely corresponding to large fire events in sierran landscapes. Together, elevation and slope provide complementary, non-redundant information: elevation captures broad physiographic and hydrological gradients that determine where continuous fuels develop, while slope distinguishes the flat or gently inclined surfaces that permit lateral spread from rugged terrains that constrain it. Their combined behavior explains why topography consistently emerges as the strongest predictor of fire size across all RF configurations.

LC evenness and LC entropy display opposite but complementary patterns because they describe different dimensions of landscape heterogeneity. Evenness decreases when one or two land-cover classes dominate the patch, creating long continuous fuel runs that favor sustained spread, whereas entropy increases with the number and diversity of cover types, even when their proportions are uneven. Both indices are zero when only one class is present, creating a structural bias toward low values for homogeneous patches typically associated with small or moderate fires. In the global SHAP summary (**Figs. 13b** and **15**), many of the largest fires occur where a dominant class (low evenness) coexists with several secondary LC types (intermediate entropy), coherent with the idea of a continuous flammable matrix with patches of secondary fuels, providing both continuity and diversity of burnable material.

The regional PDPs (**Figs. S17–S19**) confirm and refine these relationships. Evenness shows a consistently negative SHAP gradient across the Wet, Dry and Very Dry Chaco, with the transition to negative contributions near 0.6 in all regions, although small and large fires occur across the full range, indicating modulation rather than strict control. Entropy exhibits a more complex U-shaped structure regionally, with SHAP values decreasing up to ~0.2 and rising toward intermediate entropies, where large fires concentrate, before declining again at high entropy values, where only small fires are observed. These regional patterns reinforce the global interpretation: large fires are most likely to occur in landscapes characterized by a dominant continuous fuel bed enriched by a limited variety of secondary flammable types, whereas highly homogeneous or highly fragmented patches constrain fire growth.

LC fractions modulate fire size through their control on fuel characteristics, continuity and structural barriers, and their SHAP dependence patterns (**Figs. 13b**, **15**, **S17–S19**) are consistent with the heterogeneity indices described above. The tree–shrub–herb mosaic class shows a strong and monotonic negative relationship with fire size across the entire Gran Chaco and in all three regions: high fractional cover of mosaics systematically shifts SHAP values toward smaller fires, whereas the largest fires

appear at lower fractions of the mosaic class. Because mosaics are represented as a single categorical class in CCI-MRLC, patches dominated by mosaics behave as homogeneous units in the evenness and entropy indices because they count as a single LC class. Tree cover displays a broadly similar negative trend in the global model and in the Wet Chaco, reflecting their role of barriers to lateral propagation under a certain threshold of fire intensity. Regional PDPs refine this picture: in the Very Dry Chaco the decline in SHAP values is nearly linear across the tree-cover gradient, whereas in the Dry Chaco a secondary rise in SHAP values at high fractional tree cover suggests the presence of large fires in recently deforested or thinly wooded areas still mapped as forest, where cured understory fuels or active land-clearing may cause or enhance the fire spread.

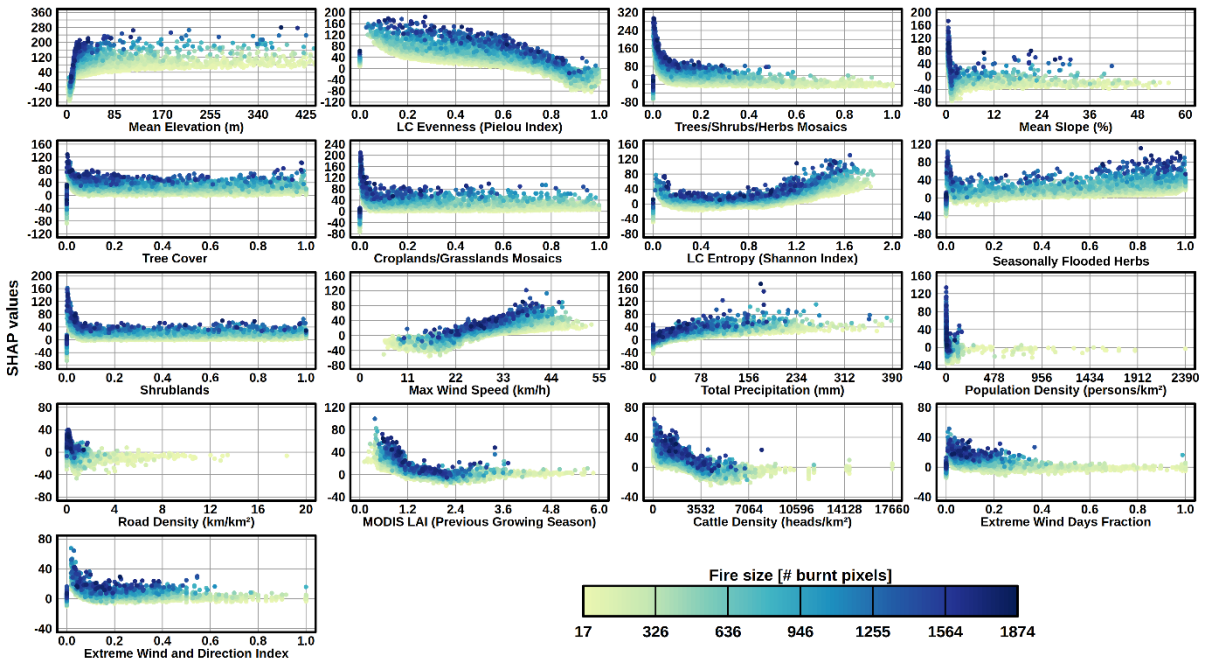

Fig. 15. SHAP dependence plots for ~~all~~the 17 explanatory variables used to predict fire ~~polygon~~patch size (n_cell) with the Random Forest model trained on ~~all~~ fire patches between 1 km² and 100 km~~²~~.² in the entire Gran Chaco between 2001 and 2022. Each panel shows the SHAP value (y-axis) across the range between 0 and the 0.995 quantile of a given feature (x-axis), illustrating the marginal effect of that feature on the model's output. Dots are colored by fire size (number of burned pixels), with darker tones indicating larger fires. Land cover classes represented as fractions.

~~SHAP dependence plots (**Fig. 15**) revealed clear non-linear responses. Elevation had a steep positive effect up to ~70 m, plateauing thereafter, suggesting that slightly elevated terrain favors larger fires, while low-lying areas may be constrained by water bodies or vegetation type. Slope effects were similar: flat to gently undulating terrain (≤10 %) supported larger fires, while steeper slopes curtailed spread. Lower LC evenness (i.e. more homogeneous fuels) and sparse tree cover were associated with larger predicted sizes, reflecting the role of fuel continuity and open vegetation in promoting spread; conversely, heterogeneous landscapes and dense tree cover dampened fire growth.~~

~~Most other predictors showed weak or flat SHAP responses. Only maximum wind speed displayed a consistent positive association with fire size among the dynamic variables, indicating a secondary but detectable influence compared with dominant topographic and structural gradients.~~

~~4~~ Shrublands exhibit more heterogeneous behavior, underscoring their different ecological roles across the precipitation–aridity gradient. In the global model and in the Wet Chaco, shrub fractions show a steep negative exponential decay, with the largest fires concentrated at low shrub cover and exclusively small fires at high shrub dominance, consistent with shrublands forming natural barriers within floodplain matrices. The Dry Chaco shows the opposite pattern: SHAP values increase with shrub cover, indicating that flammable shrublands, which are common on higher, drier terraces, can support large fires when fuels are continuous and well cured. The Very Dry Chaco exhibits a distinct, strongly non-linear shape, with SHAP values stable at low and intermediate shrub fractions but increasing sharply around ~0.8-0.9, before declining at the extreme upper tail; this reflects the concentration of the largest fires in extensive shrub-dominated matrices typical of the western Chaco drylands.

Flooded herbaceous vegetation shows a mixed response globally: SHAP values initially decrease between 0 and ~0.1 but become increasingly positive toward higher fractions, indicating that fires occurring in seasonally desiccated wetlands often reach large sizes. Regional PDPs confirm that this effect is strongest in the Wet Chaco, where dark points cluster at high flooded-herbaceous fractions, and absent in the Very Dry Chaco, where large fires occur only where flooded cover is ~0. Cropland/grassland mosaics mirror the global shrubland pattern, with a clear negative exponential relationship in all regions: large fires almost exclusively occur at low fractions, whereas patches dominated by these mosaics generate small fires. This behavior reflects both their intrinsically discontinuous fuel structure and the fact that agricultural and improved-pasture landscapes are heavily subdivided by field boundaries, roads, and irrigation infrastructure that limit lateral spread. In addition, active fire suppression, systematic fuel removal, and prescribed burning practices in productive cropland and grazing areas further reduce the likelihood that fires in these mosaics evolve into large, contiguous events.

The influence of pre-fire biomass accumulation, represented by previous-season LAI, is modest in global importance but shows consistent region-specific patterns that reflect its role as a broad proxy for vegetation productivity (**Fig. 15**; **Figs. S17–S19**). At the scale of the entire Gran Chaco, SHAP values decrease strongly from low to moderate LAI, with the largest fires concentrated at LAI < 1–1.5, consistent with highly open herbaceous or sparsely wooded systems where fine, continuous fuels dominate. Higher LAI values correspond to increasingly negative SHAP contributions across all regions, indicating vegetation types with greater structural complexity or woody dominance that constrain lateral spread. Regional PDPs refine this interpretation: in the Wet Chaco, increases in LAI coincide with vegetation types that tend to reduce spread regardless of their biomass; in the Very Dry Chaco, the compressed LAI range reflects lower overall productivity (0-4 vs 0-6 in the other regions), and large fires remain associated with the lowest values; in the Dry Chaco, a weak secondary rise in SHAP values at intermediate LAI, forming a U-shape curve, likely reflects biomass accumulation in flammable shrubland systems where moderate productivity enhances fuel availability. Overall, LAI

emerges not as a universal driver of fire size but as a vegetation-structure proxy whose meaning shifts along the Gran Chaco's precipitation–aridity gradient.

Meteorological predictors show consistent but secondary influences relative to topography and vegetation structure (**Figs. 13b**, **15**, **S17–S19**). Maximum wind speed exhibits the clearest signal: SHAP values increase steadily with maximum wind speed up to roughly 40–45 km/h, beyond which they form a plateau. In all regions, large fires cluster toward the upper half of the wind-speed distribution, with a shallow positive slope that reflects the well-known effect of stronger winds enhancing the forward spread of fire fronts. In the FWT-specific RF models, this effect becomes more prominent in Drought-Driven configurations, where maximum wind speed attains higher SHAP-based importance ranks and larger absolute SHAP amplitudes than in Neutral or Wind-Driven FWTs (**Fig. 14**). This pattern indicates that strong winds have greater leverage on fire size when fuels are already cured and moisture is low, while under more benign or mixed weather conditions their influence remains positive but more muted. The similarity of the response among the Wet, Dry and Very Dry Chaco indicates that this relationship is robust across contrasting fuel types and landscape configurations.

In contrast, the two extreme-wind metrics (extreme wind days fraction and extreme wind-and-direction index) display weak negative or near-flat SHAP responses. SHAP values decline from slightly positive to near-zero between fractions of 0 and ~0.2, after which only small fires occur in all regions. The Very Dry Chaco shows a shallow positive segment at very low fractions but converges toward the same pattern. These tendencies likely arise because the extreme-wind variables summarize the frequency of extreme conditions rather than the instantaneous wind state during fire growth, and because extreme-wind events are typically rare and dispersed, producing SHAP structures dominated by the large mass of low-fraction observations. Their behavior therefore does not contradict the positive effect of maximum wind speed but instead reflects the different statistical role of occurrence-based indices in the RF model.

Total precipitation shows uniformly weak contributions across regions. Although the global SHAP curve appears moderately positive at low to intermediate precipitation totals, large fires are clearly concentrated at low rainfall values in all regional PDPs, and small fires dominate wetter intervals. The apparent positive SHAP slope between 0 and ~150 mm results from the construction of the variable itself: precipitation represents the fire-duration-integrated rainfall, which is confounded with event duration. Larger, longer-lasting fires have more opportunity to accumulate rainfall even if spread occurred primarily under dry conditions. This duration bias explains why some large fires appear at relatively high precipitation totals despite the overall negative association between wet conditions and fire growth. Thus, precipitation contributes only marginally to the RF predictions once static fuel and topographic structure are accounted for.

Human-pressure variables (road density, population density, cattle density) have consistently low mean SHAP importance across all RF models (**Fig. 13a**), indicating that they explain only a minor portion of the variance in fire size once topography and vegetation structure are accounted for. Nevertheless, their

marginal SHAP responses (**Figs. 15**, **S17–S19**) reveal systematic gradients that are interpretable in a fire-management context.

Cattle density shows the clearest pattern: SHAP values decline almost monotonically with increasing cattle density, and the largest fires are concentrated at low to moderate densities. At high densities, SHAP values are strongly negative and large fires are absent. This trend is constant across all regions. The most plausible interpretation is indirect: highly stocked ranching systems typically involve intensive fuel management, pasture renewal, and active fire control, reducing the likelihood that ignitions develop into large, contiguous fire patches. However, this mechanism cannot be tested directly with the available data and should be regarded as a behavioral correlation rather than a causal inference.

Road density and population density exhibit parallel patterns. SHAP values are positive at low densities and become increasingly negative as infrastructure or settlement density increases. Large fires occur almost exclusively where road and population density are low, whereas high-density areas are dominated by small fires. These gradients hold in each region, though they are most pronounced in the Wet and Dry Chaco and slightly attenuated in the Very Dry Chaco, where human populations and infrastructure are sparser overall. The interpretation is consistent with broad-scale patterns of fire management: remote areas with limited access generally allow fires to grow larger, whereas areas with more roads, people, and managed landscapes tend to suppress or fragment fires earlier.

Despite these coherent marginal trends, the overall contribution of human-pressure variables remains secondary. Their effects are largely overshadowed by static topographic structure and LC composition, and their marginal signals do not alter the dominance hierarchy observed in **Fig. 14**. Taken together, these results indicate that anthropogenic influences on fire size operate mainly through long-term land-use changes embedded within topographic and vegetation-structure variables, rather than through direct effects captured by density proxies alone.

3.7 Sensitivity experiments

To assess the robustness of the models and the sources of explanatory power, we performed two targeted sensitivity experiments: (i) training a RF without topographic variables, and (ii) replacing the baseline road density product for another with more road detections.

In the No-Topography experiment, the most important observation is that the overall ordering of non-topographic predictors remained stable (**Fig. S20**): vegetation-structure metrics (LC evenness, mosaic cover, tree cover, LC entropy) continued to dominate, while human-pressure and weather variables remained secondary. Despite this stability in feature hierarchy, removing topography resulted in a marked decline in predictive performance (test COR decreasing from ~0.74 to ~0.67; test RMSE increasing from ~110 to ~119 pixels; **Table S3**). SHAP rankings also became less coherent, with several land-cover variables inflating artefactually in importance to compensate for the absence of structural information. These changes confirm that elevation and slope do not act as direct physical drivers but

capture slow-varying ecological gradients that distinguish floodplain herbaceous systems from slightly elevated woody landscapes, which strongly condition the potential for large fire growth.

Before evaluating the effect of substituting OSM with MS road density in the RF models, we quantified how the two datasets differ across the landscape. OSM, being community-curated, captures paved and unpaved major roads reliably but tends to underrepresent informal, secondary, and seasonal tracks, particularly in remote ranching landscapes and sparsely populated areas of the western Dry and Very Dry Chaco. In our dataset, OSM identified 1.12 million km of linear features, whereas MS mapped 1.95 million km, an increase of roughly 74 % in total detected road length. By contrast, the MS product, generated through automated detection from high-resolution imagery, identifies a much larger set of linear features: about 45–60 % of MS segments have no corresponding OSM segment within 50 m, and a large fraction consist of faint, narrow dirt tracks, fencing lines, internal ranch access paths, and grid-aligned extraction routes. These additional features increase the apparent density of minor routes in areas where OSM shows little or no coverage. As a consequence, MS tends to expand the low-to-moderate density classes (0.1–2 km km^{-2}) by 30–50 % in frequency, while suppressing the long extreme tail of OSM, generating a smoother and more homogeneous density surface.

These differences are not spatially uniform. In the Wet Chaco, where agriculture, fragmentation, and population density are higher, the two datasets converge strongly, with Pearson correlations of 0.85–0.90, mean absolute differences of 0.12–0.18 km km^{-2}, and only modest discrepancies in the upper tail. In the Dry Chaco, the correlation drops to 0.80–0.83, as MS detects 40–65 % more low-density tracks than OSM, especially in cattle-ranching corridors and logging frontiers. The Very Dry Chaco shows the largest divergence, with correlations of 0.65–0.72: MS maps a more continuous network of faint tracks and straight-line property boundaries, whereas OSM retains extensive areas of near-zero density but captures some mountainous trail systems that MS misses. Consequently, MS compresses the density distribution (IQR: 0.05–0.45 km km^{-2}) and produces a quasi-normal shape, while OSM remains highly skewed with a dominant zero-density mode and occasional extreme values exceeding 5 km km^{-2}. Nonetheless, median density values remain comparable (OSM: 0.21 km km^{-2}; MS: 0.27 km km^{-2}), and both datasets reproduce the broad east–west gradient in accessibility.

Because road density interacts strongly with landscape structure, we also compared differences across LC contexts and heterogeneity indices. OSM-based density is highest in mosaic-dominated landscapes and cropland–grassland transitions, where road networks are well established and frequently used, reaching median values of 0.8–1.2 km km^{-2}. MS broadens this association by detecting a widespread network of faint tracks within shrublands and semi-open dry forests, raising densities in those classes by 0.1–0.3 km km^{-2} and reducing the contrast between mosaic-rich areas and large, relatively homogeneous herbaceous or woody expanses. When cross-referenced with LC evenness and Shannon entropy, OSM systematically highlights high-density pockets in highly heterogeneous areas ($E > 0.7$, $H > 1.2$), while MS produces weaker gradients and spreads low-to-moderate values more widely across structural classes. These differences suggest that OSM reinforces the tight connectivity between road

density and heterogeneity in mixed landscapes, whereas MS dilutes it by mapping a more pervasive set of minor linear features.

Despite these large structural differences, substituting OSM with MS in the RF models produced negligible changes in predictive performance and no change in feature rankings. Test COR remained at 0.74 for both datasets and test RMSE shifted only marginally from 110.4 to 111.2 pixels (**Table S3**). Road density retained a similarly low mean absolute SHAP value (2–3 % of total importance), and the SHAP dependence curves were nearly identical, showing positive contributions at very low densities (<0.3 km km^{-2}) and increasingly negative contributions as accessibility increases. This indicates that the additional detail captured by MS—particularly the dense network of faint tracks in remote dry areas—does not provide additional explanatory power.

Taken together, these findings support the same conclusions drawn from the original sensitivity experiment: (i) road density is strongly collinear with land-cover composition and landscape heterogeneity; (ii) patch-level aggregation of road metrics reduces the discriminating power of fine-scale differences between datasets; (iii) roads exert only a modest direct influence on final fire size at this regional scale, with most anthropogenic effects being mediated by geography, vegetation structure and long-term land-use patterns.

As a result, neither OSM nor MS provides independent explanatory power beyond what is already captured by topography and LC, and the RF hierarchy of predictors remains stable across both configurations.

4 DISCUSSION

Building on event-level fire ~~polygons~~patches (FPs), we examine how meteorology, landscape structure, and human pressures shape fire size and morphology across the Wet, Dry, and Very Dry Chaco.

4.1 Fire regime and extreme events

FP data reveal a strongly skewed size distribution: many small fires (<5 km²) and a few very large events that dominate burned area (BA), consistent with global patterns ~~(Archibald et al., 2009; García et al., 2022b; Haas et al., 2022; Hantson et al., 2015, 2017). Megafires (>100 km²) are most frequent in the Wet Chaco, where continuous herbaceous fuels in savannas and seasonally flooded vegetation support spread. Gigafires (>1000 km²), although rare, occur almost exclusively in the drier subregions, often in remote areas with limited suppression access, higher shrub biomass, and lower humidity. In extreme years such as 2019–2022, a handful of these events contributed a substantial share of total BA in their respective regions.~~(Archibald et al., 2009; Hantson et al., 2015, 2017; García et al., 2022; Haas et al., 2022). Megafires (>100 km²) are most frequent in the Wet Chaco, where continuous herbaceous fuels in savannas and seasonally flooded vegetation support spread. Gigafires (>1000 km²), although rare, occur predominantly in the Dry Chaco and are often concentrated in remote areas where suppression access may be limited, and where seasonally cured fuels and low humidity can favor sustained spread. ~~These size patterns indicate that both fuel configuration and atmospheric conditions influence the potential for very large fires. We therefore examined how short-term fire weather relates to BA across subregions. Fire weather–BA coupling shows marked spatial variability: in the Wet Chaco, high FWI is consistently associated with large BA, confirming moisture limitation and strong sensitivity to atmospheric conditions, in line with earlier BA-based analyses (San Martín et al., 2023). In the Dry and Very Dry Chaco, correlations are weaker and more heterogeneous, indicating partial decoupling between short-term fire weather and final size, mediated by fuel continuity and antecedent conditions. Lagged relationships clarify this contrast: in drier areas, positive rainfall and vegetation productivity 4–6 months before fire are followed by higher BA once fuels cure, supporting the fire–productivity hypothesis (Pausas and Bradstock, 2007). In wetter areas, where fuels are rarely limiting, short dry spells immediately prior to fire are more predictive of activity, consistent with a moisture-limited regime within varying constraint frameworks across resource gradients (Krawchuk and Moritz, 2011).~~

~~4.2 Fire-weather types across the Chaco region~~

~~To assess how daily fire weather influences fire size, we built on the framework of Hernandez et al. (2015) and Ruffault et al. (2016, 2020), who classified Mediterranean wildfires into Fire-Weather Types (FWTs) based on pre-fire meteorological anomalies (heat, drought, wind) and found that Hot-Drought and Wind-Driven types were strongly linked to large events. Applying a similar pre-fire clustering in~~

~~the Gran Chaco (Neutral, Drought-Driven, Wind-Driven) captured ignition contexts but explained little variation in final size or shape.~~

In the Gran Chaco, most ignitions are human-caused and fire use remains widespread across rural activities (Bravo et al., 2010, 2025), so the spatial and temporal distribution of fire occurrence largely reflects anthropogenic pressure. However, once a fire is ignited, its final size depends more strongly on fuel continuity, landscape structure and fire-weather conditions than on ignition source. Human pressures and their proxies are discussed in *Section 4.5*.

Feron et al. (2024) show that the Gran Chaco region in South America has experienced an increase in the frequency of warm, dry and flammable days, together with a rise in compound warm-dry anomalies over recent decades. Although these diagnostics do not quantify fire behavior, they indicate a background shift toward more frequent atmospheric conditions conducive to high flammability. In our record, 2019–2022 coincides with strongly positive FWI anomalies and multiple large fire years, particularly in the Wet Chaco. Despite the overall decline in BA between 2001 and the mid-2010s, the clustering of extreme years at the end of the time series is consistent with increasing exposure to periods of elevated fire weather under recurrent drought and large-scale climate variability (e.g. intensified La Niña conditions), while noting that the satellite era remains short for robust trend detection.

Extreme fire periods, such as the 2019–2022 season, illustrate this sensitivity. In our record, a handful of very large fires contributed a substantial share of total BA across the three subregions. This pattern aligns with reconstructions of twentieth-century fire activity showing that the Gran Chaco woodlands experience relatively frequent but generally low-to-moderate severity fires, with large fire seasons emerging when fuel accumulation coincides with prolonged dry periods (Bravo et al., 2021, 2025; San Martín et al., 2023; Vidal-Riveros et al., 2023). During 2019–2022, multi-year drought affected large parts of the La Plata basin, including the Gran Chaco, reducing river discharge, soil moisture and wetland extent (Naumann et al., 2023). Consistent with this hydroclimatic context, we observe widespread positive BA anomalies and high FWI, particularly during 2020–2021 and especially in the Wet Chaco, where rivers and floodplains typically constrain lateral spread.

Additionally, as discussed in the Introduction, the COVID-19 pandemic altered mobility, enforcement and on-the-ground fire management across South America, with contrasted effects on fire activity depending on whether restrictions reduced ignitions or weakened surveillance and suppression (Garcia et al., 2021; Eklund et al., 2022; Kumar et al., 2022; Naval Fernández et al., 2023). In the Gran Chaco, mobility declined during peak fire months, yet suppression capacity remained relatively stable due to the continued availability of volunteer brigades, while agrarian expansion and land-clearing dynamics, including deforestation burns and infrastructure projects, continued during lockdown (Castilla, 2021; Naval Fernández et al., 2023; Schmidt and Castilla, 2023). Together, these observations indicate that the persistence of extreme fire seasons during 2020–2022 cannot be explained solely by pandemic-related changes in human activity, and that concurrent drought and elevated fire weather likely played a central role in enabling large fire spread.

We therefore examined how short-term fire weather relates to BA across subregions and found strong spatial contrasts consistent with a fuel-limited to moisture-limited continuum across the Gran Chaco. In the Wet Chaco, high FWI is consistently associated with large BA, confirming moisture limitation and strong sensitivity to atmospheric conditions, in line with earlier BA-based analyses (San Martín et al., 2023) and with varying-constraint frameworks across resource gradients (Krawchuk and Moritz, 2011). In the Dry and Very Dry Chaco, correlations are weaker and more heterogeneous, indicating partial decoupling between short-term fire weather and final size, with FWI effects mediated by antecedent fuel conditions and landscape continuity, consistent with evidence that wildfire activity peaks at intermediate rainfall and productivity levels in semiarid Chaco landscapes, where fuel loads are sufficient but seasonal curing remains pronounced (Bravo et al., 2010; Argañaraz et al., 2015; San Martín et al., 2023). Lagged relationships reinforce this contrast: in drier areas, positive rainfall and vegetation productivity 4–6 months before fire are followed by higher BA once fuels cure, supporting the fire–productivity hypothesis (Pausas and Bradstock, 2007) and matching wet-to-dry sequences linked to widespread burns in western and central Chaco forests (Bravo et al., 2010; Argañaraz et al., 2015; San Martín et al., 2023), whereas in wetter areas short dry spells immediately prior to fire are more predictive of activity because fuels are rarely limiting (Krawchuk and Moritz, 2011).

4.2 Fire-weather types across the Chaco region

To assess how daily fire weather influences fire size, we built on the framework of Hernandez et al. (2015) and Ruffault et al. (2016, 2020), who classified Mediterranean wildfires into Fire-Weather Types (FWTs) based on pre-fire meteorological anomalies (heat, drought, wind) and found that Hot-Drought and Wind-Driven types were strongly linked to large events. Applying a similar pre-fire clustering in the Gran Chaco (Neutral, Drought-Driven, Wind-Driven) captured ignition contexts but explained little variation in final size or shape. This limited explanatory power is consistent with flat, fuel-rich systems where pre-fire anomalies modulate the probability of fire occurrence but do not reliably predict how far fires will spread once ignited.

In contrast, clustering based on during-fire variables (maximum wind speed, total precipitation, drought indices, and the Extreme Wind Directionality Index developed in this study) clearly separated groups with significant differences in size and morphology. Dry, windy days during the fire, favored rapid and large expansion.

~~Our findings contrast with Ruffault et al. (2016, 2020) and Belhadj-Kheder et al. (2020), who found pre-fire or near-ignition anomalies predictive in Mediterranean and North African settings, respectively, with the latter highlighting anomaly duration in low-suppression contexts. This stronger size–weather link for during-fire meteorology likely reflects Chaco-specific traits such as flat terrain, continuous fuels, and permissive fire conditions (Bucher, 1982; Vidal-Riveros et al., 2023), which make wind and humidity more decisive than pre-fire anomalies. In the Mediterranean, fragmented fuels, complex~~

~~topography, and strong suppression (Ruffault and Mouillot, 2015, 2017), translate into ignition-day extremes mattering more. Similar modulation by suppression capacity occurs in western U.S. forests (Higuera et al., 2015).~~

~~Our clustering extends fire-weather typologies to a tropical dry forest context and complements recent Gran Chaco regime classifications (Vidal-Riveros et al., 2024; Naval-Fernández et al., 2025) that omitted meteorological variables, highlighting the key role of fire-active weather in shaping fire morphology.~~

~~Separately, our results also showed that La Niña phases, characterised by precipitation deficits in the Gran Chaco, coincided with elevated FWI, higher BA, and a greater likelihood of large fire events. This pattern was particularly evident during the extreme fire seasons of 2019–2022, illustrating how interannual climate variability modulates fire size potential at regional scales.~~

~~4.3 Landscape pattern influence on fire types~~

~~Beyond meteorological effects, anthropogenic and structural landscape factors~~Our findings contrast with Ruffault et al. (2016, 2020) and Belhadj-Kheder et al. (2020), who found pre-fire or near-ignition anomalies predictive in Mediterranean and North African settings, respectively, with the latter highlighting anomaly duration in low-suppression contexts. The stronger size–weather link for during-fire meteorology that we found likely reflects Chaco-specific traits such as a relatively flat terrain, continuous fuels, and permissive fire conditions (Bucher, 1982; Vidal-Riveros et al., 2023), which make wind and humidity more decisive than pre-fire anomalies. In the Mediterranean, fragmented fuels, complex topography, and strong suppression (Ruffault and Mouillot, 2015, 2017), translate into ignition-day extremes mattering more. A similar modulation by suppression capacity occurs in western U.S. forests (Higuera et al., 2015).

In semiarid mountain landscapes of the Very Dry Chaco, Argañaraz et al. (2015) showed that climatic gradients and productivity govern where fires tend to occur, while topography and land-use mosaics constrain their spatial extent. Although their study addressed fire frequency rather than fire size, the distinction reinforces that the drivers of fire occurrence and the drivers of fire spread are related but not identical, and that landscape context mediates how daily fire weather translates into final fire extent.

Our clustering extends fire-weather typologies to a tropical dry forest context and complements recent Gran Chaco regime classifications (Vidal-Riveros et al., 2024; Naval-Fernández et al., 2025) that omitted meteorological variables, highlighting the key role of fire-active weather in shaping fire morphology.

These fire-weather patterns operate within a landscape where ignitions are predominantly anthropogenic, meaning that, aside from the few lightning-ignited events, human activities largely determine when and where fires start. The eventual size of these events, however, depends more strongly ~~modulated fire size.~~ on daily meteorological conditions and fuel continuity, in a context where fire

suppression capacity is uneven and often limited in remote areas. This contrasts with Mediterranean systems, where highly effective suppression can dampen the influence of during-fire weather on final fire size.

4.3 Topography and landscape structure as primary controls of fire size

Random Forest (RF) models ~~consistently identified~~identified topographic, land cover (LC) and landscape-structure variables as the dominant predictors of final fire size in the Gran Chaco, with mean elevation~~ as the most important predictor across all subregions and seasons, followed by land cover~~, LC evenness, the tree~~ cover, and~~ shrub–herb mosaic LC class and mean slope ~~(Fig. 14). While~~consistently ranking at the top of the SHAP-based hierarchy across all regional, seasonal and fire-weather configurations. The ordering remained stable in sensitivity experiments, and model performance declined when elevation ~~is not a direct control on combustion, it reflects broad ecological gradients in vegetation composition, fuel moisture regimes, and land use history~~ and slope were removed (**Fig. S20**, **Table S3**), confirming that topography acts as an integrative proxy for geomorphological, hydrological and ecological gradients that shape the ~~conditions under which fires develop. In the Chaco, these gradients often translate into water presence and seasonal flooding in lowlands, which can~~spatial context in which fires propagate. A mechanistic interpretation of vegetation effects in terms of fuel continuity and fuel moisture is developed in *Section 4.4*; here we focus on how elevation and slope structure the physical template of fire growth and why they dominate RF-based fire size prediction.

Elevation captures the major physiographic contrasts that structure fuel continuity across the Gran Chaco. In the Wet Chaco, extensive low-lying floodplains and seasonal wetlands generally limit ~~spread, and stronger, more persistent winds in higher~~fire spread but can become highly flammable during the dry season, especially following multi-year droughts when herbaceous biomass cures over broad, continuous surfaces. The marked increase in SHAP values below approximately 20–40 m reflects these drought-prone floodplain and marsh systems, where cured grasses form highly connected fuel beds that facilitate large fire growth. In contrast, slightly elevated terraces and woody islets ("montes" or "albardones") interrupt fuel continuity and act as natural barriers that constrain lateral fire propagation. Spatial patterns in representative Wet Chaco landscapes (**Figs. S21–S22**) support this interpretation, with large fire patches consistently associated with drought-exposed, low-elevation herbaceous systems. In the Dry Chaco, elevation contrasts distinguish floodplain matrices from agricultural mosaics and post-deforestation surfaces that break continuity. Here, the largest fires tend to occur on flat to gently elevated terrain~~, which can enhance it~~ where broad, relatively homogeneous landscape units maintain sufficiently connected fine fuels to support lateral fire growth. These tendencies align with landscape-level analyses in semi-arid central Argentina, where shrub-dominated fuel beds and topographically channeled winds promote the expansion of fire fronts (Fischer et al., 2012). In deforested landscapes, the spatial configuration of fuels is strongly shaped by clearing patterns rather than by geomorphological gradients.

As a result, BA within highly fragmented agricultural or recently cleared regions (**Fig. S23**) often exhibit weaker visual correspondence with elevation contrasts, since fuel continuity arises from land-use structure rather than from topographic controls.

In the Very Dry Chaco, rising elevation leads into sierran landscapes where open shrublands and xeric woodlands dominate. We found a near-linear positive association between fires and elevation up to several hundred meters, consistent with the concentration of large fires in shrub-dominated belts with continuous cured fuels along the mountains. Local examples from the Sierras de Córdoba (**Fig. S23**) demonstrate how topographic position aligns with vegetation structure. Similar relationships between physiographic position, shrub cover and extensive fire spread have been documented in other semi-arid regions of central Argentina (Fischer et al., 2012), underscoring that topography often serves as an effective proxy for the spatial organization of continuous fuels.

Slope provides complementary information to elevation. The largest fires overwhelmingly occur on surfaces with slopes below approximately 2-3 %, where lateral propagation is mostly unrestricted and drainage patterns do not fragment fuels. Steeper terrain consistently hosts smaller fires across the Wet and Dry Chaco, reflecting natural fuel discontinuities. In the Very Dry Chaco, most large fires also occur at low slopes, although some events exploit elongated ridge–valley structures at intermediate slopes, particularly in the sierran environments (**Fig. S23**). The combined behavior of elevation and slope explains why removing both variables in the sensitivity experiment substantially reduced model skill (**Fig. S20**).

Overall, these results indicate that topography structures the physical template within which fire growth unfolds, summarizing geomorphological and hydrological contrasts that influence where large, spatially connected burning conditions can develop. Although ignitions and land management are predominantly human-driven in the Gran Chaco, event-scale human-pressure proxies add limited incremental explanatory power once topography and landscape structure are accounted for; implications for fire use and land-use driven fuel restructuring are developed in *Section 4.5*.

4.4 Vegetation ~~composition exerted a strong influence on size outcomes. Areas dominated by herbaceous or shrub cover, often linked to past or ongoing land-use change, were more prone to large fires, whereas higher tree cover was associated with smaller fires. This pattern aligns with global~~structure, fuel continuity and fuel moisture

Vegetation structure exerts a central influence on fire behavior in the Gran Chaco by shaping fuel continuity and the potential for lateral spread. Across the precipitation gradient, the largest fires occur in herbaceous and shrub-dominated systems where fine fuels can become continuous and seasonally flammable, whereas woody vegetation and heterogeneous mosaics constrain propagation (San Martín et al., 2023). These patterns align with long-standing ecological characterizations of Chaco fire regimes, in which open woodlands, grass–shrub mixtures and seasonally flooded herbaceous vegetation burn more extensively and more frequently than denser forest formations (Bravo et al., 2010, 2025; Naval-Fernández et al., 2025; San Martín et al., 2023; Vidal-Riveros et al., 2023). As discussed in *Section 4.3*,

these vegetation effects operate within a topographic template, but they control fire growth primarily through the composition and spatial continuity of burnable fuels.

A key mechanism emerging from our results is the role of fuel continuity rather than fuel abundance per se. Herbaceous floodplain systems in the Wet Chaco and shrub-dominated systems in the Dry and Very Dry Chaco can provide highly connected fuel matrices during drought years, while woody islets, post-deforestation mosaics, cropland–grassland interfaces and other managed landscapes introduce sharp discontinuities that restrict spread. This mechanism is directly reflected in the strong importance of land cover evenness: low evenness (dominance by a single flammable class) is associated with large fires, whereas high evenness or high entropy corresponds to smaller events due to fragmentation. Similarly, the tree–shrub–herb mosaic class shows a strong negative influence, consistent with mixed woody patches acting as barriers and breaking connectivity.

These structure effects are also coherent with broader evidence that increasing tree cover ~~generally~~often reduces burned area ~~(Bistinas et al., 2014; Haas et al., 2022), although~~ by limiting fine-fuel continuity and increasing shade and moisture retention (Bistinas et al., 2014; Haas et al., 2022). However, exceptions ~~occur~~are well documented where ~~certain~~particular forest types~~, such as~~ can be more flammable than native broadleaf formations, including introduced pine plantations~~, have higher flammability than native broadleaf evergreen forests (Barros and Pereira, 2014; Paritsis et al., 2018; Vidal-Riveros et al., 2023).~~ in some regions (Barros and Pereira, 2014; Paritsis et al., 2018; Vidal-Riveros et al., 2023). In the Chaco context, this underscores that "woody cover" is not a single fire-behavior category: the relevant control is how vegetation structure translates into horizontal continuity of ignitable fuels and seasonal drying.

A second dimension is fuel moisture seasonality, which varies markedly among growth forms. Experimental and remote-sensing work in the Southern Gran Chaco indicates that shrubs and grasses reach low live fuel moisture thresholds earlier in the dry season and maintain these conditions longer than tree species (Bianchi et al., 2014; Argañaraz et al., 2016, 2018). Differences in live fuel moisture ~~between growth forms (Yebra et al., 2019) further explain the greater spread potential in shrub- and grass-dominated systems~~among growth forms provide a mechanistic basis for the contrasting role of shrublands along the gradient, with shrub patches often limiting spread in wetter floodplain landscapes but promoting larger fires in drier regions where shrub matrices cure rapidly and sustain combustion over large areas. This is consistent with the broader finding that shrubs and grasses can reach lower moisture contents during the dry season than tree species (Yebra et al., 2019). Flooded herbaceous vegetation likewise can function either as a barrier or as a flammable matrix depending on hydrological conditions, becoming a major driver of large burns when multi-year droughts desiccate wetlands.

~~Landscape heterogeneity, expressed as lower land-cover evenness (i.e., more homogeneous fuels), was also linked to larger fires, reflecting the role of continuous fuel beds in enabling propagation. Conversely, heterogeneous mosaics with high evenness disrupted spread, acting as natural firebreaks (Povak et al., 2018). Together, these results show that while fire-active weather is an important~~

determinant of spread (**Section 4.2**), the physical and vegetative structure of the landscape sets the upper limits for how large fires can become.

4.4 Fire shape as an indicator of fire weather

Building on the fire-weather clustering (**Section 4.2**) and landscape controls (**Section 4.3**), we examined whether fire morphology can reveal the influence of landscape or climatic drivers of spread, taking advantage of the detailed FP-level shape and size metrics provided by FRYv2.0 (Laurent et al., 2018; Chen, 2025). We hypothesized that elongation and perimeter complexity would be enhanced by strong, steady winds, whereas complex topography or fragmented fuels would produce more irregular shapes. In the Gran Chaco, fires occurring under strong, persistent winds displayed significantly larger perimeters and greater elongation, supporting our hypothesis and highlighting morphology as a signature of wind-driven fire types.

To our knowledge, the hypothesis that fire elongation and perimeter complexity can serve as indicators of prevailing wind influence on fire spread has rarely been tested directly, making this a novel contribution of our study. Barros et al. (2012, 2013) showed that watershed orientation influenced fire spread in California, and Mansuy et al. (2014) reported similar effects in Canadian boreal forests, but neither explicitly linked shape to dominant wind direction. We propose that the combined analysis of shape and size offers a valuable benchmark for process-based fire models, which often rely on simplified ellipsoidal spread assumptions (Hantson et al., 2016), and could help train emerging machine-learning approaches for global fire hazard prediction (Li et al., 2023; Liu et al., 2025; Zhang et al., 2023).

4.5 Deforestation and Prescribed Burning

Anthropogenic influences on the Gran Chaco fire regime include the advancing agricultural frontier, characterized by rapid land-use change and deforestation (Arriaga-Velasco-Aceves et al., 2021; Boletta et al., 2006), and the widespread use of fire as a management tool. Prescribed burning typically occurs in late winter and early spring, before the wet season (San Martín et al., 2023), and is generally limited to periods with lower wind speed and limited drought, following decision-support guidelines for ignition (Hsu et al., 2025). However, forecasts are uncertain, and fire-prone conditions can quickly develop after ignition, allowing burns to escape their intended boundaries. Such escaped prescribed fires, although often managed to limit societal impacts, remain a recurrent hazard (Black et al., 2020; Li et al., 2025). FRYv2.0 and other global burned-area products cannot distinguish between wildfires and prescribed burns, restricting our ability to assess their occurrence in the region. Although Hsu et al. (2025) compiled a global prescribed fire dataset, the Gran Chaco is not covered. Many spring fires are likely prescribed burns, but systematic monitoring is lacking. Similarly, we could not isolate deforestation fires, which in the region tend to occur mostly within three years after forest clearing (San Martín et al., 2023). High-

~~resolution burned area products combined with tree cover data could help identify such events, as demonstrated for Africa (Khairoun et al., 2024).~~

~~Improved detection of prescribed and deforestation fires would enable better risk assessment of escaped burns and could promote greater societal acceptance of prescribed fire as part of integrated fire management for hazard mitigation (Oliveras Menor et al., 2025).~~

Productivity effects on fire behavior also emerge at broader temporal scales. We showed that vegetation greenness anomalies (EVI) respond tightly to antecedent rainfall and covary with FWI during the fire season, highlighting a classic fuel–productivity pathway: wet periods promote biomass accumulation, followed by curing during dry spells that increases flammability. This mechanism is widely documented in semi-arid Chaco systems (Bravo et al., 2010; Argañaraz et al., 2015; San Martín et al., 2023). In contrast, previous-season LAI, used here as a coarse proxy for accumulated biomass, played a comparatively minor role. LAI integrates total canopy foliage, including woody components, and therefore does not isolate the herbaceous and shrub layers most critical for fire spread. This likely explains its weak association with fire size in our models and reinforces the importance of considering fuel type and structure, rather than total leaf area, when interpreting vegetation controls on fire behavior in the Chaco.

Taken together, these results show that vegetation structure mediates fire size in the Gran Chaco through three complementary mechanisms: (i) the fuel type and its degree of continuity across the landscape, which determines how far fires can propagate; (ii) the seasonal and interannual dynamics of fuel moisture, which vary among plant growth forms and strongly influence the timing and intensity of burning; and (iii) the productivity–curing sequence that links antecedent rainfall, herbaceous biomass accumulation and subsequent desiccation. These mechanisms operate differently along the precipitation–aridity gradient, producing distinct spatial fire regimes but a consistent overall pattern: large fires emerge primarily in continuous, fine-fuel systems that undergo strong seasonal drying, while fragmented or woody-dominated landscapes constrain spread regardless of weather conditions.

4.5 Human pressures and fire use in the Gran Chaco

Fire regimes worldwide are tightly linked to human activity: most ignitions are anthropogenic, and both land-use change and active suppression have reshaped BA patterns in many regions (Bowman et al., 2009, 2011; Archibald et al., 2013; Andela and van der Werf, 2014; Andela et al., 2017). The Gran Chaco fits within this global picture. It is a human-dominated dry forest and savanna system where fire is at once a natural ecological process and a widespread management tool, particularly in rangelands and agricultural frontiers (Bucher, 1982; Kunst and Bravo, 2003; Bravo et al., 2010, 2025).

Within the Gran Chaco, fire use is deeply embedded in pastoral and agricultural practices. Historical and ethnographic accounts document the use of fire by indigenous and rural communities in the Chaco

and neighboring ecoregions for hunting, communication, warfare and the management of plant resources (Arenas, 2003; Junk and Nunes da Cunha, 2012; Sugiyama et al., 2025). As in other tropical dry regions, most events are human-ignited and intentional, associated with land clearing, slash-and-burn deforestation or the disposal of residues, with a smaller fraction being accidental or natural (Baumann et al., 2018; De Marzo et al., 2023; Gasparri and Baldi, 2013; Gürtler, 2009). Modern land users routinely burn grasslands and savannas at the end of the dry season to stimulate grass regrowth and improve forage quality, often under informal or weakly regulated conditions (Kunst and Bravo, 2003; Kunst et al., 2016; Coronel et al., 2021; San Martín et al., 2023; Bravo et al., 2025). Many fires start in managed or unmanaged grasslands, savannas or croplands and subsequently spread into neighboring forests and shrublands (Bravo et al., 2010; Tálamo et al., 2013; Loto and Bravo, 2020; Giorgis et al., 2021; De Marzo et al., 2022). In this context, exotic grasses have been shown to enhance fuel continuity and fire intensity in several dryland systems (D'Antonio and Vitousek, 1992; Kunst et al., 2016; Bravo et al., 2025), but their spatial extent and dominance within the Gran Chaco remain heterogeneous and poorly constrained at regional scales. They should therefore be regarded as one of several possible mechanisms influencing fuel structure, rather than as a pervasive or dominant driver of large fires.

A further anthropogenic dimension concerns deforestation fires and the diverse forms of land-clearing burns that accompany agricultural expansion. In the Gran Chaco, the agricultural frontier has advanced rapidly over the past decades, and fire is routinely used to remove woody debris and prepare newly cleared fields, often as part of slash-and-burn cycles (Baumann et al., 2018, 2022; Boletta et al., 2006; De Marzo et al., 2023; Gasparri and Baldi, 2013; Gürtler, 2009). These fires can be extensive, but their spatial footprint depends strongly on how clearing interacts with fuel continuity, woody debris loads and local weather (San Martín et al., 2023).

A similar challenge applies to prescribed and semi-prescribed burns, which are widespread in rangeland management but rarely conducted under formal prescriptions or systematic monitoring frameworks (Bravo et al., 2025; Coria et al., 2021, p.202; Kunst et al., 2016; Kunst and Bravo, 2003). Many burns are intended to be low-intensity pasture treatments undertaken in late winter or early spring, yet under drought or wind anomalies they may escape control and evolve into landscape-scale events, as documented in multiple regions of the Chaco. Although global inventories of prescribed fire exist (Hsu et al., 2025), they do not cover the Gran Chaco, underscoring the need for regional efforts to differentiate intentional, escaped and accidental fires. The lack of this information helps explain why our human-pressure variables account for little variance in final fire size: the signal of fire use is embedded within vegetation structure, fuel loads and land-cover mosaics, rather than through independent demographic metrics or ignition proxies that lack temporal and operational detail.

In this context, our finding that human-pressure variables play a secondary role in predicting final fire size does not imply that humans are unimportant for the fire regime, but rather that their influence is mediated primarily through long-term land-use change and fuel restructuring. FRY v2.0 and related satellite products cannot distinguish between wildfires, escaped prescribed burns, deforestation fires or

routine pasture burns, and thus the anthropogenic component enters the analysis mainly through its imprint on vegetation structure, land-cover mosaics and fuel continuity. As discussed in *Sections 4.1* and *4.4*, the extreme fire seasons of 2019–2022 occurred during a prolonged La Niña episode that produced exceptional drought across the La Plata basin (Naumann et al., 2023; San Martín, 2024; Bravo et al., 2025). Despite changes in mobility and surveillance during the COVID-19 pandemic, large fires remained concentrated in fuel-rich, drought-stressed landscapes, indicating that climatic anomalies and fuel structure set the upper bound for fire size, while humans primarily determine ignition timing and location.

Livestock production offers a clear example of how human pressures modulate fire regimes indirectly. Grazing can interrupt the positive feedback between grasses and fire by reducing fine fuels, altering vegetation composition and promoting woody encroachment (Adámoli et al., 1990; Cingolani et al., 2013; Coria et al., 2021; Bravo et al., 2025). A global analysis showed that higher livestock densities in tropical rangelands are associated with lower fire frequency and increased shrub and dwarf tree cover (Bernardi et al., 2019), and regional syntheses for the Gran Chaco report that grazing interferes with fire–grass feedbacks and contributes to shrub expansion (Alessio et al., 2008; Alinari et al., 2015; Vidal-Riveros et al., 2023). The SHAP gradients we obtained for cattle density mirror these findings: large fires are concentrated at low to moderate densities, while high-density ranching landscapes are dominated by small events, consistent with a scenario where heavy grazing reduces continuous fine fuels and increases woody cover, thereby limiting maximum fire size even if fire weather remains conducive.

Road density and accessibility show a similar, albeit more complex, relationship. Numerous studies indicate that road expansion can both increase ignitions and fragment landscapes, thereby reducing the maximum size of individual fires (Andela and van der Werf, 2014; Bowring et al., 2024). In our analysis, both OpenStreetMap and Microsoft road detections density exhibited the same marginal pattern: large fires occur predominantly in areas with low road density, whereas regions with high road density are dominated by small fires. The sensitivity experiment substituting OSM with Microsoft roads confirmed that this pattern is robust and that differences in road datasets have negligible impact on predictive performance when medium to high resolution topography and LC mapping are included. The low overall importance of road density likely reflects two structural issues. First, road networks are strongly collinear with geography, LC composition and landscape heterogeneity, so much of their influence on fragmentation and suppression potential is already encoded by those variables. Second, averaging road density at the FP scale erases the spatial configuration of roads relative to ignition points and spread pathways, which is critical for understanding how roads constrain or redirect fire fronts.

Population density exhibits a comparable gradient, with sparse human presence associated with larger fires and densely populated areas dominated by smaller events, consistent with more active suppression, earlier detection and greater fuel management in productive landscapes. However, remotely sensed data and coarse demographic layers cannot capture the full social dimension of fire, including local

perceptions, traditional burning practices and informal suppression. Recent reviews emphasize that the perspectives and knowledge of local communities are rarely incorporated into peer-reviewed fire research in the Gran Chaco, despite being widely discussed in grey literature and the media (McDaniel et al., 2005; Devisscher et al., 2016, 2019; Coronel et al., 2021; Vidal-Riveros et al., 2023). San Martín et al. (2023) and Bravo et al. (2025) explicitly call for interdisciplinary approaches that combine environmental and social sciences to better understand human–fire interactions in this region.

Overall, our results suggest that anthropogenic influences on fire size in the Gran Chaco operate mainly through their cumulative effects on vegetation structure, fuel continuity and landscape fragmentation, rather than through direct, independently measurable controls at the event scale. Ignitions are overwhelmingly human-driven, but the final size of fires is governed by the interaction between this ignition pressure, long-term land-use trajectories and the windows of opportunity created by drought and fire-conducive weather. Future work that integrates spatially explicit ignition records, fine-scale fuel management data, and socio-cultural information on fire use would allow a more complete quantification of the human contribution to fire size distributions in this rapidly changing dry forest biome. One good example of the potential of such interactions is presented in Hernández et al. (2022), who show that climate-related risks in rural Chaco communities can only be understood through frameworks that combine environmental diagnostics with local practices, knowledge systems and power relations. Their coproduction process demonstrates that the way people perceive, monitor and respond to climatic hazards fundamentally shapes exposure and outcomes. A comparable socio-environmental approach applied to fire research could reveal how decisions about land clearing, burning, suppression and access interact with drought and fuel conditions to determine whether an ignition remains small or develops into a large fire.

4.6 Limitations and perspectives

~~Direct human influences, such as ignition sources, suppression actions, and fire management practices, could not be explicitly included in this study due to limited data availability. Their effects are likely reflected indirectly through variables such as vegetation structure, road density, population density, and land cover, but their absence restricts our ability to fully capture anthropogenic modulation of fire size. The ERA5-Land reanalysis at 0.1° (~9 km) resolution, although considered high for a global meteorological dataset, remains too coarse to fully represent local-scale wind variability, solar radiation heterogeneity, and terrain-induced thermal gradients that can influence fire spread. Advances in downscaling techniques for wind (Dujardin and Lehning, 2022), solar radiation (Druel et al., 2025), and temperature (Kusch and Davy, 2022) may improve the spatial realism of these variables in future fire regime analyses, especially in complex landscapes. However, these approaches were not applied here. More fundamentally, the absence of dynamic coupling between fire behaviour and atmospheric processes remains a key constraint, as fire–atmosphere feedbacks are not represented in our predictors.~~

~~The FRYv2.0 fire dataset is based on the global 250 m FireCCI51 product, which can both overestimate and underestimate fire size. Overestimation may occur when partially burned pixels are classified as fully burned, particularly along fire edges or within heterogeneous scars (Pettinari et al., 2021). Underestimation arises from omission errors, which are common for small, low-intensity, or fragmented fires that fall below the detection threshold, or in areas affected by cloud cover, dense smoke, or mixed land cover (Lizundia-Loiola et al., 2022).~~

~~Other FireCCI51 specific limitations should also be acknowledged. BA is likely underestimated during the early period of the dataset (2001 to mid-2002) when only Terra MODIS data were available. Ignition dates may contain biases depending on satellite detection quality and meteorological conditions (Lizundia-Loiola et al., 2020). Furthermore, the aggregation of pixels into FPs depends on temporal thresholds used to group neighbouring pixels within the same event (Moreno et al., 2021; Oom et al., 2016).~~

~~Future developments in fine-resolution burned area products (e.g. 20 m), such as FireCCISFD20, have already demonstrated substantial improvements in Africa, detecting 80–120 % more burned area (Chuvieco et al., 2022). Delivering similar products at continental or global scale, as long requested by the fire science community (Mouillot et al., 2014), will be critical to reduce both overestimation from coarse-pixel classification and underestimation from omission errors, and to improve the accuracy of fire size and distribution assessments.~~

Several limitations of this study stem from the nature of the available datasets and from methodological constraints. First, the meteorological information used to characterize fire weather, which relies on ERA5-Land at 0.1° resolution and cannot resolve local wind acceleration, channeled flows, shading, or fine-scale thermal gradients that influence fire spread in heterogeneous terrains. Although maximum wind speed and directional persistence emerged as meaningful predictors, the coarse resolution likely under-represents sub-kilometer variability in fire-atmosphere coupling, particularly in sierran environments. In addition, ERA5-Land precipitation is not bias-corrected, and its known tendency to smooth short-lived convective events at sub-daily scales may influence variables derived from it, such as total precipitation during the fire, potentially dampening the detection of sharp wetting or drying transitions within the time window of fire growth. Advances in downscaling techniques for wind (Dujardin and Lehning, 2022), solar radiation (Druel et al., 2025), and temperature (Kusch and Davy, 2022) may improve the spatial realism of these variables in future fire regime analyses, especially in complex landscapes. However, these approaches were not applied here.

Second, the FRY v2.0 dataset inherits all structural uncertainties of FireCCI51, including omission of small or low-intensity burns, overestimation in heterogeneous pixels, and potential inconsistencies in early MODIS years (Lizundia-Loiola et al., 2020; Pettinari et al., 2021). The reconstruction of FPs also depends on temporal grouping parameters that merge or split neighboring pixel clusters (Oom et al., 2016; Moreno et al., 2021). These issues constrain our ability to resolve very small events, the fine-scale

geometry of scars, and rapid-fire spread fronts. The development of higher-resolution BA products has been repeatedly requested by the fire science community (Mouillot et al., 2014), and regional examples, such as the FireCCISFD20 product at 20 m for Africa (Chuvieco et al., 2022), have already demonstrated large gains in BA detection. Such advances will be essential to quantify fire size distributions and fire spread processes more accurately across the Gran Chaco.

Third, the satellite BA products used here do not provide information on fire type and therefore cannot distinguish among wildfires, escaped prescribed burns, deforestation fires, and routine rangeland burns. This restricts our capacity to attribute human-driven fire dynamics directly, since the anthropogenic signal enters the models primarily through long-term structural changes in vegetation composition, fragmentation and fuel continuity rather than through explicit information on ignition sources or operational decisions. The absence of spatially explicit ignition datasets, suppression records and fine-scale fuel management layers further limits our ability to separate environmental controls from management outcomes.

In the absence of direct information on fire type or ignition mechanism, human-pressure variables such as road density, population density or cattle density are used as indirect proxies for socio-environmental processes. Their weak importance in the RF models should therefore not be interpreted as evidence that human influence is negligible, but rather as a reflection of the limited thematic precision, spatial resolution and temporal representativeness of the available demographic and infrastructure datasets. These proxies capture only broad accessibility and land-use patterns, and they cannot represent operational decisions, intentional fire use or suppression capacity. As a result, landscape and LC variables at the scale of our analysis absorb much of the anthropogenic signal in our models.

Fourth, additional limitations arise from the interaction between the RF framework and the structure of the predictor datasets. Tree-based ensembles and SHAP-based rankings can be sensitive to differences in data quality, spatial support and collinearity among predictors. These conditions are better met by high-quality satellite-derived predictors such as elevation and annual land-cover layers than by demographic or infrastructure datasets, which are often coarser, noisier or less spatially complete. As a result, part of the dominant SHAP importance of topography and vegetation likely reflects both genuine structural controls on fuel continuity and the statistical advantages associated with these higher-quality predictors, rather than their purely mechanistic influence. The sensitivity experiment without topography confirms that elevation and slope summarize multiple unobserved gradients, partly compensating for limitations in other predictors. Although cross-validation diagnostics suggest limited overfitting, the RF remains bound to the chosen feature set and to the aggregation scale of fire patches. Future work could evaluate machine-learning architectures that operate directly on high-resolution imagery or spatial neighborhoods, for example through convolutional or graph-based neural networks combined with richer socio-economic layers, to test whether the predictor hierarchy found here is robust.

Fifth, several environmental variables used in this study should be interpreted as proxies rather than mechanistic drivers. Elevation and slope summarize hydrological, geomorphological and ecological

gradients rather than exerting direct effects on combustion. Similarly, the previous-season LAI integrates productivity and vegetation structure but does not explicitly represent live fuel moisture or curing dynamics. Incorporating finer-resolution fuel moisture content datasets, daily vegetation optical depth or in situ biomass measurements (Argañaraz et al., 2016, 2018) would strengthen mechanistic interpretations.

Finally, our statistical models do not capture feedbacks between fire behavior and atmospheric processes, nor do they represent dynamic suppression, diurnal cycles of wind and humidity, or sub-daily fire-growth stages. Mechanistic fire-spread models and hybrid statistical–physical approaches could help resolve these processes and offer a complementary perspective.

Despite these limitations, our results provide a consistent regional picture: static landscape structure, summarized by topography and vegetation composition, dominates fire-size outcomes, while meteorology governs the windows of opportunity for rapid spread. Future work that combines high-resolution BA mapping, improved fire-weather fields, ignition and management records, and socio-cultural dimensions of fire use would allow a more comprehensive understanding of the evolving fire regime of the Gran Chaco.

5 CONCLUSIONS

This study advances understanding of fire regimes across the Wet, Dry, and Very Dry Chaco through a spatially explicit analysis of fire events from 2001–2022. We document strong regional contrasts in fire size, seasonality~~,~~ and ~~drivers, shaped by interactions between fuels,~~morphology, and show that these patterns arise from the combined effects of fuel structure, fire weather~~,~~ and long-term land use change. Fire patch (FP) sizes were highly skewed: over 80% of detected fires were <5 km², yet large events dominated total burned area (BA). Megafires (>100 km²) occurred in all subregions, with the Wet Chaco recording the most. Gigafires (>1000 km²) were rare but concentrated in the Dry Chaco, where some single events exceeded 50% of annual BA. The Wet Chaco burned most extensively (~2× the Dry Chaco), with the highest fire frequency and ignition density, reflecting greater biomass productivity and continuous fuels. The Very Dry Chaco, although it contributes the smallest share of total BA, is characterized by sporadic large, mega and gigafires that produce abrupt interannual peaks, consistent with a more stochastic fire regime where a few extreme events dominate variability.

The Fire Weather Index (FWI) ~~showed~~displayed its strongest~~,~~ and most coherent relationship with BA and fire counts in the Wet Chaco ~~(r~~, where most pixels (93%) showed positive correlations between monthly FWI and BA anomalies (R up to 0.7), ~~while drier subregions displayed~~ confirming a moisture limited regime. In the Dry and Very Dry Chaco, correlations were weaker~~,~~ and more heterogeneous ~~patterns~~, indicating ~~additional controls.~~that short term fire weather alone cannot explain spatial and interannual variability in BA. The ~~2020~~extreme fire seasons of 2019–2022 ~~drought produced unprecedented fire activity, though large outbreaks also~~coincided with a prolonged La Niña event and widespread positive FWI anomalies, especially in the Wet, yet some years with extensive burning occurred without ~~extreme~~exceptional FWI, underscoring the ~~role of~~ additional roles of fuel continuity, antecedent conditions and ignition patterns ~~and fuel availability. In the Wet Chaco, 93% of pixels had positive FWI–fire correlations, compared to ~60% in the Dry and Very Dry Chaco~~.

~~Lag~~Lagged analyses revealed ~~dual mechanisms:~~a fuel productivity mechanism in drier areas~~, wet~~ and a short-term drying control in wetter ones. In the Dry and Very Dry Chaco, positive rainfall and greenness anomalies several months before the fire season were followed by higher BA once fuels cured, consistent with a productivity–curing sequence where wet periods build biomass ~~buildup (4–6 months prior) preceded high~~that later dries and burns. In wetter sectors of the Chaco, shorter dry spells immediately before the fire season were more closely associated with BA peaks, reflecting conditions where fuels are rarely limiting and fire activity~~, while in wetter areas, short-term pre-fire dryness was more predictive.~~ responds primarily to transient moisture deficits. La Niña phases ~~amplified~~strengthened fire potential ~~via~~across the region through reduced rainfall and elevated ~~FWI.~~

~~During~~ fire weather, and the clustering of ~~fire-weather types (FWTs) identified wind intensity and directionality as stronger predictors of fire morphology than other pre-fire conditions. Persistent winds produced larger, elongated, and cohesive burns, highlighting morphology as an indicator of wind-driven~~

~~dynamics~~extreme fire years at the end of the record suggests increasing exposure to such windows of opportunity.

Fire weather types (FWT) provided additional insight into how daily meteorology shapes fire outcomes. Pre-fire clustering captured ignition contexts but showed limited discrimination in final size or shape, consistent with a system where ignitions are predominantly anthropogenic and occur under broadly permissive conditions. In contrast, clustering based on during-fire meteorology separated neutral, drought-driven and wind-driven fires with clear differences in size and morphology. Wind-driven events were larger, more elongated and more cohesive than drought-driven fires, highlighting fire patch morphology as a signature of strong, persistent winds that could be used to benchmark process-based fire models and emerging machine learning approaches for fire behavior prediction.

Random Forest models ~~ranked mean~~ showed that static landscape structure dominates fire size outcomes. Mean elevation, land cover evenness, a tree–shrub–herb mosaic land cover~~,~~ class and mean slope consistently ranked highest in ~~size prediction. Larger fires occurred~~SHAP based importance across regions, seasons and FWTs, ahead of meteorological and human pressure variables. With regional variations, large fires mostly concentrated in flat, low~~-elevation areas with low tree cover;~~ lying or gently elevated areas that host continuous herbaceous or shrub fuels, while steeper slopes and higher ~~forest~~tree cover limited spread. Shrublands and flooded herbaceous vegetation played contrasted roles along the precipitation gradient, inhibiting spread in wetter, fragmented floodplains and supporting large fires in drier, shrub dominated matrices.

~~In the Dry and Very Dry Chaco, part of the BA comes from one-time deforestation fires occurring after clearing, generally small to moderate in size. Extreme megafires and gigafires instead resulted from rare alignments of continuous fuels and exceptional weather, especially persistent winds and prolonged dryness, which exceeded suppression capacity. This distinction is critical for separating land-use related burns from large climatic extremes in risk assessments.~~

Human pressures in the Gran Chaco are essential for ignition but emerged as secondary for explaining the variation in final fire size once landscape structure is accounted for. Cattle, road, and population density all showed interpretable SHAP gradients, with larger fires occurring in remote, sparsely populated landscapes with low accessibility and low to moderate grazing pressure, and smaller fires in heavily managed areas with high road density or high stocking levels. However, their overall importance in the models was low, reflecting that most anthropogenic effects on fire size operate indirectly through long term transformations of vegetation structure, fuel continuity and fragmentation, or that they are hard to account for through remote sensing. Deforestation and land clearing fires contributed to BA, particularly in expanding agricultural frontiers, but the largest megafires and gigafires arose when continuous fine fuels, drought and wind aligned in ways that exceeded available suppression capacity.

By combining medium- resolution ~~fire patch~~FP data, reanalysis-based weather metrics, machine learning~~,~~ and landscape analysis, we identify key biophysical, climatic~~,~~ and anthropogenic determinants of fire size and shape~~.~~ in a major South American ecoregion, the Gran Chaco. Our results emphasize

that topography and vegetation structure set the primary template for fire spread, that during-fire meteorology governs when ignited fires evolve into large, elongated events, and that human activities shape fire size mainly through their cumulative imprint on fuels and landscape configuration rather than through simple demographic gradients. These findings inform fire risk ~~forecasting~~assessment and management under ongoing land-_use intensification and climate variability in the Gran Chaco, and highlight the ~~potential of morphology and during-fire wind metrics to benchmark and improve process-based global fire models.~~

~~6 APPENDIX A~~

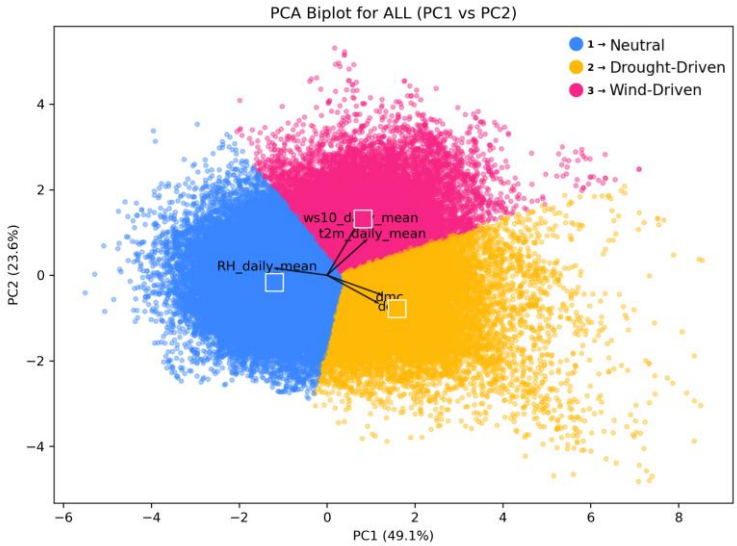

~~**Fig. A1:** Principal Component Analysis (PCA) biplot of pre-fire meteorological anomalies used for K-means clustering, showing the distribution~~need for high resolution BA products, improved fire weather fields, explicit ignition and management records and stronger integration of ~~fire patches across the first two principal components (PC1 and PC2), which explain 49.1% and 23.6%~~socio-cultural dimensions of ~~the total variance, respectively. The three clusters are color-coded and numbered as follows: Cluster 1 (blue) corresponds to Neutral conditions, Cluster 2 (orange) to Drought-Driven conditions (with high DC and DMC anomalies), and Cluster 3 (pink) to Wind-Driven conditions (characterized by elevated wind speed and temperature anomalies). Arrows represent the contribution of the original variables to the PCA axes. This ordination was used to guide the semantic naming of clusters.~~

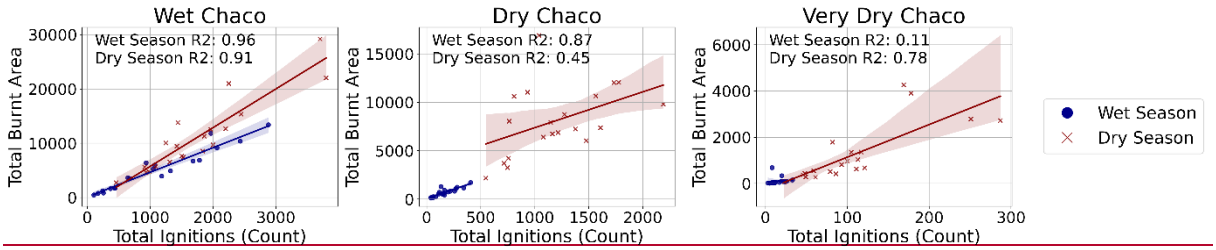

~~**Fig. A2:** Scatter plots and linear regressions between total annual BA and total annual ignitions between 2001 and 2022 in the Wet, Dry- and Very Dry Chaco, divided into wet season fires (blue circles) and dry season fires (red crosses).~~

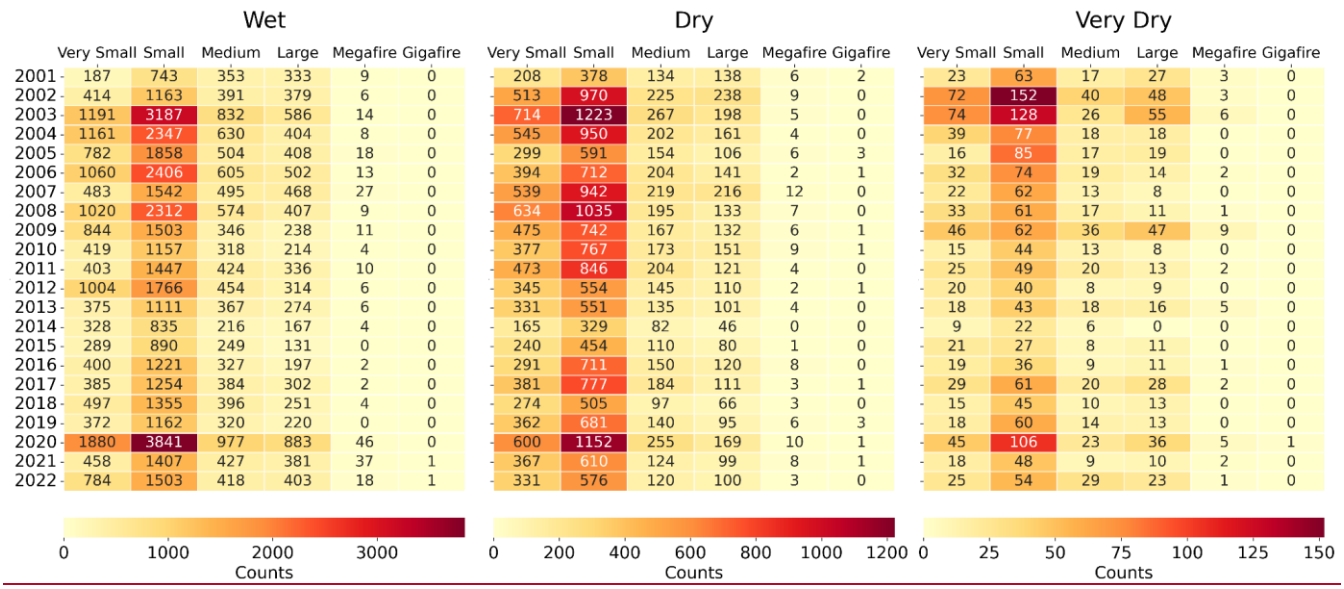

~~**Fig. A3:** Total counts of fire polygons separated by size category between 2001 and 2022 in the Wet, Dry, and Very Dry Chaco.~~

~~**Table A1.** Number of fires detected by FRYv2.0 between 2001 and 2022 classified by fire size. WS: wet season; DS: dry season.~~

~~Region~~	~~Very Small (0-1 km²)~~		~~Small (1-5 km²)~~		~~Medium (5-10 km²)~~		~~Large (10-100 km²)~~		~~Megafire (100-1000 km²)~~		~~Gigafire (> 1000 km²)~~		~~Total~~
~~Season~~	~~WS~~	~~DS~~	~~WS~~	~~DS~~	~~WS~~	~~DS~~	~~WS~~	~~DS~~	~~WS~~	~~DS~~	~~WS~~	~~DS~~	
~~Wet~~	~~8414~~	~~6322~~	~~17,018~~	~~18,992~~	~~4340~~	~~5667~~	~~3264~~	~~4534~~	~~91~~	~~163~~	~~2~~	~~0~~	~~68,807~~
	~~14,736~~		~~36,010~~		~~10,007~~		~~7,798~~		~~254~~		~~2~~		
~~Dry~~	~~3526~~	~~5332~~	~~5754~~	~~10,302~~	~~1201~~	~~2485~~	~~841~~	~~1991~~	~~24~~	~~94~~	~~0~~	~~15~~	~~31,565~~
	~~8,858~~		~~16,056~~		~~3,686~~		~~2,832~~		~~118~~		~~15~~		
~~Very Dry~~	~~334~~	~~300~~	~~708~~	~~691~~	~~187~~	~~203~~	~~200~~	~~238~~	~~13~~	~~29~~	~~0~~	~~1~~	~~2,904~~
	~~634~~		~~1,399~~		~~390~~		~~438~~		~~42~~		~~1~~		
~~Total~~	~~24,228~~		~~53,465~~		~~14,083~~		~~11,068~~		~~414~~		~~18~~		~~103,276~~

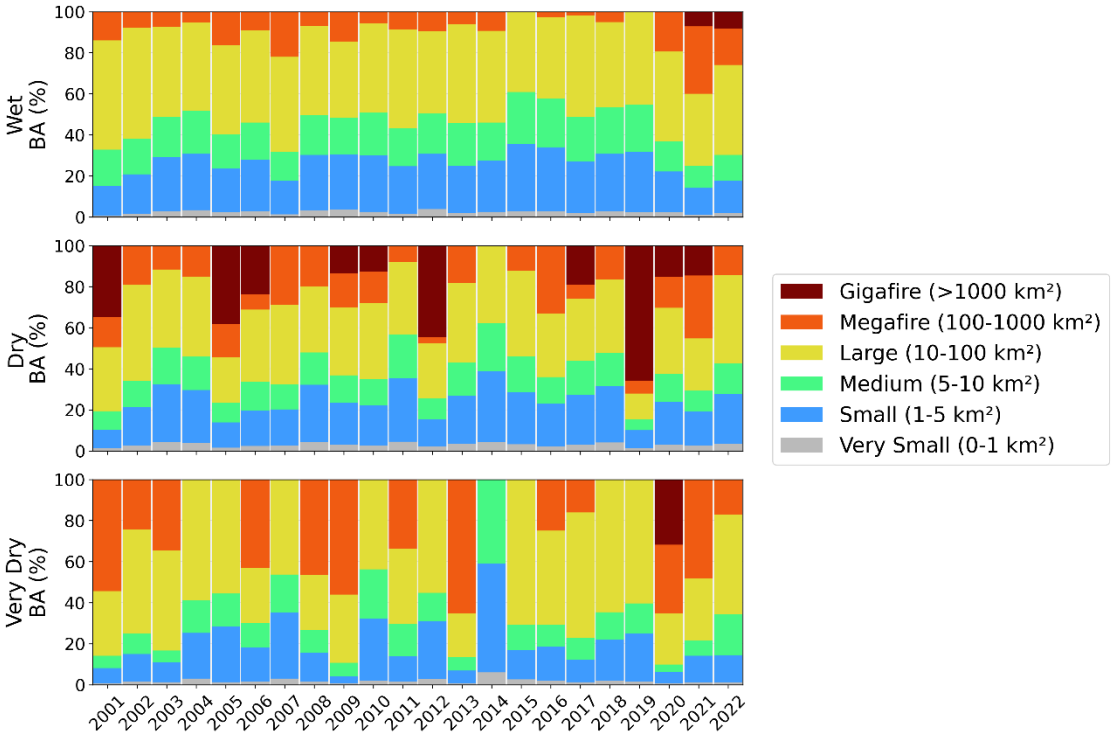

~~**Fig. A4:** Annual percentage distribution of burned areas across different size categories between 2001 and 2022 in the Wet, Dry, and Very Dry Chaco.~~

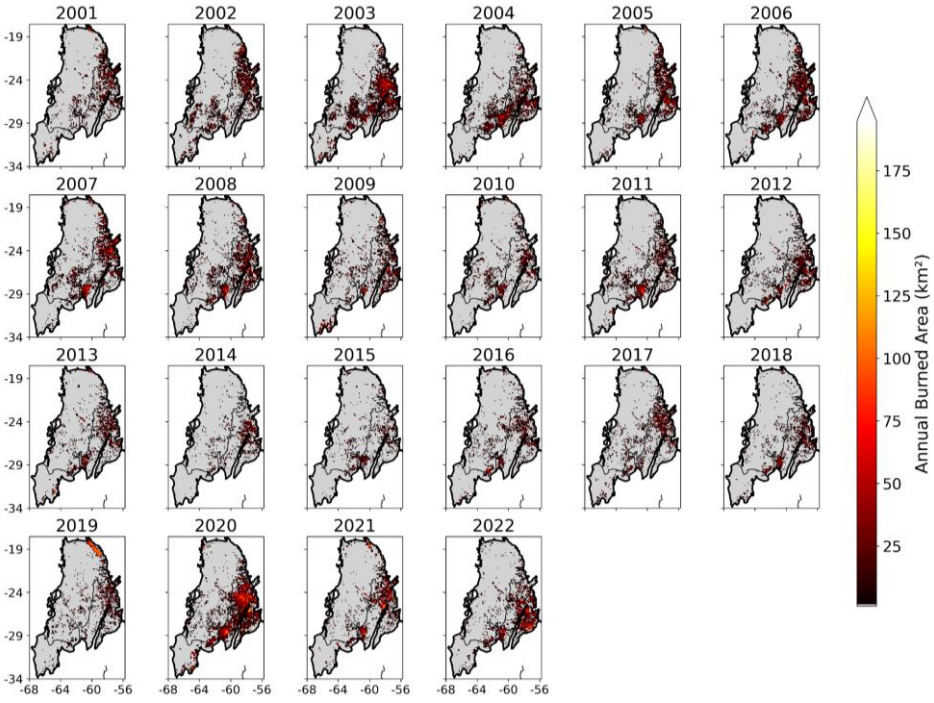

~~**Fig. A5:** Annual burned area maps of the Chaco region between 2001 and 2022. Burned areas extracted from FRYv2.0.~~

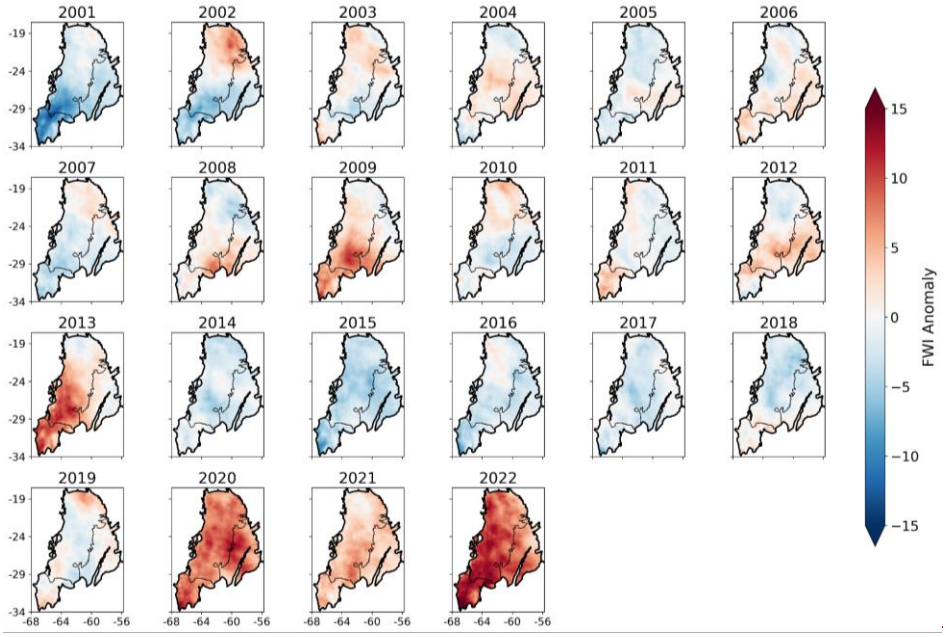

~~**Fig. A6:** Annual mean Fire Weather Index (FWI) anomalies with respect to the period 2001–2020, averaged for the Chaco region for each year between 2001 and 2022. FWI built from ERA5-Land.~~

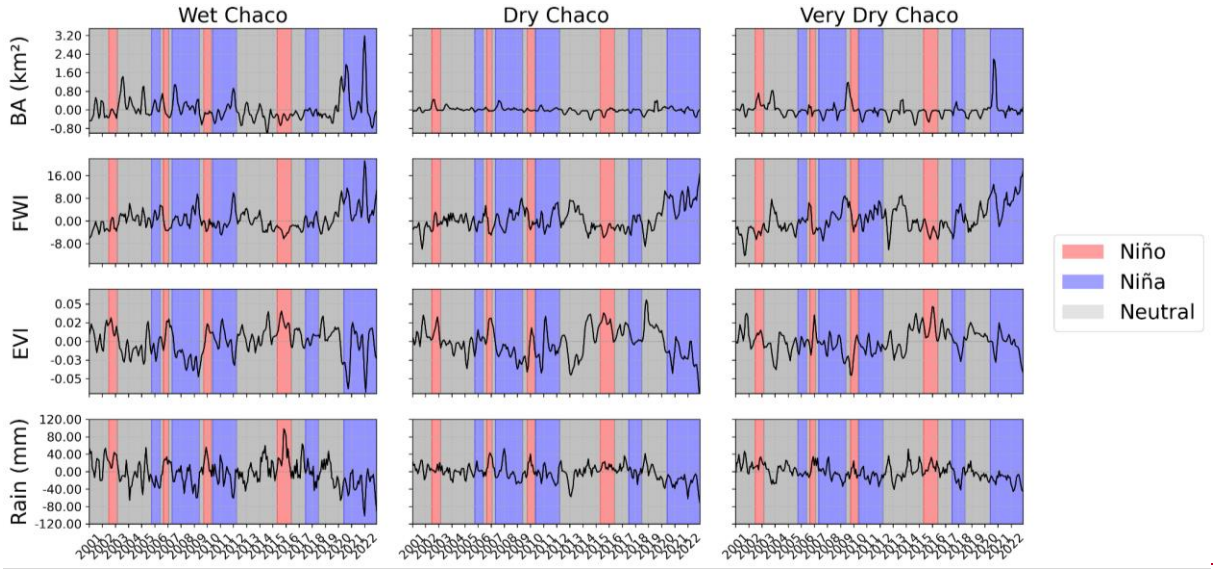

~~**Fig. A7:** Monthly anomalies of rainfall, vegetation (EVI), fuel dryness (FWI), and burned area in the Chaco subregions. Panels show 3-month running means of region-averaged anomalies for each variable, calculated from gridded (pixel-based) data and averaged over the Wet, Dry, and Very Dry Chaco subregions. Shaded backgrounds in the burned area panel indicate ENSO phases (red for El Niño, blue for La Niña), calculated with the Multivariate ENSO index (MEI).~~

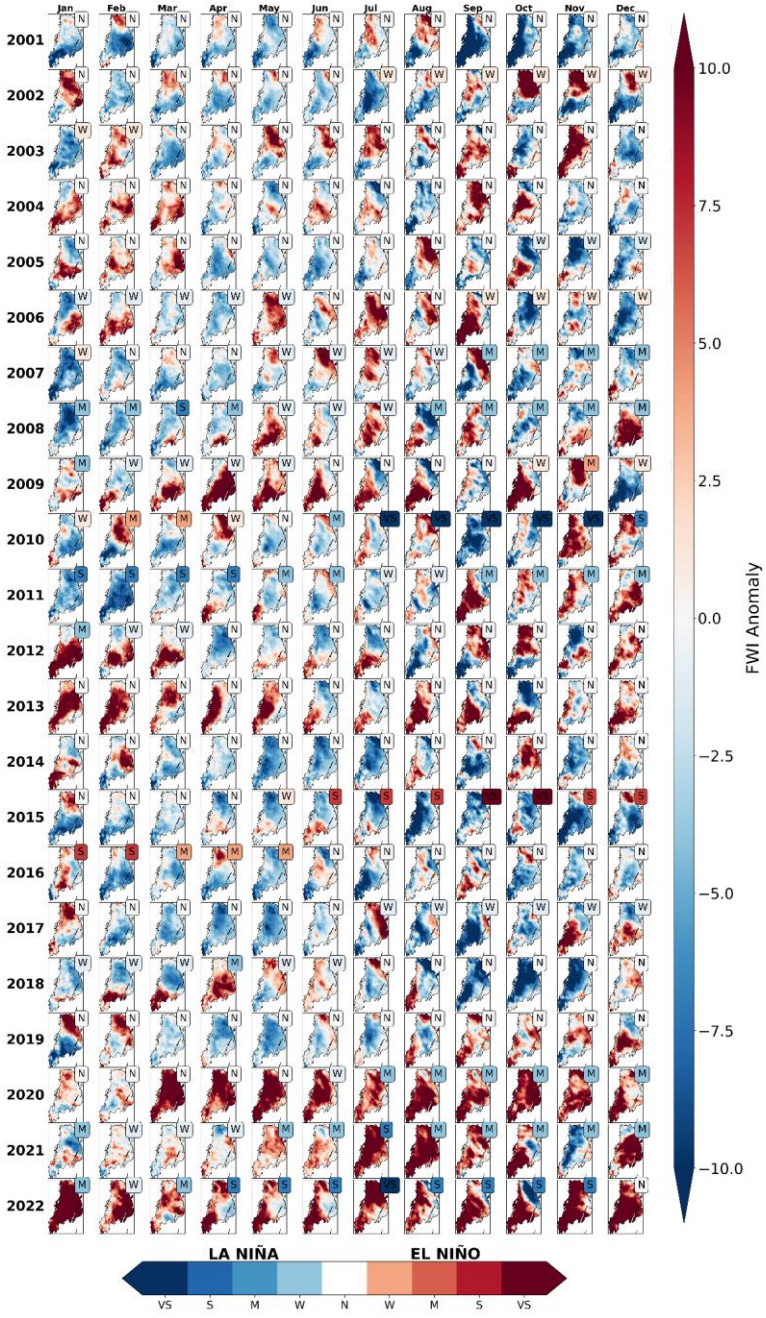

Fig. A8: The maps display the monthly anomalies (with 2001–2021 as the baseline) for the Chaco region for each year within the period. Additionally, each map counts with the Multivariate ENSO Index (MEI) showing the presence of an El Niño (EN; red) or La Niña (LN; blue) when during five consecutive three-month periods, MEI values are above +0.5 or below -0.5, respectively. Otherwise, the months are in a neutral (N) phase. The Niño/Niña events are classified by intensity based on the absolute MEI values. W: Weak (≥ 0.5); M: Moderate (≥ 1); S: Strong (≥ 1.5); VS: Very Strong (≥ 2).

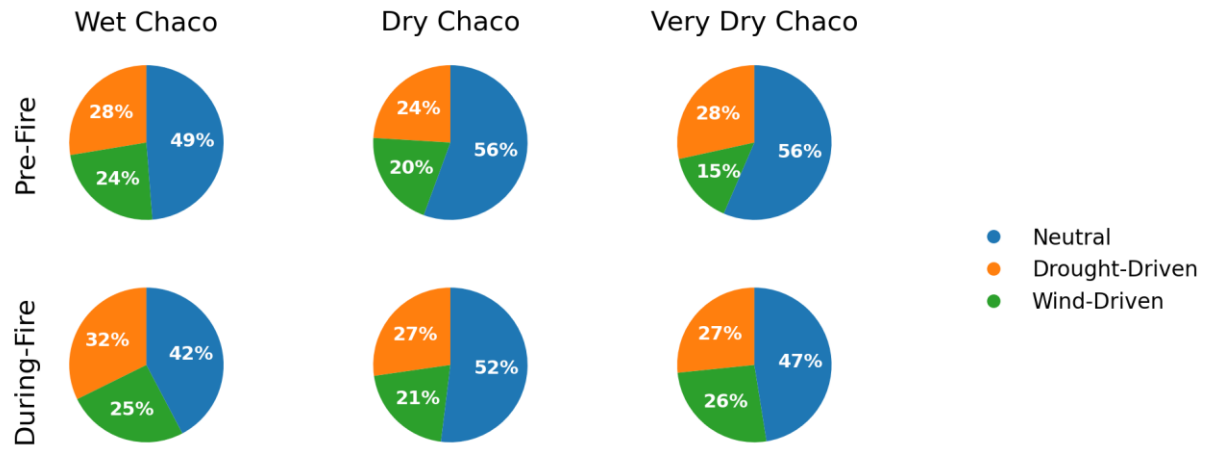

Fig. A9: Regional distribution of fire-weather types (FWTs) across the three Chaco subregions based on the Pre-Fire clustering (top row) and the During-Fire clustering (bottom row). Pie charts represent the proportion of fire patches assigned to each cluster—Drought-Driven (orange), Wind-Driven (green), and Neutral (blue)—based on pre-fire (0–3 days before ignition) and during-fire meteorological conditions.

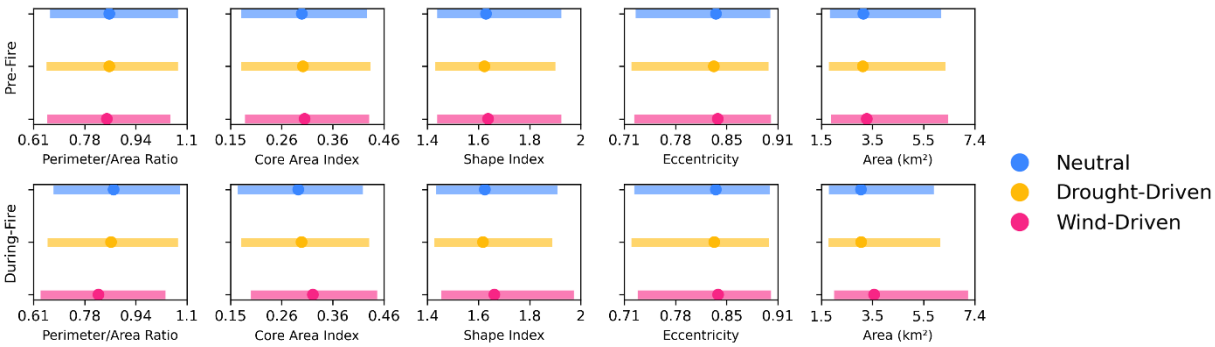

Fig. A10: Distribution of morphology variables by cluster (quartile–dot plots). For each morphology variable, the interquartile range (IQR; thick horizontal bar) and median (dot) are shown for each cluster, separately for Pre-Fire and During-Fire clusterings (first and second rows, respectively). This visualizes the spread and central tendency of each variable within clusters, highlighting differences in fire patch morphology between cluster types and fire periods.

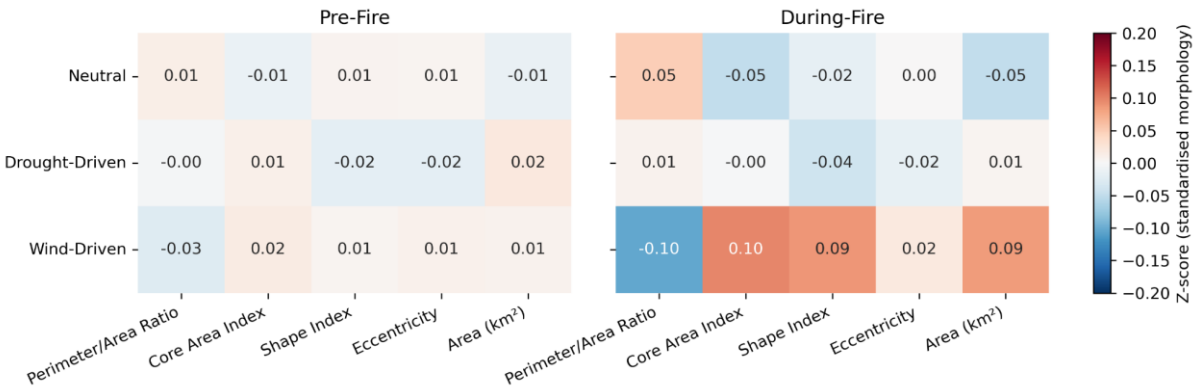

Fig. A11: Each heatmap shows the mean z-score (standardised value) of key fire patch morphology variables for each cluster, separately for Pre-Fire (left) and During-Fire (right) cluster assignments. Rows correspond to clusters (Neutral, Drought-Driven, Wind-Driven), and columns

~~to morphology variables. The color scale indicates the relative position of each cluster's mean within the overall distribution, highlighting differences in~~use in order to anticipate how this fire ~~patch shape and size between clusters and fire periods.~~

regime will respond to future environmental and societal change.

~~7~~

~~6~~ 6 AUTHOR CONTRIBUTION

RSM collected and processed the data, analyzed the results, and drafted the manuscript. CO and AS conceived the idea and led the project. PVA contributed to data analysis, specifically by performing Random Forest modeling. All co-authors discussed the results, provided critical feedback, and reviewed the manuscript.

~~8~~ 7 COMPETING INTERESTS

The authors declare that they have no conflict of interest.

~~9~~ 8 ACKNOWLEDGEMENTS

The authors thank all the researchers and institutions involved in providing open-access datasets, including ESA CCI, ERA5-Land, and the Copernicus Climate Data Store (CDS). We acknowledge the computational infrastructure and support provided by the Laboratoire des Sciences du Climat et de l'Environnement (LSCE/IPSL). We also express our gratitude to Dr. Sandra Bravo for her important collaboration and contributions to our understanding of the fire regime in the region, as well as colleagues from CONICET for their valuable insights into Chaco ecology. The authors also acknowledge the use of AI-based tools to assist with text editing, code debugging, and figure scripting throughout the preparation of the manuscript.

9 FINANCIAL SUPPORT

This research was partially funded by the European Space Agency through the Climate Change Initiative programme, under contract numbers ESA/No. 4000126564 (Land_Cover_cci) and ESA ESRIN/No. 4000125259/18/I-NB. A. Sörensson acknowledges support from the Agencia Nacional de Promoción Científica y Tecnológica (ANPCyT, Argentina) via project PICT 2018-02511, and from the Consejo Nacional de Investigaciones Científicas y Técnicas (CONICET, Argentina) through grant PIP 11220200102141CO. R. San Martin received doctoral funding from the Environmental Science Doctoral School of Île-de-France (DS 129).

10 REFERENCES

Alencar, A. A., Brando, P. M., Asner, G. P., and Putz, F. E.: Landscape fragmentation, severe drought, and the new Amazon forest fire regime, Ecol. Appl., 25, 1493–1505, https://doi.org/10.1890/14-1528.1, 2015.

Andela, N., Morton, D. C., Giglio, L., Chen, Y., van der Werf, G. R., Kasibhatla, P. S., DeFries, R. S., Collatz, G. J., Hantson, S., Kloster, S., Bachelet, D., Forrest, M., Lasslop, G., Li, F., Mangeon, S., Melton, J. R., Yue, C., and Randerson, J. T.: A human-driven decline in global burned area, Science, 356, 1356–1362, https://doi.org/10.1126/science.aal4108, 2017.

Andela, N., Morton, D. C., Giglio, L., Paugam, R., Chen, Y., and Hantson, S.: The Global Fire Atlas of individual fire size, duration, speed and direction, 2019.

Archibald, S., Roy, D. P., Van WILGEN, B. W., and Scholes, R. J.: What limits fire? An examination of drivers of burnt area in Southern Africa, Glob. Change Biol., 15, 613–630, https://doi.org/10.1111/j.1365-2486.2008.01754.x, 2009.

Archibald, S., Lehmann, C. E. R., Gómez-Dans, J. L., and Bradstock, R. A.: Defining pyromes and global syndromes of fire regimes, Proc. Natl. Acad. Sci., 110, 6442–6447, https://doi.org/10.1073/pnas.1211466110, 2013.

Archibald, S., Lehmann, C. E. R., Belcher, C. M., Bond, W. J., Bradstock, R. A., Daniau, A. L., Dexter, K. G., Forrestel, E. J., Greve, M., He, T., Higgins, S. I., Hoffmann, W. A., Lamont, B. B., McGlinn, D. J., Moncrieff, G. R., Osborne, C. P., Pausas, J. G., Price, O., Ripley, B. S., Rogers, B. M., Schwilk, D. W., Simon, M. F., Turetsky, M. R., Van der Werf, G. R., and Zanne, A. E.: Biological and geophysical feedbacks with fire in the Earth system, Environ. Res. Lett., 13, 033003, https://doi.org/10.1088/1748-9326/aa9ead, 2018.

Arias, P. A., Rivera, J. A., Sörensson, A. A., Zachariah, M., Barnes, C., Philip, S., Kew, S., Vautard, R., Koren, G., Pinto, I., Vahlberg, M., Singh, R., Raju, E., Li, S., Yang, W., Vecchi, G. A., and Otto, F. E. L.: Interplay between climate change and climate variability: the 2022 drought in Central South America, Clim. Change, 177, 6, https://doi.org/10.1007/s10584-023-03664-4, 2024.

Arriaga-Velasco-Aceves, P., Xu, C. Y., and Ginzburg, R.: Chaco region: Forest loss and fragmentation in the context of the territorial planning law. Remote sensing assessment in Formosa, Argentina application case, Glob. Ecol. Conserv., 31, e01846, https://doi.org/10.1016/j.gecco.2021.e01846, 2021.

Barros, A. M. G. and Pereira, J. M. C.: Wildfire Selectivity for Land Cover Type: Does Size Matter?, PLOS ONE, 9, e84760, https://doi.org/10.1371/journal.pone.0084760, 2014.

Barros, A. M. G., Pereira, J. M. C., and Lund, U. J.: Identifying geographical patterns of wildfire orientation: A watershed-based analysis, For. Ecol. Manag., 264, 98–107, https://doi.org/10.1016/j.foreco.2011.09.027, 2012.

Barros, A. M. G., Pereira, J. M. C., Moritz, M. A., and Stephens, S. L.: Spatial Characterization of Wildfire Orientation Patterns in California, Forests, 4, 197–217, https://doi.org/10.3390/f4010197, 2013.

Baumann, M., Levers, C., Macchi, L., Bluhm, H., Waske, B., Gasparri, N. I., and Kuemmerle, T.: Mapping continuous fields of tree and shrub cover across the Gran Chaco using Landsat 8 and Sentinel-1 data, Remote Sens. Environ., 216, 201–211, https://doi.org/10.1016/j.rse.2018.06.044, 2018.

Baumann, M., Gasparri, I., Buchadas, A., Oeser, J., Meyfroidt, P., Levers, C., Romero-Muñoz, A., le

Polain de Waroux, Y., Müller, D., and Kuemmerle, T.: Frontier metrics for a process based understanding of deforestation dynamics, Environ. Res. Lett., 17, 095010, https://doi.org/10.1088/1748-9326/ac8b9a, 2022.

Belhadj-Khedher, C., El-Melki, T., and Mouillot, F.: Saharan Hot and Dry Sirocco Winds Drive Extreme Fire Events in Mediterranean Tunisia (North Africa), Atmosphere, 11, 590, https://doi.org/10.3390/atmos11060590, 2020.

Bistinas, I., Harrison, S. P., Prentice, I. C., and Pereira, J. M. C.: Causal relationships versus emergent patterns in the global controls of fire frequency, Biogeosciences, 11, 5087–5101, https://doi.org/10.5194/bg-11-5087-2014, 2014.

Black, A. E., Hayes, P., and Strickland, R.: Organizational Learning from Prescribed Fire Escapes: a Review of Developments Over the Last 10 Years in the USA and Australia, Curr. For. Rep., 6, 41–59, https://doi.org/10.1007/s40725-019-00108-0, 2020.

Boletta, P. E., Ravelo, A. C., Planchuelo, A. M., and Grilli, M.: Assessing deforestation in the Argentine Chaco, For. Ecol. Manag., 228, 108–114, https://doi.org/10.1016/j.foreco.2006.02.045, 2006.

Bowman, Balch, J., Artaxo, P., Bond, W. J., Cochrane, M. A., D'Antonio, C. M., DeFries, R., Johnston, F. H., Keeley, J. E., Krawchuk, M. A., Kull, C. A., Mack, M., Moritz, M. A., Pyne, S., Roos, C. I., Scott, A. C., Sodhi, N. S., and Swetnam, T. W.: The human dimension of fire regimes on Earth: The human dimension of fire regimes on Earth, J. Biogeogr., 38, 2223–2236, https://doi.org/10.1111/j.1365-2699.2011.02595.x, 2011.

Bowman, D. M. J. S., Balch, J. K., Artaxo, P., Bond, W. J., Carlson, J. M., Cochrane, M. A., D'Antonio, C. M., DeFries, R. S., Doyle, J. C., Harrison, S. P., Johnston, F. H., Keeley, J. E., Krawchuk, M. A., Kull, C. A., Marston, J. B., Moritz, M. A., Prentice, I. C., Roos, C. I., Scott, A. C., Swetnam, T. W., van der Werf, G. R., and Pyne, S. J.: Fire in the Earth System, Science, 324, 481–484, https://doi.org/10.1126/science.1163886, 2009.

Bowring, S. P. K., Li, W., Mouillot, F., Rosan, T. M., and Ciais, P.: Road fragment edges enhance wildfire incidence and intensity, while suppressing global burned area, Nat. Commun., 15, 9176, https://doi.org/10.1038/s41467-024-53460-6, 2024.

Bravo, S., Kunst, C., Leiva, M., and Ledesma, R.: Response of hardwood tree regeneration to surface fires, western Chaco region, Argentina, For. Ecol. Manag., 326, 36–45, https://doi.org/10.1016/j.foreco.2014.04.009, 2014.

Bucher, E. H.: Chaco and Caatinga — South American Arid Savannas, Woodlands and Thickets, in: Ecology of Tropical Savannas, vol. 42, edited by: Huntley, B. J. and Walker, B. H., Springer Berlin Heidelberg, Berlin, Heidelberg, 48–79, https://doi.org/10.1007/978-3-642-68786-0_4, 1982.

Bucher, E. H. and Huszar, P. C.: Sustainable management of the Gran Chaco of South America: Ecological promise and economic constraints, J. Environ. Manage., 57, 99–108, https://doi.org/10.1006/jema.1999.0290, 1999.

Center For International Earth Science Information Network-CIESIN-Columbia University: Gridded Population of the World, Version 4 (GPWv4): Population Density, Revision 11, https://doi.org/10.7927/H49C6VHW, 2017.

Chen, W.: FRY version 2.0 provisional, [online] Available from: osf.io/rjvz5, 2025.

Chuvieco, E., Aguado, I., Salas, J., García, M., Yebra, M., and Oliva, P.: Satellite Remote Sensing Contributions to Wildland Fire Science and Management, Curr. For. Rep., 6, 81–96, https://doi.org/10.1007/s40725-020-00116-5, 2020.

Chuvieco, E., Roteta, E., Sali, M., Stroppiana, D., Boettcher, M., Kirches, G., Storm, T., Khairoun, A., Pettinari, M. L., Franquesa, M., and Albergel, C.: Building a small fire database for Sub-Saharan Africa from Sentinel-2 high-resolution images, Sci. Total Environ., 845, 157139, https://doi.org/10.1016/j.scitotenv.2022.157139, 2022.

D'Antonio, C. M. and Vitousek, P. M.: Biological Invasions by Exotic Grasses, the Grass/Fire Cycle, and Global Change, Annu. Rev. Ecol. Evol. Syst., 23, 63–87, https://doi.org/10.1146/annurev.es.23.110192.000431, 1992.

De Marzo, T., Pflugmacher, D., Baumann, M., Lambin, E. F., Gasparri, I., and Kuemmerle, T.: Characterizing forest disturbances across the Argentine Dry Chaco based on Landsat time series, Int. J. Appl. Earth Obs. Geoinformation, 98, 102310, https://doi.org/10.1016/j.jag.2021.102310, 2021.

De Marzo, T., Pratzer, M., Baumann, M., Gasparri, N. I., Pötzschner, F., and Kuemmerle, T.: Linking disturbance history to current forest structure to assess the impact of disturbances in tropical dry forests, For. Ecol. Manag., 539, 120989, https://doi.org/10.1016/j.foreco.2023.120989, 2023.

Doblas-Reyes, F. J., Sorensson, A. A., Almazroui, M., Dosio, A., Gutowski, W. J., Haarsma, R., Hamdi, R., Hewitson, B., Kwon, W. T., Lamptey, B. L., Maraun, D., Stephenson, T. S., Takayabu, I., Terray, L., Turner, A., and Zuo, Z.: Linking global to regional climate change, edited by: Masson-Delmotte, V., Zhai, P., Pirani, A., Connors, S. L., Pean, C., Berger, S., Caud, N., Chen, Y., Goldfarb, L., Gomis, M. I., Huang, M., Leitzell, K., Lonnoy, E., Matthews, J. B. R., Maycock, T. K., Waterfield, T., Yelekci, O., Yu, R., and Zhou, B., Cambridge University Press, 2021.

Druel, A., Ruffault, J., Davi, H., Chanzy, A., Marloie, O., De Cáceres, M., Olioso, A., Mouillot, F., François, C., Soudani, K., and Martin-StPaul, N. K.: Enhancing environmental models with a new downscaling method for global radiation in complex terrain, Biogeosciences, 22, 1–18, https://doi.org/10.5194/bg-22-1-2025, 2025.

Dujardin, J. and Lehning, M.: Wind-Topo: Downscaling near-surface wind fields to high-resolution topography in highly complex terrain with deep learning, Q. J. R. Meteorol. Soc., 148, 1368–1388, https://doi.org/10.1002/qj.4265, 2022.

SRTM | Earthdata: https://www.earthdata.nasa.gov/sensors/srtm, last access: 4 September 2024.

García, M., Pettinari, M. L., Chuvieco, E., Salas, J., Mouillot, F., Chen, W., and Aguado, I.: Characterizing Global Fire Regimes from Satellite-Derived Products, Forests, 13, 699, https://doi.org/10.3390/f13050699, 2022a.

García, M., Pettinari, M. L., Chuvieco, E., Salas, J., Mouillot, F., Chen, W., and Aguado, I.: Characterizing Global Fire Regimes from Satellite-Derived Products, Forests, 13, 699, https://doi.org/10.3390/f13050699, 2022b.

Gasparri, N. I., Grau, H. R., and Manghi, E.: Carbon Pools and Emissions from Deforestation in Extra-Tropical Forests of Northern Argentina Between 1900 and 2005, Ecosystems, 11, 1247–1261, https://doi.org/10.1007/s10021-008-9190-8, 2008.

Ginzburg, R., Adámoli, J., Herrera, P., and Torrella, S.: Los Humedales del Chaco: clasificación, inventario y mapeo a escala regional, Miscelánea, 14, 121–138, 2005.

Haas, O., Prentice, I. C., and Harrison, S. P.: Global environmental controls on wildfire burnt area, size, and intensity, Environ. Res. Lett., 17, 065004, https://doi.org/10.1088/1748-9326/ac6a69, 2022.

Hantson, S., Pueyo, S., and Chuvieco, E.: Global fire size distribution is driven by human impact and climate, Glob. Ecol. Biogeogr., 24, 77–86, https://doi.org/10.1111/geb.12246, 2015.

Hantson, S., Arneth, A., Harrison, S. P., Kelley, D. I., Prentice, I. C., Rabin, S. S., Archibald, S., Mouillot, F., Arnold, S. R., Artaxo, P., Bachelet, D., Ciais, P., Forrest, M., Friedlingstein, P., Hickler, T., Kaplan, J. O., Kloster, S., Knorr, W., Lasslop, G., Li, F., Mangeon, S., Melton, J. R., Meyn, A., Sitch, S., Spessa, A., van der Werf, G. R., Voulgarakis, A., and Yue, C.: The status and challenge of global fire modelling, Biogeosciences, 13, 3359–3375, https://doi.org/10.5194/bg-13-3359-2016, 2016.

Hantson, S., Scheffer, M., Pueyo, S., Xu, C., Lasslop, G., Nes, E. H., and Mendelsohn, J.: Rare, Intense, Big fires dominate the global tropics under drier conditions, Sci. Rep., 7, 1–5, 2017.

Hengl, T., Mendes De Jesus, J., Heuvelink, G. B. M., Ruiperez Gonzalez, M., Kilibarda, M., Blagotić, A., Shangguan, W., Wright, M. N., Geng, X., Bauer-Marschallinger, B., Guevara, M. A., Vargas, R., MacMillan, R. A., Batjes, N. H., Leenaars, J. G. B., Ribeiro, E., Wheeler, I., Mantel, S., and Kempen, B.: SoilGrids250m: Global gridded soil information based on machine learning, PLOS ONE, 12, e0169748, https://doi.org/10.1371/journal.pone.0169748, 2017.

Hernandez, C., Drobinski, P., and Turquety, S.: How much does weather control fire size and intensity in the Mediterranean region?, Ann. Geophys., 33, 931–939, https://doi.org/10.5194/angeo-33-931-2015, 2015.

Higuera, P. E., Abatzoglou, J. T., Littell, J. S., and Morgan, P.: The Changing Strength and Nature of Fire-Climate Relationships in the Northern Rocky Mountains, U.S.A., 1902–2008, PLOS ONE, 10, e0127563, https://doi.org/10.1371/journal.pone.0127563, 2015.

Hsu, A., Jones, M. W., Thurgood, J. R., Smith, A. J. P., Carmenta, R., Abatzoglou, J. T., Anderson, L. O., Clarke, H., Doerr, S. H., Fernandes, P. M., Kolden, C. A., Santín, C., Strydom, T., Le Quéré, C., Ascoli, D., Castellnou, M., Goldammer, J. G., Guiomar, N. R. G. N., Kukavskaya, E. A., Rigolot, E., Tanpipat, V., Varner, M., Yamashita, Y., Baard, J., Barreto, R., Becerra, J., Brunn, E., Bergius, N., Carlsson, J., Cheney, C., Druce, D., Elliot, A., Evans, J., De Moraes Falleiro, R., Prat-Guitart, N., Hiers, J. K., Kaiser, J. W., Macher, L., Morris, D., Park, J., Robles, C., Román-Cuesta, R. M., Rücker, G., Senra, F., Steil, L., Valverde, J. A. L., and Zerr, E.: A global assemblage of regional prescribed burn records – GlobalRx, Sci. Data, 12, 1083, https://doi.org/10.1038/s41597-025-04941-w, 2025.

Jolly, W. M., Cochrane, M. A., Freeborn, P. H., Holden, Z. A., Brown, T. J., Williamson, G. J., and Bowman, D. M. J. S.: Climate-induced variations in global wildfire danger from 1979 to 2013, Nat. Commun., 6, 7537, https://doi.org/10.1038/ncomms8537, 2015.

Jones, Abatzoglou, J. T., Veraverbeke, S., Andela, N., Lasslop, G., and Forkel, M.: Global and regional trends and drivers of fire under climate change, Rev. Geophys., 60, 2020–000726, https://doi.org/10.1029/2020RG000726, 2022.

Kelley, D. I., Bistinas, I., Whitley, R., Burton, C., Marthews, T. R., and Dong, N.: How contemporary bioclimatic and human controls change global fire regimes, Nat. Clim. Change, 9, 690–696, https://doi.org/10.1038/s41558-019-0540-7, 2019.

Khairoun, A., Mouillot, F., Chen, W., Ciais, P., and Chuvieco, E.: Coarse-resolution burned area datasets severely underestimate fire-related forest loss, Sci. Total Environ., 920, 170599, https://doi.org/10.1016/j.scitotenv.2024.170599, 2024.

Krawchuk, M. A. and Moritz, M. A.: Constraints on global fire activity vary across a resource gradient, Ecology, 92, 121–132, https://doi.org/10.1890/09-1843.1, 2011.

Krawchuk, M. A., Cumming, S. G., and Flannigan, M. D.: Predicted changes in fire weather suggest increases in lightning fire initiation and future area burned in the mixedwood boreal forest, Clim. Change, 92, 83–97, https://doi.org/10.1007/s10584-008-9460-7, 2009.

Kuemmerle, T., Altrichter, M., Baldi, G., Cabido, M., Camino, M., Cuellar, E., and Zak, M.: Forest conservation: remember gran chaco, Science, 355, 465–465, 2017.

Kunst, C., Bravo, S., Monti, E., Cornacchione, M., and Godoy, J.: El fuego y el manejo de pasturas naturales y cultivadas de la región chaqueña, Fuego En Los Ecosistemas Argent. Ediciones INTA, 21, 239–247, 2003.

Kusch, E. and Davy, R.: KrigR – A tool for downloading and statistically downscaling climate reanalysis data, Environ. Res. Lett., 17, https://doi.org/10.1088/1748-9326/ac48b3, 2022.

Laurent, P., Mouillot, F., Yue, C., Ciais, P., Moreno, M. V., and Nogueira, J. M. P.: FRY, a global database of fire patch functional traits derived from space-borne burned area products, Sci. Data, 5, 180132, https://doi.org/10.1038/sdata.2018.132, 2018.

Lehner, B., Verdin, K., and Jarvis, A.: New Global Hydrography Derived From Spaceborne Elevation Data, Eos Trans. Am. Geophys. Union, 89, 93–94, https://doi.org/10.1029/2008eo100001, 2008.

Levers, C., Piquer-Rodríguez, M., Gollnow, F., Baumann, M., Camino, M., Gasparri, N. I., Gavier-Pizarro, G. I., le Polain de Waroux, Y., Müller, D., Nori, J., Pötzschner, F., Romero-Muñoz, A., and Kuemmerle, T.: What is still at stake in the Gran Chaco? Social-ecological impacts of alternative land-system futures in a global deforestation hotspot, Environ. Res. Lett., 19, 064003, https://doi.org/10.1088/1748-9326/ad44b6, 2024.

Li, F., Zhu, Q., Riley, W. J., Zhao, L., Xu, L., Yuan, K., Chen, M., Wu, H., Gui, Z., Gong, J., and Randerson, J. T.: AttentionFire_v1.0: interpretable machine learning fire model for burned-area predictions over tropics, Geosci. Model Dev., 16, 869–884, https://doi.org/10.5194/gmd-16-869-2023, 2023.

Li, S., Baijnath-Rodino, J. A., York, R. A., Quinn-Davidson, L. N., and Banerjee, T.: Temporal and spatial pattern analysis of escaped prescribed fires in California from 1991 to 2020, Fire Ecol., 21, 3, https://doi.org/10.1186/s42408-024-00342-3, 2025.

Linley, G. D., Jolly, C. J., Doherty, T. S., Geary, W. L., Armenteras, D., Belcher, C. M., Bliege Bird, R., Duane, A., Fletcher, M., Giorgis, M. A., Haslem, A., Jones, G. M., Kelly, L. T., Lee, C. K. F., Nolan, R. H., Parr, C. L., Pausas, J. G., Price, J. N., Regos, A., Ritchie, E. G., Ruffault, J., Williamson, G. J., Wu, Q., and Nimmo, D. G.: What do you mean, 'megafire'?, Glob. Ecol. Biogeogr., 31, 1906–1922, https://doi.org/10.1111/geb.13499, 2022.

Liu, Y., Huang, H., Wang, S. C., Zhang, T., Xu, D., and Chen, Y.: ELM2.1-XGBfire1.0: improving wildfire prediction by integrating a machine learning fire model in a land surface model, Geosci. Model Dev., 18, 4103–4117, https://doi.org/10.5194/gmd-18-4103-2025, 2025.

Lizundia-Loiola, J., Otón, G., Ramo, R., and Chuvieco, E.: A spatio-temporal active-fire clustering approach for global burned area mapping at 250 m from MODIS data, Remote Sens. Environ., 236, 111493, https://doi.org/10.1016/j.rse.2019.111493, 2020.

Lizundia-Loiola, J., Franquesa, M., Khairoun, A., and Chuvieco, E.: Global burned area mapping from Sentinel-3 Synergy and VIIRS active fires, Remote Sens. Environ., 282, 113298, https://doi.org/10.1016/j.rse.2022.113298, 2022.

MacQueen, J.: Some methods for classification and analysis of multivariate observations, in: Proceedings of the Fifth Berkeley Symposium on Mathematical Statistics and Probability, Volume 1: Statistics, 281–298, 1967.

Mansuy, N., Boulanger, Y., Terrier, A., Gauthier, S., Robitaille, A., and Bergeron, Y.: Spatial attributes of fire regime in eastern Canada: influences of regional landscape physiography and climate, Landsc.

Ecol., 29, 1157–1170, https://doi.org/10.1007/s10980-014-0049-4, 2014.

Marengo, J., Martinez, R., Tapia, B., Allen, T., Basantes, R., Hernandez Espinoza, K., Alvarado, L., Baddour, O., Ransom, C., Silva, Á., Báez, J., Gomez, F., Costa, F., Avalos, G., Estella, J., and Kennedy, J.: State of the Climate in Latin America and the Caribbean 2021 (WMO No. 1295), 2022.

Meinshausen, N.: Quantile Regression Forests, J. Mach. Learn. Res., 7, 983–999, 2006.

Meteorological Organization, Naumann, G., Podestá, G., Marengo, J. A., Luterbacher, J., Bavera, D., Arias Muñoz, C., Barbosa, P., Cammalleri, C., Acosta Navarro, J. C., Cuartas, L. A., Jager, A. de, Escobar, C., Hidalgo, C., Mazzeschi, M., Leal de Moraes, O. L., Estrada, M. de, Maetens, W., Magni, D., Masante, D., Seluchi, M. E., Milagros Skansi, M. de los, Felice, M. de, Fioravanti, G., Giordano, L., Hrast Essenfelder, A., Osman, M., Rossi, L., Spennemann, P., Spinoni, J., Toreti, A., and Vera, C.: Extreme and long-term drought in the La Plata Basin: event evolution and impact assessment until September 2022 : a joint report from EC JRC, CEMADEN, SISSA and WMO, Publications Office of the European Union, 2023.

Morello, J. H. and Adámoli, J. M.: Las grandes unidades de vegetación y ambiente del Chaco argentino, 1968.

Moreno, M. V., Laurent, P., and Mouillot, F.: Global intercomparison of functional pyrodiversity from two satellite sensors, Int. J. Remote Sens., 42, 9523–9541, https://doi.org/10.1080/01431161.2021.1999529, 2021.

Mouillot, F., Schultz, M. G., Yue, C., Cadule, P., Tansey, K., Ciais, P., and Chuvieco, E.: Ten years of global burned area products from spaceborne remote sensing—A review: Analysis of user needs and recommendations for future developments, Int. J. Appl. Earth Obs. Geoinformation, 26, 64–79, https://doi.org/10.1016/j.jag.2013.05.014, 2014.

Muñoz Sabater, J., Dutra, E., Agustí Panareda, A., Albergel, C., Arduini, G., Balsamo, G., Boussetta, S., Choulga, M., Harrigan, S., Hersbach, H., Martens, B., Miralles, D. G., Piles, M., Rodríguez Fernández, N. J., Zsoter, E., Buontempo, C., and Thépaut, J. N.: ERA5 Land: a state of the art global reanalysis dataset for land applications, Earth Syst. Sci. Data, 13, 4349–4383, https://doi.org/10.5194/essd-13-4349-2021, 2021.

Musser, K.: Río de la Plata, Wikipedia, 2024.

Naumann, G., Podesta, G., Marengo, J., Luterbacher, J., Bavera, D., Acosta, N. J., Arias Muñoz, C., Barbosa, P., Cammalleri, C., Cuartas, L. A., De, E. M., De, F. M., De, J. A., Escobar, C., Fioravanti, G., Giordano, L., Hrast, E. A., Hidalgo, C., Leal, D. M. O. L., Maetens, W., Magni, D., Masante, D., Mazzeschi, M., Osman, M., Rossi, L., Seluchi, M., De, L. M. S. M., Spennemann, P., Spinoni, J., Toreti, A., and Vera, C.: Extreme and long-term drought in the La Plata Basin: event evolution and impact assessment until September 2022, https://doi.org/10.2760/62557, 2023.

Naval-Fernández, M. C., Elia, M., Giannico, V., Bellis, L. M., Bravo, S. J., and Argañaraz, J. P.: The Pyrogeography of the Gran Chaco's Dry Forest: A Comparison of Clustering Algorithms and the Scale of Analysis, Forests, 16, 1114, https://doi.org/10.3390/f16071114, 2025.

Nori, J., Torres, R., Lescano, J. N., Cordier, J. M., Periago, M. E., and Baldo, D.: Protected areas and spatial conservation priorities for endemic vertebrates of the Gran Chaco, one of the most threatened ecoregions of the world, Divers. Distrib., 22, 1212–1219, https://doi.org/10.1111/ddi.12497, 2016.

Oliveras Menor, I., Prat-Guitart, N., Spadoni, G. L., Hsu, A., Fernandes, P. M., Puig-Gironès, R., Ascoli, D., Bilbao, B. A., Bacciu, V., Brotons, L., Carmenta, R., de-Miguel, S., Gonçalves, L. G., Humphrey, G., Ibarnegaray, V., Jones, M. W., Machado, M. S., Millán, A., de Morais Falleiro, R., Mouillot, F.,

Pinto, C., Pons, P., Regos, A., Senra de Oliveira, M., Harrison, S. P., and Armenteras Pascual, D.: Integrated fire management as an adaptation and mitigation strategy to altered fire regimes, Commun. Earth Environ., 6, 202, https://doi.org/10.1038/s43247-025-02165-9, 2025.

Olson, D. M., Dinerstein, E., Wikramanayake, E. D., Burgess, N. D., Powell, G. V., Underwood, E. C., and Kassem, K. R.: Terrestrial Ecoregions of the World: A New Map of Life on EarthA new global map of terrestrial ecoregions provides an innovative tool for conserving biodiversity, BioScience, 51, 933–938, 2001.

Oom, D., Silva, P. C., Bistinas, I., and Pereira, J. M. C.: Highlighting Biome-Specific Sensitivity of Fire Size Distributions to Time Gap Parameter Using a New Algorithm for Fire Event Individuation, Remote Sens., 8, 663, https://doi.org/10.3390/rs8080663, 2016.

Paritsis, J., Landesmann, J. B., Kitzberger, T., Tiribelli, F., Sasal, Y., Quintero, C., and Nuñez, M. A.: Pine plantations and invasion alter fuel structure and potential fire behavior in a Patagonian forest-steppe ecotone, Forests, 9, 117, https://doi.org/10.3390/f9030117, 2018.

Pausas, J. G. and Bradstock, R. A.: Fire persistence traits of plants along a productivity and disturbance gradient in mediterranean shrublands of south east Australia, Glob. Ecol. Biogeogr., 16, 330–340, https://doi.org/10.1111/j.1466-8238.2006.00283.x, 2007.

Pettinari, M. L., Lizundia-Loiola, J., and Chuvieco, E.: ESA CCI ECV fire disturbance: D4. 2.1 product user guide–MODIS, version 1.1, 2021.

Pielou, E. C.: The measurement of diversity in different types of biological collections, J. Theor. Biol., 13, 131–144, https://doi.org/10.1016/0022-5193(66)90013-0, 1966.

Povak, N. A., Hessburg, P. F., and Salter, R. B.: Evidence for scale-dependent topographic controls on wildfire spread, Ecosphere, 9, e02443, https://doi.org/10.1002/ecs2.2443, 2018.

Redford, K. H., Taber, A., and Simonetti, J. A.: There is More to Biodiversity than the Tropical Rain Forests, Conserv. Biol., 4, 328–330, 1990.

Ruffault, J. and Mouillot, F.: How a new fire-suppression policy can abruptly reshape the fire-weather relationship, Ecosphere, 6, art199, https://doi.org/10.1890/ES15-00182.1, 2015.

Ruffault, J. and Mouillot, F.: Contribution of human and biophysical factors to the spatial distribution of forest fire ignitions and large wildfires in a French Mediterranean region, Int. J. Wildland Fire, 26, 498–508, https://doi.org/10.1071/WF16181, 2017.

Ruffault, J., Moron, V., Trigo, R. M., and Curt, T.: Objective identification of multiple large fire climatologies: an application to a Mediterranean ecosystem, Environ. Res. Lett., 11, 075006, https://doi.org/10.1088/1748-9326/11/7/075006, 2016.

Ruffault, J., Curt, T., Moron, V., Trigo, R. M., Mouillot, F., Koutsias, N., Pimont, F., Martin-StPaul, N., Barbero, R., Dupuy, J. L., Russo, A., and Belhadj-Khedher, C.: Increased likelihood of heat-induced large wildfires in the Mediterranean Basin, Sci. Rep., 10, 13790, https://doi.org/10.1038/s41598-020-70069-z, 2020.

San Martín, R.: Fires, land use, and forest loss in the South American Chaco : understanding the links between fires, climate, ecosystems, and human activity through remote sensing, PhD Thesis, Université Paris-Saclay, 2024.

San Martín, R., Ottlé, C., and Sörensson, A.: Fires in the South American Chaco, from dry forests to wetlands: response to climate depends on land cover, Fire Ecol., 19, 57, https://doi.org/10.1186/s42408-023-00212-4, 2023.

Saucedo, G. I. and Kurtz, D. B.: Seasonality and post-fire recovery in a wetland-dominated region: Insights from satellite data analysis in northern Argentina, Remote Sens. Appl. Soc. Environ., 37, 101480, https://doi.org/10.1016/j.rsase.2025.101480, 2025.

Shannon, C. E.: A Mathematical Theory of Communication, Bell Syst. Tech. J., 27, 379–423, https://doi.org/10.1002/j.1538-7305.1948.tb01338.x, 1948.

Sugiyama, M. S., Mendoza, M., and Carpio, M. B.: Resilience and Recovery in the Dry Chaco: Ecological Knowledge Encoded in Forager Wildfire Narratives, J. Ethnobiol., 45, 76–94, https://doi.org/10.1177/02780771241303896, 2025.

Takacs, S., Schulte to Bühne, H., and Pettorelli, N.: What shapes fire size and spread in African savannahs?, Remote Sens. Ecol. Conserv., 7, 610–620, https://doi.org/10.1002/rse2.212, 2021.

Torrella, S. A. and Adámoli, J.: Situación ambiental de la ecorregión del Chaco Seco, Situac. Ambient. Argent., 75–82, 2005.

Van Wagner, C. E.: Development and structure of the Canadian Forest Fire Weather Index System, Minister of Supply and Services Canada, Ottawa, 37 pp., 1987.

Vidal Riveros, C., Souza-Alonso, P., Bravo, S., Laino, R., and Ngo Bieng, M. A.: A review of wildfires effects across the Gran Chaco region, For. Ecol. Manag., 549, 121432, https://doi.org/10.1016/j.foreco.2023.121432, 2023.

Vidal Riveros, C., Watler Reyes, W. J., Ngo Bieng, M. A., and Souza Alonso, P.: Assessing Fire Regimes in the Paraguayan Chaco: Implications for Ecological and Fire Management, Fire, 7, 347, https://doi.org/10.3390/fire7100347, 2024.

Vitolo, C., Di Giuseppe, F., Barnard, C., Coughlan, R., San-Miguel-Ayanz, J., Libertá, G., and Krzeminski, B.: ERA5-based global meteorological wildfire danger maps, Sci. Data, 7, 216, https://doi.org/10.1038/s41597-020-0554-z, 2020.

Wright, M. N. and Ziegler, A.: ranger: A Fast Implementation of Random Forests for High Dimensional Data in C++ and R, J. Stat. Softw., 77, 1–17, https://doi.org/10.18637/jss.v077.i01, 2017.

Yebra, M., Scortechini, G., Badi, A., Beget, M. E., Boer, M. M., Bradstock, R., Chuvieco, E., Danson, F. M., Dennison, P., Resco de Dios, V., Di Bella, C. M., Forsyth, G., Frost, P., Garcia, M., Hamdi, A., He, B., Jolly, M., Kraaij, T., Martín, M. P., Mouillot, F., Newnham, G., Nolan, R. H., Pellizzaro, G., Qi, Y., Quan, X., Riaño, D., Roberts, D., Sow, M., and Ustin, S.: Globe-LFMC, a global plant water status database for vegetation ecophysiology and wildfire applications, Sci. Data, 6, 155, https://doi.org/10.1038/s41597-019-0164-9, 2019.

Zhang, Y., Mao, J., Ricciuto, D. M., Jin, M., Yu, Y., Shi, X., Wullschleger, S., Tang, R., and Liu, J.: Global fire modelling and control attributions based on the ensemble machine learning and satellite observations, Sci. Remote Sens., 7, 100088, https://doi.org/10.1016/j.srs.2023.100088, 2023.Adámoli, J., Sennhauser, E., Acero, J. M., and Rescia, A.: Stress and Disturbance: Vegetation Dynamics in the Dry Chaco Region of Argentina, Journal of Biogeography, 17, 491–500, https://doi.org/10.2307/2845381, 1990.

Alencar, A. A., Brando, P. M., Asner, G. P., and Putz, F. E.: Landscape fragmentation, severe drought, and the new Amazon forest fire regime, Ecological Applications, 25, 1493–1505, https://doi.org/10.1890/14-1528.1, 2015.

Alessio, G. A., Peñuelas, J., Llusià, J., Ogaya, R., Estiarte, M., and De Lillis, M.: Influence of water and terpenes on flammability in some dominant Mediterranean species, Int J Wildland Fire, 17, 274–286, https://doi.org/10.1071/WF07038, 2008.

Alinari, J., Muller, A. von, and Renison, D.: The contribution of fire damage to restricting high mountain Polylepis australis forests to ravines: Insights from an un-replicated comparison, Ecología Austral, 25, 11–18, https://doi.org/10.25260/EA.15.25.1.0.53, 2015.

Andela, N. and van der Werf, G. R.: Recent trends in African fires driven by cropland expansion and El Niño to La Niña transition, Nature Clim Change, 4, 791–795, https://doi.org/10.1038/nclimate2313, 2014.

Andela, N., Morton, D. C., Giglio, L., Chen, Y., van der Werf, G. R., Kasibhatla, P. S., DeFries, R. S., Collatz, G. J., Hantson, S., Kloster, S., Bachelet, D., Forrest, M., Lasslop, G., Li, F., Mangeon, S., Melton, J. R., Yue, C., and Randerson, J. T.: A human-driven decline in global burned area, Science, 356, 1356–1362, https://doi.org/10.1126/science.aal4108, 2017.

Andela, N., Morton, D. C., Giglio, L., Paugam, R., Chen, Y., and Hantson, S.: The Global Fire Atlas of individual fire size, duration, speed and direction, 2019.

Archibald, S., Roy, D. P., Van WILGEN, B. W., and Scholes, R. J.: What limits fire? An examination of drivers of burnt area in Southern Africa, Global Change Biology, 15, 613–630, https://doi.org/10.1111/j.1365-2486.2008.01754.x, 2009.

Archibald, S., Lehmann, C. E. R., Gómez-Dans, J. L., and Bradstock, R. A.: Defining pyromes and global syndromes of fire regimes, Proceedings of the National Academy of Sciences, 110, 6442–6447, https://doi.org/10.1073/pnas.1211466110, 2013.

Archibald, S., Lehmann, C. E. R., Belcher, C. M., Bond, W. J., Bradstock, R. A., Daniau, A.-L., Dexter, K. G., Forrestel, E. J., Greve, M., He, T., Higgins, S. I., Hoffmann, W. A., Lamont, B. B., McGlinn, D. J., Moncrieff, G. R., Osborne, C. P., Pausas, J. G., Price, O., Ripley, B. S., Rogers, B. M., Schwilk, D. W., Simon, M. F., Turetsky, M. R., Van der Werf, G. R., and Zanne, A. E.: Biological and geophysical feedbacks with fire in the Earth system, Environ. Res. Lett., 13, 033003, https://doi.org/10.1088/1748-9326/aa9ead, 2018.

Arenas, P.: ARENAS, Pastor. 2003. Etnografía y alimentación entre los toba-ñachilamole#ek y wichí- lhuku'tas del Chaco Central (Argentina). Buenos Aires, Edición del autor, 562 p. 24x17 cm. ISBN 987-43-6483-1., Book, 2003.

Argañaraz, Pizarro, G. G., Zak, M., Landi, M. A., and Bellis, L. M.: Human and biophysical drivers of fires in Semiarid Chaco mountains of Central Argentina, Science of the Total Environment, 520, 1–12, 2015.

Argañaraz, Landi, M. A., Bravo, S. J., Gavier-Pizarro, G. I., Scavuzzo, C. M., and Bellis, L. M.: Estimation of Live Fuel Moisture Content From MODIS Images for Fire Danger Assessment in Southern Gran Chaco, IEEE Journal of Selected Topics in Applied Earth Observations and Remote Sensing, 9, 5339–5349, https://doi.org/10.1109/JSTARS.2016.2575366, 2016.

Argañaraz, Landi, M. A., Scavuzzo, C. M., and Bellis, L. M.: Determining fuel moisture thresholds to assess wildfire hazard: A contribution to an operational early warning system, PLoS ONE, 13, e0204889, https://doi.org/10.1371/journal.pone.0204889, 2018.

Arias, P. A., Rivera, J. A., Sörensson, A. A., Zachariah, M., Barnes, C., Philip, S., Kew, S., Vautard, R., Koren, G., Pinto, I., Vahlberg, M., Singh, R., Raju, E., Li, S., Yang, W., Vecchi, G. A., and Otto, F. E. L.: Interplay between climate change and climate variability: the 2022 drought in Central South America, Climatic Change, 177, 6, https://doi.org/10.1007/s10584-023-03664-4, 2024.

Barros, A. M. G. and Pereira, J. M. C.: Wildfire Selectivity for Land Cover Type: Does Size Matter?, PLOS ONE, 9, e84760, https://doi.org/10.1371/journal.pone.0084760, 2014.

Baumann, M., Levers, C., Macchi, L., Bluhm, H., Waske, B., Gasparri, N. I., and Kuemmerle, T.: Mapping continuous fields of tree and shrub cover across the Gran Chaco using Landsat 8 and Sentinel-1 data, Remote Sensing of Environment, 216, 201–211, https://doi.org/10.1016/j.rse.2018.06.044, 2018.

Baumann, M., Gasparri, I., Buchadas, A., Oeser, J., Meyfroidt, P., Levers, C., Romero-Muñoz, A., le Polain de Waroux, Y., Müller, D., and Kuemmerle, T.: Frontier metrics for a process-based understanding of deforestation dynamics, Environ. Res. Lett., 17, 095010, https://doi.org/10.1088/1748-9326/ac8b9a, 2022.

Belhadj-Khedher, C., El-Melki, T., and Mouillot, F.: Saharan Hot and Dry Sirocco Winds Drive Extreme Fire Events in Mediterranean Tunisia (North Africa), Atmosphere, 11, 590, https://doi.org/10.3390/atmos11060590, 2020.

Bernardi, R. E., Staal, A., Xu, C., Scheffer, M., and Holmgren, M.: Livestock Herbivory Shapes Fire Regimes and Vegetation Structure Across the Global Tropics, Ecosystems, 22, 1457–1465, https://doi.org/10.1007/s10021-019-00349-x, 2019.

Bianchi, L., Defossé, G., Dentoni, M., Kunst, C., Ledesma, R., and Bravo, S.: Dynamics of fuel moisture and its relation to the ecology and management of fire in the western Chaco region (Argentina) I: basic concepts., 2014.

Bistinas, I., Harrison, S. P., Prentice, I. C., and Pereira, J. M. C.: Causal relationships versus emergent patterns in the global controls of fire frequency, Biogeosciences, 11, 5087–5101, https://doi.org/10.5194/bg-11-5087-2014, 2014.

Boletta, P. E., Ravelo, A. C., Planchuelo, A. M., and Grilli, M.: Assessing deforestation in the Argentine Chaco, Forest Ecology and Management, 228, 108–114, https://doi.org/10.1016/j.foreco.2006.02.045, 2006.

Bowman, Balch, J., Artaxo, P., Bond, W. J., Cochrane, M. A., D'Antonio, C. M., DeFries, R., Johnston, F. H., Keeley, J. E., Krawchuk, M. A., Kull, C. A., Mack, M., Moritz, M. A., Pyne, S., Roos, C. I., Scott, A. C., Sodhi, N. S., and Swetnam, T. W.: The human dimension of fire regimes on Earth: The human dimension of fire regimes on Earth, Journal of Biogeography, 38, 2223–2236, https://doi.org/10.1111/j.1365-2699.2011.02595.x, 2011.

Bowman, D. M. J. S., Balch, J. K., Artaxo, P., Bond, W. J., Carlson, J. M., Cochrane, M. A., D'Antonio, C. M., DeFries, R. S., Doyle, J. C., Harrison, S. P., Johnston, F. H., Keeley, J. E., Krawchuk, M. A., Kull, C. A., Marston, J. B., Moritz, M. A., Prentice, I. C., Roos, C. I., Scott, A. C., Swetnam, T. W., van der Werf, G. R., and Pyne, S. J.: Fire in the Earth System, Science, 324, 481–484, https://doi.org/10.1126/science.1163886, 2009.

Bowring, S. P. K., Li, W., Mouillot, F., Rosan, T. M., and Ciais, P.: Road fragment edges enhance wildfire incidence and intensity, while suppressing global burned area, Nat Commun, 15, 9176, https://doi.org/10.1038/s41467-024-53460-6, 2024.

Bravo, S., Kunst, C., Grau, R., and Aráoz, E.: Fire–rainfall relationships in Argentine Chaco savannas, Journal of Arid Environments, 74, 1319–1323, https://doi.org/10.1016/j.jaridenv.2010.04.010, 2010.

Bravo, S., Kunst, C., Leiva, M., and Ledesma, R.: Response of hardwood tree regeneration to surface fires, western Chaco region, Argentina, Forest Ecology and Management, 326, 36–45, https://doi.org/10.1016/j.foreco.2014.04.009, 2014.

Bravo, S., Bogino, S., Leiva, M., Lepiscopo, M., Cendoya, M., Kunst, C., and Biurrun, F.: Wood anatomy, fire wounds and dendrochronological potential of Prosopis pugionata Burkart (Fabaceae) in arid Argentine Chaco, IAWA journal / International Association of Wood Anatomists, 42, 1–10, https://doi.org/10.1163/22941932-bja10056, 2021.

Bravo, S., Ledesma, R., Coria, D., and Loto, D.: Fire in the Chaco Region: Ecological Aspects and Land Management, in: Fire in the South American Ecosystems, edited by: Fidelis, A. and Pivello, V. R., Springer Nature Switzerland, Cham, 213–241, https://doi.org/10.1007/978-3-031-89372-8_8, 2025.

Bucher, E. H.: Chaco and Caatinga — South American Arid Savannas, Woodlands and Thickets, in: Ecology of Tropical Savannas, vol. 42, edited by: Huntley, B. J. and Walker, B. H., Springer Berlin Heidelberg, Berlin, Heidelberg, 48–79, https://doi.org/10.1007/978-3-642-68786-0_4, 1982.

Bucher, E. H. and Huszar, P. C.: Sustainable management of the Gran Chaco of South America: Ecological promise and economic constraints, Journal of Environmental Management, 57, 99–108, https://doi.org/10.1006/jema.1999.0290, 1999.

Castilla, M.: " Ahora tenemos este virus, pero cuando tenés tantos problemas en la zona nada alcanza": Extractivismo, segregación y pandemia en la provincia del Chaco, 2021.

Center For International Earth Science Information Network-CIESIN-Columbia University: Gridded Population of the World, Version 4 (GPWv4): Population Density, Revision 11, https://doi.org/10.7927/H49C6VHW, 2017.

Chuvieco, E., Aguado, I., Salas, J., García, M., Yebra, M., and Oliva, P.: Satellite Remote Sensing Contributions to Wildland Fire Science and Management, Curr Forestry Rep, 6, 81–96, https://doi.org/10.1007/s40725-020-00116-5, 2020.

Chuvieco, E., Roteta, E., Sali, M., Stroppiana, D., Boettcher, M., Kirches, G., Storm, T., Khairoun, A., Pettinari, M. L., Franquesa, M., and Albergel, C.: Building a small fire database for Sub-Saharan Africa from Sentinel-2 high-resolution images, Science of The Total Environment, 845, 157139, https://doi.org/10.1016/j.scitotenv.2022.157139, 2022.

Cingolani, A. M., Vaieretti, M. V., Giorgis, M. A., La Torre, N., Whitworth-Hulse, J. I., and Renison, D.: Can livestock and fires convert the sub-tropical mountain rangelands of central Argentina into a rocky desert?, Rangel J, 35, 285–297, https://doi.org/10.1071/RJ12095, 2013.

Coria, R. D., Kunst, C. R., and Bravo, S. J.: A contribution to the understanding of the woody encroachment in grasslands/savannas from the South American Semiarid Chaco., 2021.

Coronel, G., Pastén, M., Breuer, N., Celeste, A., Rejalaga, L., Domecq, F. M., and Nagy, G. J.: Wildfires in Paraguay: Environmental and Human Impacts, in: Sustainability in Natural Resources Management and Land Planning, edited by: Leal Filho, W., Azeiteiro, U. M., and Setti, A. F. F., Springer International Publishing, Cham, 429–444, https://doi.org/10.1007/978-3-030-76624-5_25, 2021.

D'Antonio, C. M. and Vitousek, P. M.: Biological Invasions by Exotic Grasses, the Grass/Fire Cycle, and Global Change, Annual Review of Ecology and Systematics, 23, 63–87, 1992.

De Marzo, T., Pflugmacher, D., Baumann, M., Lambin, E. F., Gasparri, I., and Kuemmerle, T.: Characterizing forest disturbances across the Argentine Dry Chaco based on Landsat time series, International Journal of Applied Earth Observation and Geoinformation, 98, 102310, https://doi.org/10.1016/j.jag.2021.102310, 2021.

De Marzo, T., Gasparri, N. I., Lambin, E. F., and Kuemmerle, T.: Agents of Forest Disturbance in the Argentine Dry Chaco, Remote Sensing, 14, 1758, https://doi.org/10.3390/rs14071758, 2022.

De Marzo, T., Pratzer, M., Baumann, M., Gasparri, N. I., Pötzschner, F., and Kuemmerle, T.: Linking disturbance history to current forest structure to assess the impact of disturbances in tropical dry forests, Forest Ecology and Management, 539, 120989, https://doi.org/10.1016/j.foreco.2023.120989, 2023.

Defourny, P., Lamarche, C., Brockmann, C., Boettcher, M., Bontemps, S., Maet, T., Duveiller, G. L. H., K., H. A., Kirches, G., Moreau, I., Peylin, P., Ottlé, C., J., R., Bogaert, E., Ramoino, F., Albergel, C., and Arino, O.: Observed annual global land-use change from 1992 to 2020 three times more dynamic than reported by inventory-based statistics, in preparation, 2023.

Devisscher, T., Boyd, E., and Malhi, Y.: Anticipating future risk in social-ecological systems using fuzzy cognitive mapping: the case of wildfire in the Chiquitania, Bolivia, Ecology and Society, 21, https://doi.org/10.5751/ES-08599-210418, 2016.

Devisscher, T., Malhi, Y., and Boyd, E.: Deliberation for wildfire risk management: Addressing conflicting views in the Chiquitania, Bolivia, The Geographical Journal, 185, 38–54, https://doi.org/10.1111/geoj.12261, 2019.

Doblas-Reyes, F. J., Sorensson, A. A., Almazroui, M., Dosio, A., Gutowski, W. J., Haarsma, R., Hamdi, R., Hewitson, B., Kwon, W.-T., Lamptey, B. L., Maraun, D., Stephenson, T. S., Takayabu, I., Terray, L., Turner, A., and Zuo, Z.: Linking global to regional climate change, edited by: Masson-Delmotte, V., Zhai, P., Pirani, A., Connors, S. L., Pean, C., Berger, S., Caud, N., Chen, Y., Goldfarb, L., Gomis, M. I., Huang, M., Leitzell, K., Lonnoy, E., Matthews, J. B. R., Maycock, T. K., Waterfield, T., Yelekci, O., Yu, R., and Zhou, B., Cambridge University Press, 2021.

Druel, A., Ruffault, J., Davi, H., Chanzy, A., Marloie, O., De Cáceres, M., Olioso, A., Mouillot, F., François, C., Soudani, K., and Martin-StPaul, N. K.: Enhancing environmental models with a new downscaling method for global radiation in complex terrain, Biogeosciences, 22, 1–18, https://doi.org/10.5194/bg-22-1-2025, 2025.

Dujardin, J. and Lehning, M.: Wind-Topo: Downscaling near-surface wind fields to high-resolution topography in highly complex terrain with deep learning, Quarterly Journal of the Royal Meteorological Society, 148, 1368–1388, https://doi.org/10.1002/qj.4265, 2022.

Eklund, J., Jones, J. P. G., Räsänen, M., Geldmann, J., Jokinen, A.-P., Pellegrini, A., Rakotobe, D., Rakotonarivo, O. S., Toivonen, T., and Balmford, A.: Elevated fires during COVID-19 lockdown and the vulnerability of protected areas, Nat Sustain, 5, 603–609, https://doi.org/10.1038/s41893-022-00884-x, 2022.

Feron, S., Cordero, R. R., Damiani, A., MacDonell, S., Pizarro, J., Goubanova, K., Valenzuela, R., Wang, C., Rester, L., and Beaulieu, A.: South America is becoming warmer, drier, and more flammable, Communications Earth & Environment, 5, https://doi.org/10.1038/s43247-024-01654-7, 2024.

Fischer, M. A., Di Bella, C. M., and Jobbágy, E. G.: Fire patterns in central semiarid Argentina, Journal of Arid Environments, 78, 161–168, https://doi.org/10.1016/j.jaridenv.2011.11.009, 2012.

Garcia, L. C., Szabo, J. K., de Oliveira Roque, F., de Matos Martins Pereira, A., Nunes da Cunha, C., Damasceno-Júnior, G. A., Morato, R. G., Tomas, W. M., Libonati, R., and Ribeiro, D. B.: Record-breaking wildfires in the world's largest continuous tropical wetland: Integrative fire management is urgently needed for both biodiversity and humans, Journal of Environmental Management, 293, 112870, https://doi.org/10.1016/j.jenvman.2021.112870, 2021.

García, M., Pettinari, M. L., Chuvieco, E., Salas, J., Mouillot, F., Chen, W., and Aguado, I.: Characterizing Global Fire Regimes from Satellite-Derived Products, Forests, 13, 699, https://doi.org/10.3390/f13050699, 2022.

Gasparri, N. I. and Baldi, G.: Regional patterns and controls of biomass in semiarid woodlands: lessons from the Northern Argentina Dry Chaco, Reg Environ Change, 13, 1131–1144, https://doi.org/10.1007/s10113-013-0422-x, 2013.

Gasparri, N. I., Grau, H. R., and Manghi, E.: Carbon Pools and Emissions from Deforestation in Extra-Tropical Forests of Northern Argentina Between 1900 and 2005, Ecosystems, 11, 1247–1261, https://doi.org/10.1007/s10021-008-9190-8, 2008.

Ginzburg, R., Adámoli, J., Herrera, P., and Torrella, S.: Los Humedales del Chaco: clasificación, inventario y mapeo a escala regional, Miscelánea, 14, 121–138, 2005.

Giorgis, M. A., Zeballos, S. R., Carbone, L., Zimmermann, H., von Wehrden, H., Aguilar, R., Ferreras, A. E., Tecco, P. A., Kowaljow, E., Barri, F., Gurvich, D. E., Villagra, P., and Jaureguiberry, P.: A review of fire effects across South American ecosystems: the role of climate and time since fire, fire ecol, 17, 11, https://doi.org/10.1186/s42408-021-00100-9, 2021.

Gürtler, R. E.: Sustainability of vector control strategies in the Gran Chaco Region: current challenges and possible approaches, Memórias do Instituto Oswaldo Cruz, 104, 52–59, 2009.

Haas, O., Prentice, I. C., and Harrison, S. P.: Global environmental controls on wildfire burnt area, size, and intensity, Environ. Res. Lett., 17, 065004, https://doi.org/10.1088/1748-9326/ac6a69, 2022.

Hantson, S., Pueyo, S., and Chuvieco, E.: Global fire size distribution is driven by human impact and climate, Global Ecology and Biogeography, 24, 77–86, https://doi.org/10.1111/geb.12246, 2015.

Hantson, S., Scheffer, M., Pueyo, S., Xu, C., Lasslop, G., Nes, E. H., and Mendelsohn, J.: Rare, Intense, Big fires dominate the global tropics under drier conditions, Scientific reports, 7, 1–5, 2017.

Harper, K. L., Lamarche, C., Hartley, A., Peylin, P., Ottlé, C., Bastrikov, V., San Martín, R., Bohnenstengel, S. I., Kirches, G., Boettcher, M., Shevchuk, R., Brockmann, C., and Defourny, P.: A 29-year time series of annual 300 m resolution plant-functional-type maps for climate models, Earth Syst. Sci. Data, 15, 1465–1499, https://doi.org/10.5194/essd-15-1465-2023, 2023.

Hernandez, C., Drobinski, P., and Turquety, S.: How much does weather control fire size and intensity in the Mediterranean region?, Annales Geophysicae, 33, 931–939, https://doi.org/10.5194/angeo-33-931-2015, 2015.

Hernández, V., Florencia Fossa Riglos, M., and Vera, C.: Addressing climate services in SouthAmerican Chaco region through a knowledge coproduction process, Global Environmental Change, 72, 102443, https://doi.org/10.1016/j.gloenvcha.2021.102443, 2022.

Higuera, P. E., Abatzoglou, J. T., Littell, J. S., and Morgan, P.: The Changing Strength and Nature of Fire-Climate Relationships in the Northern Rocky Mountains, U.S.A., 1902-2008, PLOS ONE, 10, e0127563, https://doi.org/10.1371/journal.pone.0127563, 2015.

Horn, B. K. P.: Hill shading and the reflectance map, Proceedings of the IEEE, 69, 14–47, https://doi.org/10.1109/PROC.1981.11918, 1981.

Hsu, A., Jones, M. W., Thurgood, J. R., Smith, A. J. P., Carmenta, R., Abatzoglou, J. T., Anderson, L. O., Clarke, H., Doerr, S. H., Fernandes, P. M., Kolden, C. A., Santín, C., Strydom, T., Le Quéré, C., Ascoli, D., Castellnou, M., Goldammer, J. G., Guiomar, N. R. G. N., Kukavskaya, E. A., Rigolot, E., Tanpipat, V., Varner, M., Yamashita, Y., Baard, J., Barreto, R., Becerra, J., Brunn, E., Bergius, N., Carlsson, J., Cheney, C., Druce, D., Elliot, A., Evans, J., De Moraes Falleiro, R., Prat-Guitart, N., Hiers, J. K., Kaiser, J. W., Macher, L., Morris, D., Park, J., Robles, C., Román-Cuesta, R. M., Rücker, G., Senra, F., Steil, L., Valverde, J. A. L., and Zerr, E.: A global assemblage of regional prescribed burn records — GlobalRx, Sci Data, 12, 1083, https://doi.org/10.1038/s41597-025-04941-w, 2025.

Jones, Abatzoglou, J. T., Veraverbeke, S., Andela, N., Lasslop, G., and Forkel, M.: Global and regional trends and drivers of fire under climate change, Reviews of Geophysics, 60, 2020 000726, https://doi.org/10.1029/2020RG000726, 2022.

Junk, W. J. and Nunes da Cunha, C.: Pasture clearing from invasive woody plants in the Pantanal: a tool for sustainable management or environmental destruction?, Wetlands Ecol Manage, 20, 111–122, https://doi.org/10.1007/s11273-011-9246-y, 2012.

Kelley, D. I., Bistinas, I., Whitley, R., Burton, C., Marthews, T. R., and Dong, N.: How contemporary bioclimatic and human controls change global fire regimes, Nat. Clim. Chang., 9, 690–696, https://doi.org/10.1038/s41558-019-0540-7, 2019.

Krawchuk, M. A. and Moritz, M. A.: Constraints on global fire activity vary across a resource gradient, Ecology, 92, 121–132, https://doi.org/10.1890/09-1843.1, 2011.

Kumar, S., Getirana, A., Libonati, R., Hain, C., Mahanama, S., and Andela, N.: Changes in land use enhance the sensitivity of tropical ecosystems to fire-climate extremes, Sci Rep, 12, 964, https://doi.org/10.1038/s41598-022-05130-0, 2022.

Kunst, C. and Bravo, S.: Ecología y régimen de fuego en la región chaqueña argentina, in: Fuego en los ecosistemas Argentinos, 47–59, 2003.

Kunst, C., Bravo, S., Monti, E., Cornacchione, M., and Godoy, J.: El fuego y el manejo de pasturas naturales y cultivadas de la región chaqueña, Fuego en los Ecosistemas Argentinos. Ediciones INTA, 21, 239–247, 2003.

Kunst, C., Navall, M., Ledesma, R., Silberman, J., Anríquez, A., Coria, D., Bravo, S., Gómez, A., Albanesi, A., Grasso, D., Nuñez, J. A. D., González, A., Tomsic, P., and Godoy, J.: Silvopastoral Systems in the Western Chaco Region, Argentina, in: Silvopastoral Systems in Southern South America, edited by: Peri, P. L., Dube, F., and Varella, A., Springer International Publishing, Cham, 63–87, https://doi.org/10.1007/978-3-319-24109-8_4, 2016.

Kusch, E. and Davy, R.: KrigR – A tool for downloading and statistically downscaling climate reanalysis data, Environmental Research Letters, 17, https://doi.org/10.1088/1748-9326/ac48b3, 2022.

Laurent, P., Mouillot, F., Yue, C., Ciais, P., Moreno, M. V., and Nogueira, J. M. P.: FRY, a global database of fire patch functional traits derived from space-borne burned area products, Sci Data, 5, 180132, https://doi.org/10.1038/sdata.2018.132, 2018.

Levers, C., Piquer-Rodríguez, M., Gollnow, F., Baumann, M., Camino, M., Gasparri, N. I., Gavier-Pizarro, G. I., le Polain de Waroux, Y., Müller, D., Nori, J., Pötzschner, F., Romero-Muñoz, A., and Kuemmerle, T.: What is still at stake in the Gran Chaco? Social-ecological impacts of alternative land-system futures in a global deforestation hotspot, Environ. Res. Lett., 19, 064003, https://doi.org/10.1088/1748-9326/ad44b6, 2024.

Linley, G. D., Jolly, C. J., Doherty, T. S., Geary, W. L., Armenteras, D., Belcher, C. M., Bliege Bird, R., Duane, A., Fletcher, M., Giorgis, M. A., Haslem, A., Jones, G. M., Kelly, L. T., Lee, C. K. F., Nolan, R. H., Parr, C. L., Pausas, J. G., Price, J. N., Regos, A., Ritchie, E. G., Ruffault, J., Williamson, G. J., Wu, Q., and Nimmo, D. G.: What do you mean, 'megafire'?, Global Ecol Biogeogr, 31, 1906–1922, https://doi.org/10.1111/geb.13499, 2022.

Lizundia-Loiola, J., Otón, G., Ramo, R., and Chuvieco, E.: A spatio-temporal active-fire clustering approach for global burned area mapping at 250 m from MODIS data, Remote Sensing of Environment, 236, 111493, https://doi.org/10.1016/j.rse.2019.111493, 2020.

Loto, D. and Bravo, S.: Species composition, structure, and functional traits in Argentine Chaco forests under two different disturbance histories, Ecological Indicators, 113, 106232, https://doi.org/10.1016/j.ecolind.2020.106232, 2020.

MacQueen, J.: Some methods for classification and analysis of multivariate observations, in: Proceedings of the Fifth Berkeley Symposium on Mathematical Statistics and Probability, Volume 1: Statistics, 281–298, 1967.

Marengo, J., Martinez, R., Tapia, B., Allen, T., Basantes, R., Hernandez-Espinoza, K., Alvarado, L., Baddour, O., Ransom, C., Silva, Á., Báez, J., Gomez, F., Costa, F., Avalos, G., Estella, J., and Kennedy, J.: State of the Climate in Latin America and the Caribbean 2021 (WMO-No. 1295), 2022.

McDaniel, J., Kennard, D., and Fuentes, A.: Smokey the Tapir: Traditional Fire Knowledge and Fire Prevention Campaigns in Lowland Bolivia, Society & Natural Resources, 18, 921–931, https://doi.org/10.1080/08941920500248921, 2005.

Meinshausen, N.: Quantile Regression Forests, Journal of Machine Learning Research, 7, 983–999, 2006.

Morello, J. H. and Adámoli, J. M.: Las grandes unidades de vegetación y ambiente del Chaco argentino, 1968.

Moreno, M. V., Laurent, P., and Mouillot, F.: Global intercomparison of functional pyrodiversity from two satellite sensors, International Journal of Remote Sensing, 42, 9523–9541, https://doi.org/10.1080/01431161.2021.1999529, 2021.

Mouillot, F., Schultz, M. G., Yue, C., Cadule, P., Tansey, K., Ciais, P., and Chuvieco, E.: Ten years of global burned area products from spaceborne remote sensing—A review: Analysis of user needs and recommendations for future developments, International Journal of Applied Earth Observation and Geoinformation, 26, 64–79, https://doi.org/10.1016/j.jag.2013.05.014, 2014.

Mouillot, F., Chen, W., Campagnolo, M., and Ciais, P.: FRYv2.0 : a global fire patch morphology database from FireCCI51 and MCD64A1, Copernicus Meetings, https://doi.org/10.5194/egusphere-egu23-9575, 2023.

Muñoz-Sabater, J., Dutra, E., Agustí-Panareda, A., Albergel, C., Arduini, G., Balsamo, G., Boussetta, S., Choulga, M., Harrigan, S., Hersbach, H., Martens, B., Miralles, D. G., Piles, M., Rodríguez-Fernández, N. J., Zsoter, E., Buontempo, C., and Thépaut, J.-N.: ERA5-Land: a state-of-the-art global reanalysis dataset for land applications, Earth System Science Data, 13, 4349–4383, https://doi.org/10.5194/essd-13-4349-2021, 2021.

Musser, K.: Río de la Plata, Wikipedia, 2024.

Naumann, G., Podesta, G., Marengo, J., Luterbacher, J., Bavera, D., Acosta, N. J., Arias-Muñoz, C., Barbosa, P., Cammalleri, C., Cuartas, L. A., De, E. M., De, F. M., De, J. A., Escobar, C., Fioravanti, G., Giordano, L., Hrast, E. A., Hidalgo, C., Leal, D. M. O. L., Maetens, W., Magni, D., Masante, D., Mazzeschi, M., Osman, M., Rossi, L., Seluchi, M., De, L. M. S. M., Spennemann, P., Spinoni, J., Toreti, A., and Vera, C.: Extreme and long-term drought in the La Plata Basin: event evolution and impact assessment until September 2022, https://doi.org/10.2760/62557, 2023.

Naval Fernández, Albornoz, J., Bellis, L. M., Baldini, C., Arcamone, J., Silvetti, L., Álvarez, M. P., and Argañaraz, J. P.: Megaincendios 2020 en Córdoba: Incidencia del fuego en áreas de valor ecológico y socioeconómico, Ecol. Austral, 33, 136–151, https://doi.org/10.25260/EA.23.33.1.0.2120, 2023.

Naval-Fernández, M. C., Elia, M., Giannico, V., Bellis, L. M., Bravo, S. J., and Argañaraz, J. P.: The Pyrogeography of the Gran Chaco's Dry Forest: A Comparison of Clustering

Algorithms and the Scale of Analysis, Forests, 16, 1114, https://doi.org/10.3390/f16071114, 2025.

Nori, J., Torres, R., Lescano, J. N., Cordier, J. M., Periago, M. E., and Baldo, D.: Protected areas and spatial conservation priorities for endemic vertebrates of the Gran Chaco, one of the most threatened ecoregions of the world, Diversity and Distributions, 22, 1212–1219, https://doi.org/10.1111/ddi.12497, 2016.

Olson, D. M., Dinerstein, E., Wikramanayake, E. D., Burgess, N. D., Powell, G. V., Underwood, E. C., and Kassem, K. R.: Terrestrial Ecoregions of the World: A New Map of Life on EarthA new global map of terrestrial ecoregions provides an innovative tool for conserving biodiversity, BioScience, 51, 933–938, 2001.

Oom, D., Silva, P. C., Bistinas, I., and Pereira, J. M. C.: Highlighting Biome-Specific Sensitivity of Fire Size Distributions to Time-Gap Parameter Using a New Algorithm for Fire Event Individuation, Remote Sensing, 8, 663, https://doi.org/10.3390/rs8080663, 2016.

Paritsis, J., Landesmann, J. B., Kitzberger, T., Tiribelli, F., Sasal, Y., Quintero, C., Dimarco, R. D., Barrios-García, M. N., Iglesias, A. L., Diez, J. P., Sarasola, M., and Nuñez, M. A.: Pine Plantations and Invasion Alter Fuel Structure and Potential Fire Behavior in a Patagonian Forest-Steppe Ecotone, Forests, 9, 117, https://doi.org/10.3390/f9030117, 2018.

Paudel, J.: Short-run environmental effects of COVID-19: Evidence from forest fires, World Development, 137, 105120, https://doi.org/10.1016/j.worlddev.2020.105120, 2021.

Pausas, J. G. and Bradstock, R. A.: Fire persistence traits of plants along a productivity and disturbance gradient in mediterranean shrublands of south-east Australia, Global Ecol Biogeography, 16, 330–340, https://doi.org/10.1111/j.1466-8238.2006.00283.x, 2007.

Pettinari, M. L., Lizundia-Loiola, J., and Chuvieco, E.: ESA CCI ECV fire disturbance: D4. 2.1 product user guide—MODIS, version 1.1, 2021.

Pielou, E. C.: The measurement of diversity in different types of biological collections, Journal of Theoretical Biology, 13, 131–144, https://doi.org/10.1016/0022-5193(66)90013-0, 1966.

Poulter, B., Freeborn, P., Jolly, W., and Varner, J.: COVID-19 lockdowns drive decline in active fires in southeastern United States, Proceedings of the National Academy of Sciences, 118, e2105666118, https://doi.org/10.1073/pnas.2105666118, 2021.

Redford, K. H., Taber, A., and Simonetti, J. A.: There is More to Biodiversity than the Tropical Rain Forests, Conservation Biology, 4, 328–330, 1990.

Ruffault, J. and Mouillot, F.: How a new fire-suppression policy can abruptly reshape the fire-weather relationship, Ecosphere, 6, art199, https://doi.org/10.1890/ES15-00182.1, 2015.

Ruffault, J. and Mouillot, F.: Contribution of human and biophysical factors to the spatial distribution of forest fire ignitions and large wildfires in a French Mediterranean region, Int. J. Wildland Fire, 26, 498–508, https://doi.org/10.1071/WF16181, 2017.

Ruffault, J., Moron, V., Trigo, R. M., and Curt, T.: Objective identification of multiple large fire climatologies: an application to a Mediterranean ecosystem, Environ. Res. Lett., 11, 075006, https://doi.org/10.1088/1748-9326/11/7/075006, 2016.

Ruffault, J., Curt, T., Moron, V., Trigo, R. M., Mouillot, F., Koutsias, N., Pimont, F., Martin-StPaul, N., Barbero, R., Dupuy, J.-L., Russo, A., and Belhadj-Khedher, C.: Increased likelihood of heat-induced large wildfires in the Mediterranean Basin, Sci Rep, 10, 13790, https://doi.org/10.1038/s41598-020-70069-z, 2020.

San Martín, R.: Fires, land use, and forest loss in the South American Chaco : understanding the links between fires, climate, ecosystems, and human activity through remote sensing, PhD Thesis, Université Paris-Saclay, 2024.

San Martín, R., Ottlé, C., and Sörensson, A.: Fires in the South American Chaco, from dry forests to wetlands: response to climate depends on land cover, fire ecol, 19, 57, https://doi.org/10.1186/s42408-023-00212-4, 2023.

Saucedo, G. I. and Kurtz, D. B.: Seasonality and post fire recovery in a wetland dominated region: Insights from satellite data analysis in northern Argentina, Remote Sensing Applications: Society and Environment, 37, 101480, https://doi.org/10.1016/j.rsase.2025.101480, 2025.

Schmidt, M. A. and Castilla, M.: La emergencia del fuego en un territorio hidrosocial: incendios en las provincias de Salta y Chaco, I Encuentro Territorios Hidrosociales en Disputa (ETHIS) (Chaco, 25 y 26 de agosto de 2022), 2023.

Shannon, C. E.: A Mathematical Theory of Communication, Bell System Technical Journal, 27, 379–423, https://doi.org/10.1002/j.1538-7305.1948.tb01338.x, 1948.

Sugiyama, M. S., Mendoza, M., and Carpio, M. B.: Resilience and Recovery in the Dry Chaco: Ecological Knowledge Encoded in Forager Wildfire Narratives, Journal of Ethnobiology, 45, 76–94, https://doi.org/10.1177/02780771241303896, 2025.

Takacs, S., Schulte to Bühne, H., and Pettorelli, N.: What shapes fire size and spread in African savannahs?, Remote Sensing in Ecology and Conservation, 7, 610–620, https://doi.org/10.1002/rse2.212, 2021.

Tálamo, A., Lopez De Casenave, J., Núñez-Regueiro, M., and Caziani, S. M.: Regeneración de plantas leñosas en el Chaco semiárido argentino: relación con factores bióticos y abióticos en micrositios creados por el aprovechamiento forestal, Bosque (Valdivia), 34, 13–14, https://doi.org/10.4067/S0717-92002013000100007, 2013.

Torrella, S. A. and Adámoli, J.: Situación ambiental de la ecorregión del Chaco Seco, La situación ambiental Argentina, 75–82, 2005.

Van Wagner, C. E.: Development and structure of the Canadian Forest Fire Weather Index System, Minister of Supply and Services Canada, Ottawa, 37 pp., 1987.

Vidal-Riveros, C., Souza-Alonso, P., Bravo, S., Laino, R., and Ngo Bieng, M. A.: A review of wildfires effects across the Gran Chaco region, Forest Ecology and Management, 549, 121432, https://doi.org/10.1016/j.foreco.2023.121432, 2023.

Vidal-Riveros, C., Watler Reyes, W. J., Ngo Bieng, M. A., and Souza-Alonso, P.: Assessing Fire Regimes in the Paraguayan Chaco: Implications for Ecological and Fire Management, Fire, 7, 347, https://doi.org/10.3390/fire7100347, 2024.

Vitolo, C., Di Giuseppe, F., Barnard, C., Coughlan, R., San-Miguel-Ayanz, J., Libertá, G., and Krzeminski, B.: ERA5-based global meteorological wildfire danger maps, Sci Data, 7, 216, https://doi.org/10.1038/s41597-020-0554-z, 2020.

Wright, M. N. and Ziegler, A.: ranger: A Fast Implementation of Random Forests for High Dimensional Data in C++ and R, Journal of Statistical Software, 77, 1–17, https://doi.org/10.18637/jss.v077.i01, 2017.

Yebra, M., Scortechini, G., Badi, A., Beget, M. E., Boer, M. M., Bradstock, R., Chuvieco, E., Danson, F. M., Dennison, P., Resco de Dios, V., Di Bella, C. M., Forsyth, G., Frost, P., Garcia, M., Hamdi, A., He, B., Jolly, M., Kraaij, T., Martín, M. P., Mouillot, F., Newnham, G., Nolan, R. H., Pellizzaro, G., Qi, Y., Quan, X., Riaño, D., Roberts, D., Sow, M., and Ustin, S.: Globe-LFMC, a global plant water status database for vegetation ecophysiology and wildfire applications, Sci Data, 6, 155, https://doi.org/10.1038/s41597-019-0164-9, 2019.